ENGINEERING EXPERIMENT STATION
of the Georgia Institute of Technology
Atlanta, Georgia

CR-61653

N-5

FINAL REPORT

PROJECT NO. A-512

DEVELOPMENT OF MONOLITHIC CERAMICS AND HETEROGENEOUS CERAMIC-METAL BODIES FOR AERODYNAMIC APPLICATIONS AT HIGH VELOCITIES AND TEMPERATURES

By

N. E. POULOS, S. R. EIKINS, and J. D. WALTON

NATIONAL AERONAUTICS AND SPACE ADMINISTRATION
GEORGE C. MARSHALL SPACE FLIGHT CENTER
CONTRACT NO. NAS8-8

1 JULY 1960 to 31 OCTOBER 1960

PQ-7.48657

FOREWORD

The investigation covered in this report was performed by the Engineering Experiment Station of the Georgia Institute of Technology under National Aeronautics and Space Administration, George C. Marshall Space Flight Center, Contract No. NAS8-8. The contract Technical Supervisor was Mr. Clyde M. Holmes, Special Assistant, Engineering Materials Branch, Structures and Mechanics Division, Technical Services. The contract period was 1 July 1960 to 31 October 1960. This report covers all work performed during this contract period. This contract was a continuation of U. S. Army Ordnance Contract No. DA-01-009-ORD-777.

TABLE OF CONTENTS

This report contains 97 pages.

LIST OF FIGURES

LIST OF FIGURES (Continued)

LIST OF FIGURES (Continued)

LIST OF TABLES

I. SUMMARY

A. Equipment and Procedures Used for Standard Tests

The procedures, plaster molds, brass molds, data calculations and equipment have been described and illustrated. Unless otherwise specifically noted the "standard" sample sizes, formulas, equipment, and procedures were followed in conducting all experiments as detailed and illustrated herein.

B. Hydrated Cement--Fused Silica Aggregate Mixes

Studies previously performed under U. S. Army Ordnance Contract No. DA-01-009-ORD-777 indicated that hydrated cements such as Lumnite (calcium aluminate), portland cement, and Gypsum plaster held promise as an ablative and transpiration cooling material when mixed with fused silica aggregate. The main thought in considering these hydrated cements was to utilize the combined water (water of crystallization or chemically bound water) for transpiration cooling.

One of the major disadvantages of these materials - low transverse strength - could be overcome by using these materials as a filler for honeycomb structure, thus forming a composite structure that would offer good mechanical strength, good thermal shock properties, and transpiration cooling through the release of the combined water in the filler material - hydrated cements.

Since strength problems apparently could be solved, studies were initiated to determine the effect of (1) changes in the water of plasticity (water-to-cement ratio), (2) changes in the fused silica aggregate size from -100+200 mesh to -50+100 mesh, and (3) additions of Aerolith (Vinsol resin) - 0.5 oz Aerolith per 94 lb cement to 4 oz Aerolith per 94 lb cement - on the ablation and physical properties of various combinations of Lumnite cement and portland

cement--fused silica aggregate compositions. Also studied was the effect of replacing the water used in the cements with Ludox LS (colloidal silica) on the ablation and physical properties of the materials and the effect of driving the chemically bound water out of the samples by firing at 2150° F before exposure to the exhaust gases.

Among the data obtained from the combinations of hydrated cements and fused silica aggregate mixes are per cent apparent porosity, per cent water absorption, bulk density, transverse strength, ablation or erosion rate, weight loss rate, backside temperature, differential thermal analysis, and transpiration cooling data. All of the ablation properties, backside temperature determinations, and transpiration cooling data were obtained from standard 2- x 7- x 1/2-inch rocket motor test plate samples exposed to the exhaust gases of the oxyhydrogen rocket motor at a heat flux value of 260 $Btu \cdot ft^{-2} \cdot sec^{-1}$.

The water-cement ratio studies indicated that a ratio of 1.33 produced a maximum transpiration cooling period of 114 seconds for the Lumnite cement--fused silica aggregate compositions. This same ratio produced a maximum transpiration cooling period of 55 seconds for the special Lumnite cement compositions and 58 seconds for the portland cement compositions.

The changes in the fused silica aggregate sizes in the Lumnite cement compositions from -100+200 mesh to -50+100 mesh did not indicate any dramatic increases in the transpiration cooling periods.

The Aerolith additions to Lumnite and portland cements studies indicated that a 2-oz-Aerolith-per-94-lb-cement-addition to the 30 per cent Lumnite cement--70 per cent -100+200-mesh fused silica aggregate composition with a water-cement ratio of 1.11 produced a transpiration cooling period of 114 seconds, whereas this composition without the Aerolith addition exhibited a

transpiration cooling period of 72 seconds. In the case of Aerolith additions to similar compositions of portland cement but with a water-cement ratio of 0.84, the transpiration cooling period was 41 and 46 seconds respectively with 2- and 4-oz-Aerolith-per-94-lb-cement additions. The portland composition without the Aerolith additions exhibited no definite transpiration cooling period.

The replacement of water with Ludox colloidal silica in the cement-fused silica aggregate compositions did not tend to improve the strength or ablation properties of the compositions.

A comparison of partially dehydrated with hydrated 30 per cent Lumnite cement--70 per cent -100+200-mesh fused silica aggregate rocket motor test plates graphically illustrated the transpiration cooling effect of the release of the combined water. The partially dehydrated and hydrated test plates respectively indicated transpiration cooling periods of 14 and 76 seconds. The weight loss rate was increased from 0.113 to 0.163 $gm \cdot sec^{-1}$ and the ablation or erosion rate was increased from 0.0009 to 0.0038 $in \cdot sec^{-1}$ due to partial removal of the chemically bound water.

C. Reinforced Ceramic Fiber Ceramics

A study was initiated to determine the feasibility of reinforcing (1) 30 per cent Lumnite cement--fused silica aggregate compositions and (2) 8 per cent Pyropreg AC bonding resin--fused silica slip compositions with H. I. Thompson Fiber Glass Company's Refrasil flakes and fibers and General Electric Company's pure fused silica fibers. The transverse strength of the 30-per-cent-Lumnite-cement compositions were substantially improved (as much as a 136-per-cent increase with an average increase of 65 per cent) due to the fiber and flake reinforcement. The transverse strength of the 8 per cent Pyropreg AC bonding

resin compositions in general were not improved. Due to time limitations ablation properties could not be studied.

D. Composite Structures

Composite structures were formed by (1) filling the channels of a honeycomb structure with a Lumnite cement composition and (2) coating a metal substrate with fused silica aggregate compositions. The composite structures were exposed to the exhaust gases of the oxyhydrogen rocket motor.

A 1/2-inch-diameter x 1/8-inch-width groove was cut in the backplate of one of the honeycomb panels as shown in Figure 50 for the purpose of determining any heat sink effect. The heat sink effect of the backplate is graphically shown by the lower change in backside temperature for approximately the same time and by the masking or hiding of the flat portion of curve '0', Figure 39, of the transpiration cooling effect of the Lumnite cement filler material.

The results of coating two mild steel substrates with two different fused silica aggregate compositions and of exposure to the exhaust gases indicate that there is a possibility of easily coating a metal nose cone with a ceramic material for thermal protection (in this case fused silica) and still retaining the desired properties of both the metal and ceramic.

E. Differential Thermal Analysis (DTA)

DTA data were obtained for all test samples studied in the preliminary investigation of hydrated cement, Section B. The DTA data were correlated with the transpiration cooling data and backside temperature data. It was indicated that the greater the endothermic area under the DTA curves the

longer the transpiration cooling periods during exposure to the exhaust gases of the oxyhydrogen rocket motor.

F. Ablation Studies

Ablation or erosion rates, weight loss rates, backside temperature determination, and transpiration cooling data were determined for all test samples studied in Sections B, C, and D using the standard 2- x 7- x 1/2-inch rocket motor test plates. The test plates were exposed to the exhaust gases of the oxyhydrogen rocket motor at 9-1/2 inches from the exit plane of the rocket nozzle at a flame impingement angle of 45°. Water calorimeter heat flux value for this distance and angle was 260 $Btu \cdot ft^{-2} \cdot sec^{-1}$. The results of these determinations are summarized under the corresponding headings listed above.

II. PURPOSE

The purpose of Contract No. NAS8-8 was the development of high temperature resistant materials for aerodynamic application at high velocities and temperatures.

III. EXPERIMENTAL WORK

A. Equipment and Procedures Used for Standard Tests

The following standard procedures, plaster molds, brass molds, and equipment were used to determine data for the tests indicated, unless otherwise specifically noted.

(1) Transverse Strength

All transverse strength measurements were made on a Dillon Model L Universal Tester. Certified calibrated dynamometers with capacities of 250 and 500 lb were used. A cross head speed of 0.125 inch per minute was employed. The sample size is 3/4 inch in diameter x 6 inches in length for the round bars and 4 x 3/4 x 3/4 inches for square bars. The formulas used to compute the transverse strengths are:

a. Round Bars

$$\text{Transverse strength} = \frac{8pl}{\pi d^3}$$

where

p = maximum load indicated by the testing machine in pounds.

l = distance between the supports in inches.

d = diameter of round bars in inches.

b. Square Bars

$$\text{Transverse strength} = \frac{3pl}{2bd^2}$$

where:

p = maximum load indicated by the testing machine in pounds.

l = distance between the supports in inches.

b = average overall width, face to face, of the sample in inches.

d = average overall depth, face to face, of the sample in inches.

The flexure mold and test sample for the round bars are shown in Figure 1 while the brass mold and test sample for the square bars are shown in Figure 2.

(2) Water Absorption, Bulk Density, Apparent Porosity.

a. Dry Weight, D.

1. Samples dried at 230° F

2. If during the boiling process, (b) below, some particles were noted in the bottom of the pan, the samples were redried and reweighed (this weight was then recorded as the dry weight).

b. Boiling

The samples were boiled for 2 hours, keeping samples off the bottom of the pan, and then allowed to slowly cool to room temperature.

c. Suspended Weight, S

This weight was determined after boiling by weighing the samples in water to the nearest 0.01 gm.

d. Saturated Weight, W

The samples were blotted lightly with a sponge after saturation and weighed to the nearest 0.01 gm.

e. Exterior Volume, V

$$V = W-S$$

f. Per Cent Apparent Porosity, P

$$p = \frac{W-D}{V} \times 100$$

g. Per Cent Water Absorption, A

$$A = \frac{W-D}{D} \times 100$$

h. Bulk Density, B

$$B = \frac{D}{V}$$

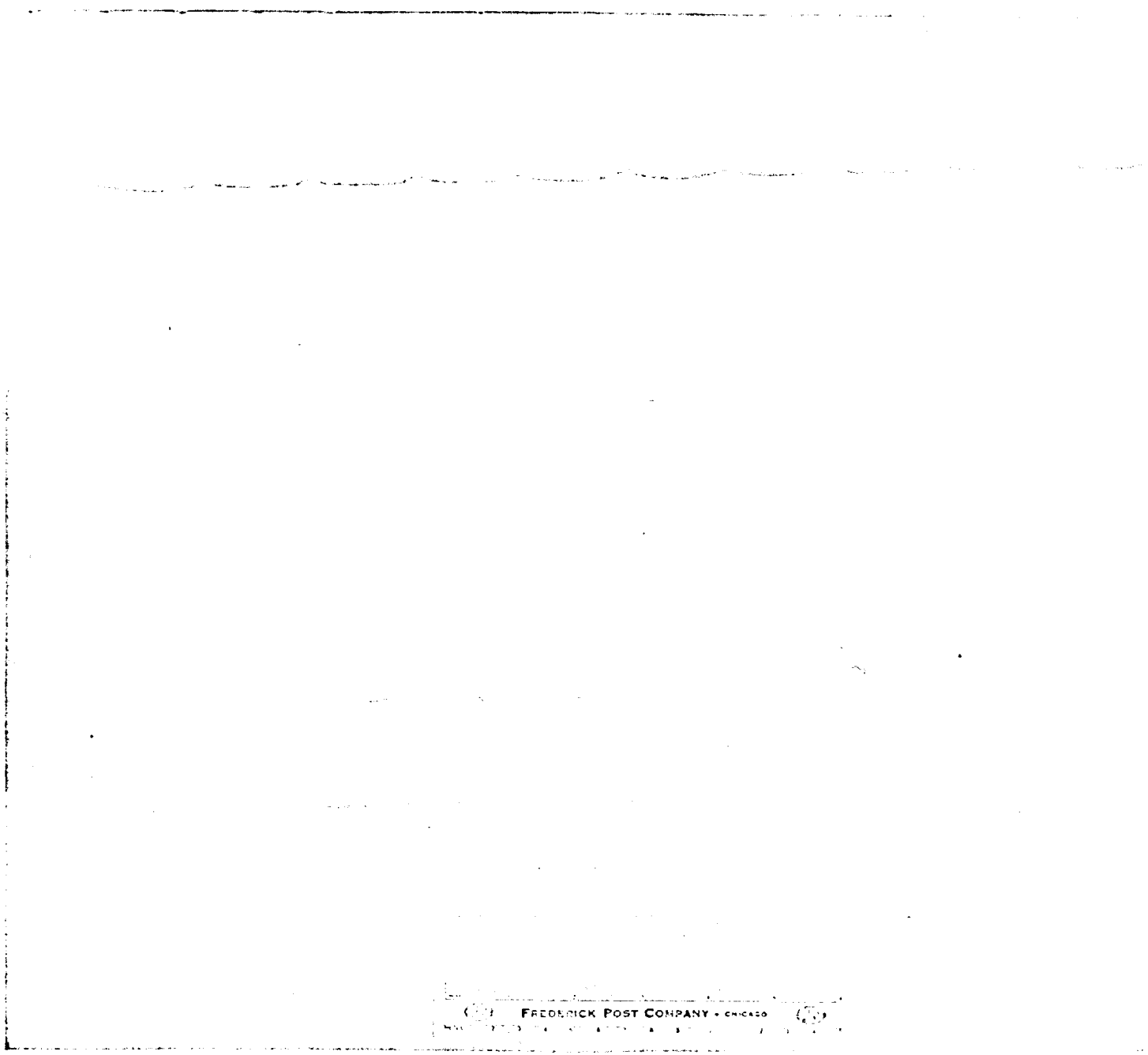

Figure 1. Gypsum Plaster Mold and Transverse Strength Test Sample for the Round Bars.

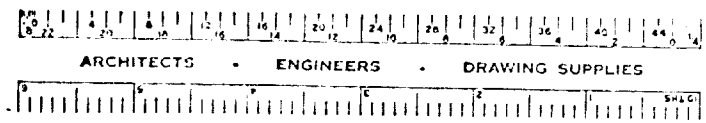

Figure 2. Brass Mold and Transverse Strength Test Sample for the Square Bars.

(3) DTA (Differential Thermal Analysis)

a. Furnace and Associated Equipment[1]

1. Furnace: A muffle furnace, heated by Kanthal resistance wire elements, was used to heat the samples for the differential thermal analysis studies. The platform, which lowered from the bottom of the furnace, held the samples in the heating zone (Figure 3).

2. Control: The furnace temperature and heating-cooling rate were controlled by a proportional-type unit which employed a pneumatic system to control the furnace through a saturable reactor and was capable of maintaining a constant heating rate of ± 1 per cent over a range of 2° to 42° F per minute. In this investigation a rate of furnace temperature rise of 20° F per minute (11.1° C per minute) was maintained throughout.

3. Recorder: The recorder used for obtaining the DTA data reported in this study employed two pens which recorded simultaneously (as a function of time) the temperature of the reference material and the electromotive force produced by the temperature differential between the reference and test samples. By means of a range selector switch, the range of the instrument could be made -5 to +5 mv or -0.5 to +0.5 mv, both with a zero-millivolt center scale position. Chromel-Alumel thermocouples were used to drive this instrument.

b. DTA Molds

Two molds were used to cast five test samples each. The molds were constructed in three parts and held together by bolts. The side walls

[1] J. D. Walton, Jr., "New Method of Preparing Clay Samples for Differential Thermal Analysis," The Journal of the American Ceramic Society 38, No. 12, 440 (December 1955).

were made from 5/8-inch steel, the bottom plates from 1/8-inch steel plate, and the thermocouple pins from 5/32-inch drill rod. The thermocouple pins were sweated into the bottom plates with silver solder. Figure 3 shows the mold and sample used for DTA studies.

(4) Ablation Studies

The standard rocket motor test plates were 7- x 2- x 1/2-inch and were cast in brass or Gypsum plaster molds shown in Figure 4. The test plates were exposed to the exhaust gases at 9-1/2 inches from the exit plane of the oxyhydrogen rocket motor nozzle. The angle of flame impingement was 45°. The indicated water calorimeter heat flux value is 260 $Btu \cdot ft^{-2} \cdot sec^{-1}$.

The backside of the test plates was insulated from the holder with Kaolin wool. A spring-loaded iron-constantan thermocouple was placed against the surface opposite the point of flame impingement for backside temperature measurements. A schematic of the sample holder, the thermocouple location, insulation, and location from the exit plane of the rocket motor is shown in Figure 5. The backside temperatures were recorded automatically with a Wheelco Model 8000 strip chart recorder.

The ablation rate of each sample was determined by measuring the thickness of the sample before testing, subtracting the minimum thickness after testing and dividing by the length of time the rocket motor was fired.

The weight loss rate was determined by weighing the sample before testing, subtracting the weight after testing, and dividing by the length of time the rocket motor was fired.

The oxyhydrogen rocket motor used in these studies was constructed during 1957. This was a combined effort by the Navy Bureau of Ordnance and the Station's Ceramics Branch. The primary purpose of this test facility is to evaluate materials for use in rocket motors, i. e., nozzles and jet vanes.

A water-cooled nozzle as shown in Figure 6 was attached to the rocket motor and the motor was evaluated for possible use as a preliminary test

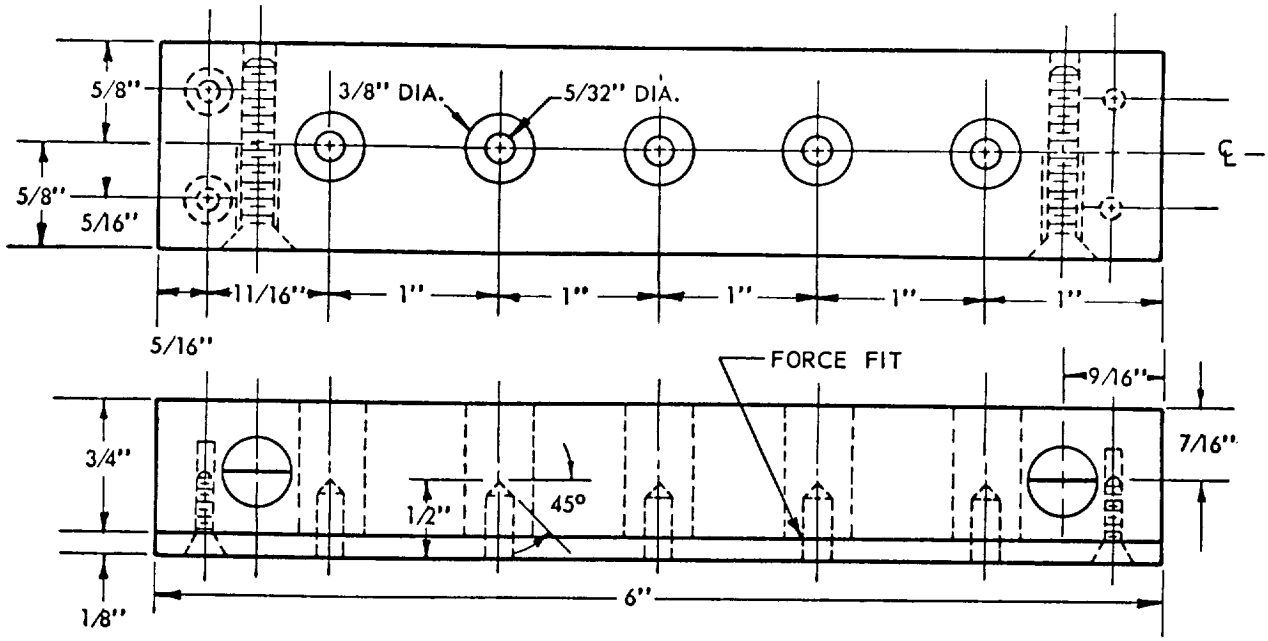

DIAGRAM OF MOLD USED FOR FORMING DTA TEST PELLETS

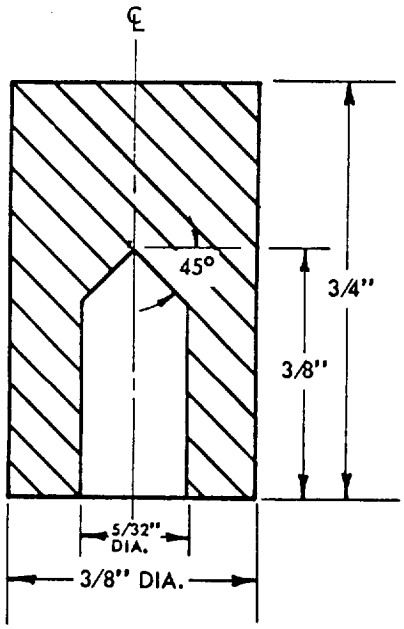

DIAGRAM OF PELLET

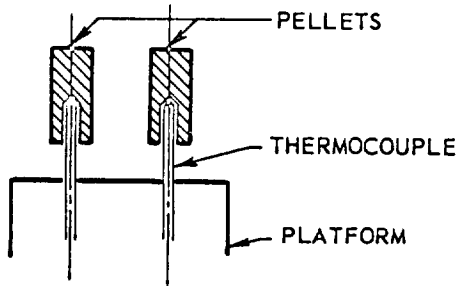

CROSS-SECTIONAL DIAGRAM FOR MOUNTING PELLETS

Figure 3. Diagram of Mold, Test Pellet, and Mounting of Test Pellets for DTA Studies.

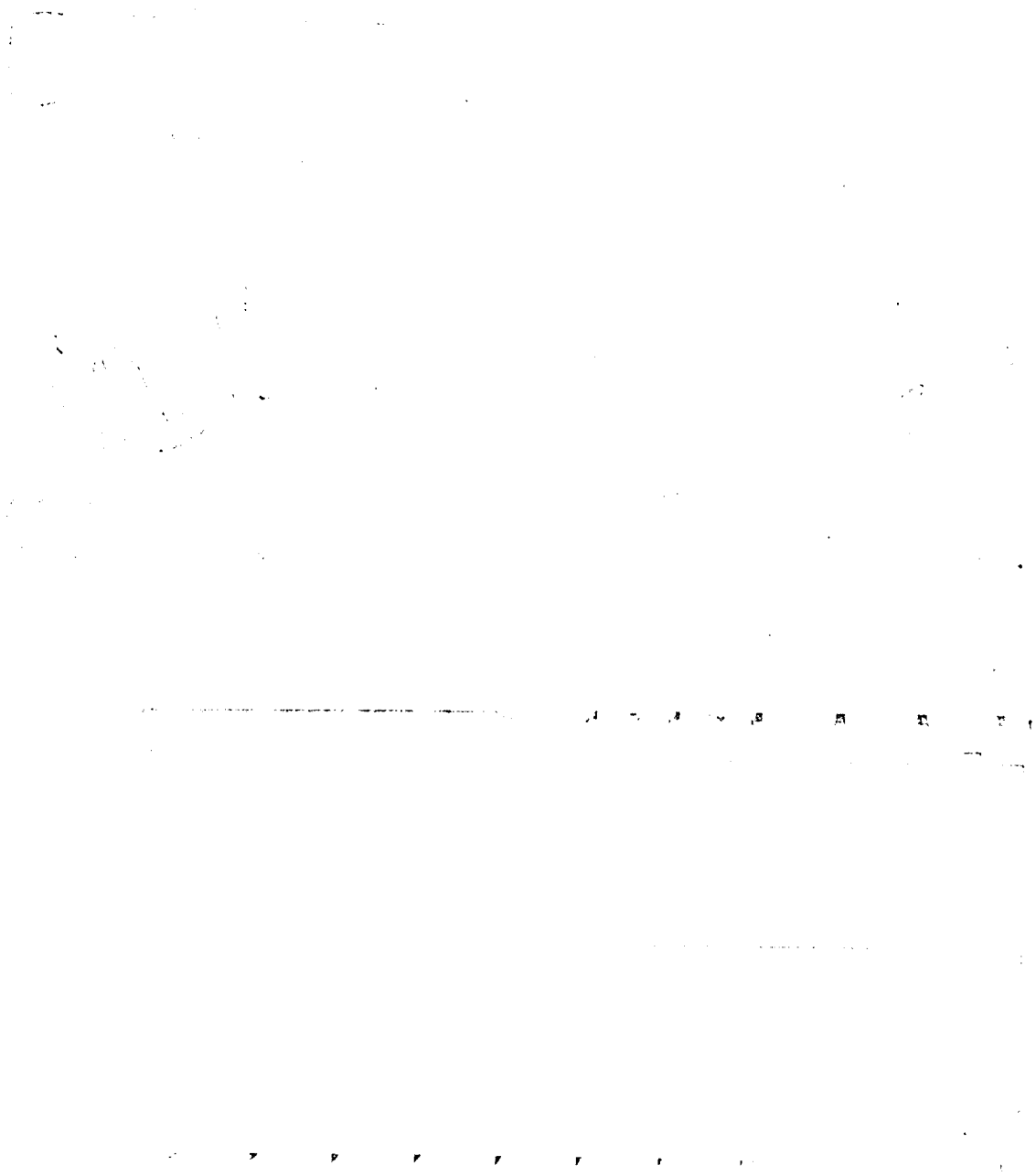

Figure 4. Brass and Plaster Molds Used to Fabricate Rocket Motor Test Samples (2 x 7 x 1/2-inch).

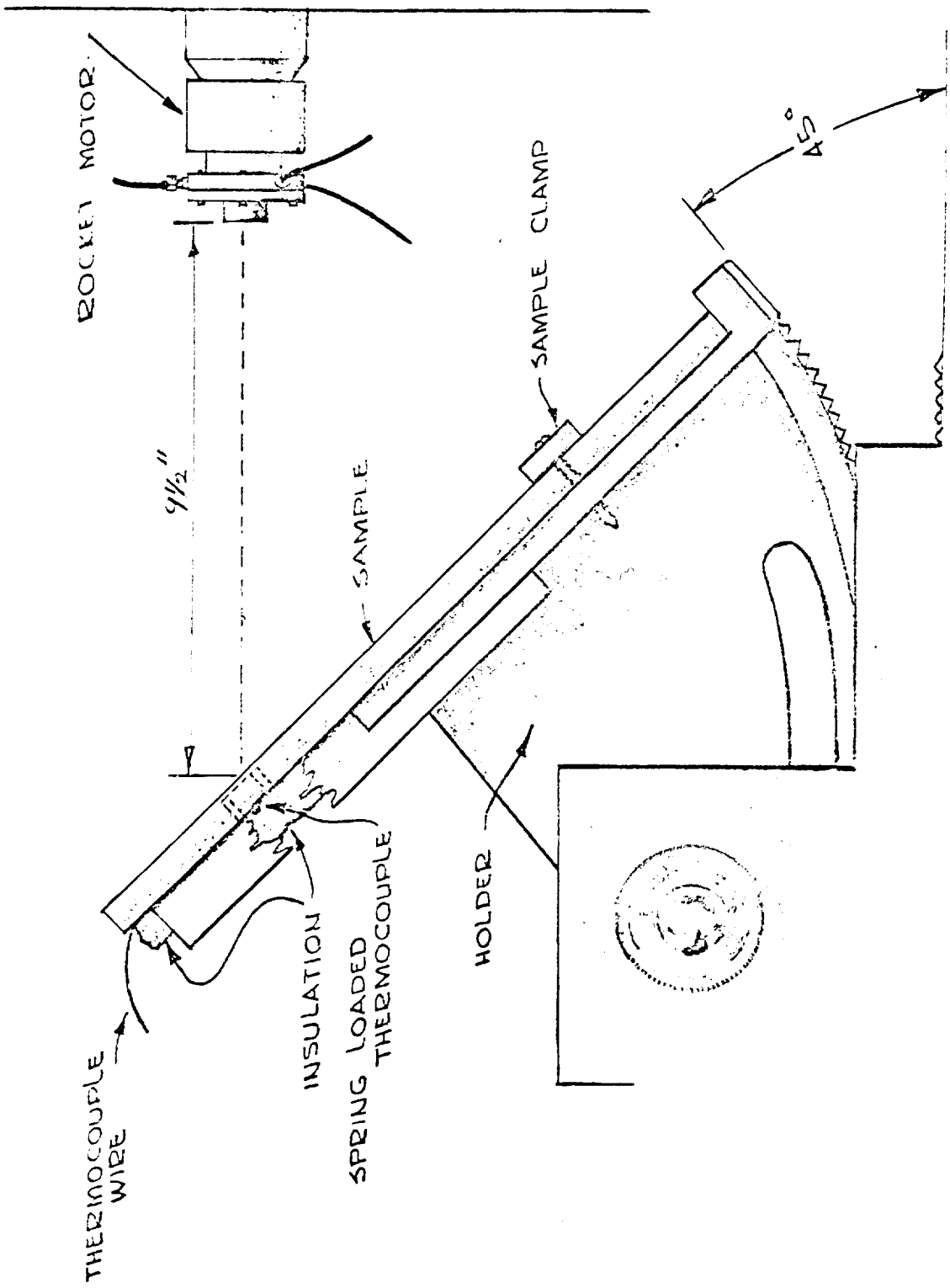

Figure 5. Schematic of Sample Setup for Evaluation in Oxyhydrogen Rocket Motor.

device for screening various compositions to be tested by Redstone Arsenal's 4HT and 164HT burners. Comparison of data obtained for Micarta with Redstone Arsenal's facility and the Station's rocket motor test facility indicated that data obtained from the two facilities could be correlated.

The maximum ablation rate obtained with the Station's facility was approximately one-half the maximum ablation rate obtained by Redstone Arsenal with their 4HT and 164 HT burners. This held true for large time limits, i.e., between 10 and 50 seconds. This ablation rate was determined by the thickness of the test sample and not the mass removed.

The heat flux of the exhaust gases was measured using a modified water calorimeter designed by Battelle Memorial Institute (Figure 7). The heat flux was determined as a function of distance from the exit plane of the rocket motor both at 90° and at 45° to the plane of the exhaust. These results are shown in Figure 8. The stagnation enthalpy and the stagnation temperature provided by the rocket motor exhaust were calculated as a function of the distance from the exit plane. The relationships are shown in Figure 9. Measured stagnation temperatures at distances between 6 and 12 inches are also shown in this figure.

The operating conditions of the oxyhydrogen rocket motor are shown in Table I.

B. Hydrated Cement--Fused Silica Aggregate Mixes

Studies performed under U. S. Army Ordnance Contract No. DA-01-009-ORD-777, of which this reported work is a continuation, indicated the merits of hydrated cement--fused silica mixes as materials for use in ablation and/or transpiration cooling systems. The hydrated cements also offered other advantages such as low cost, fabricability, and adaptability to composite structures such

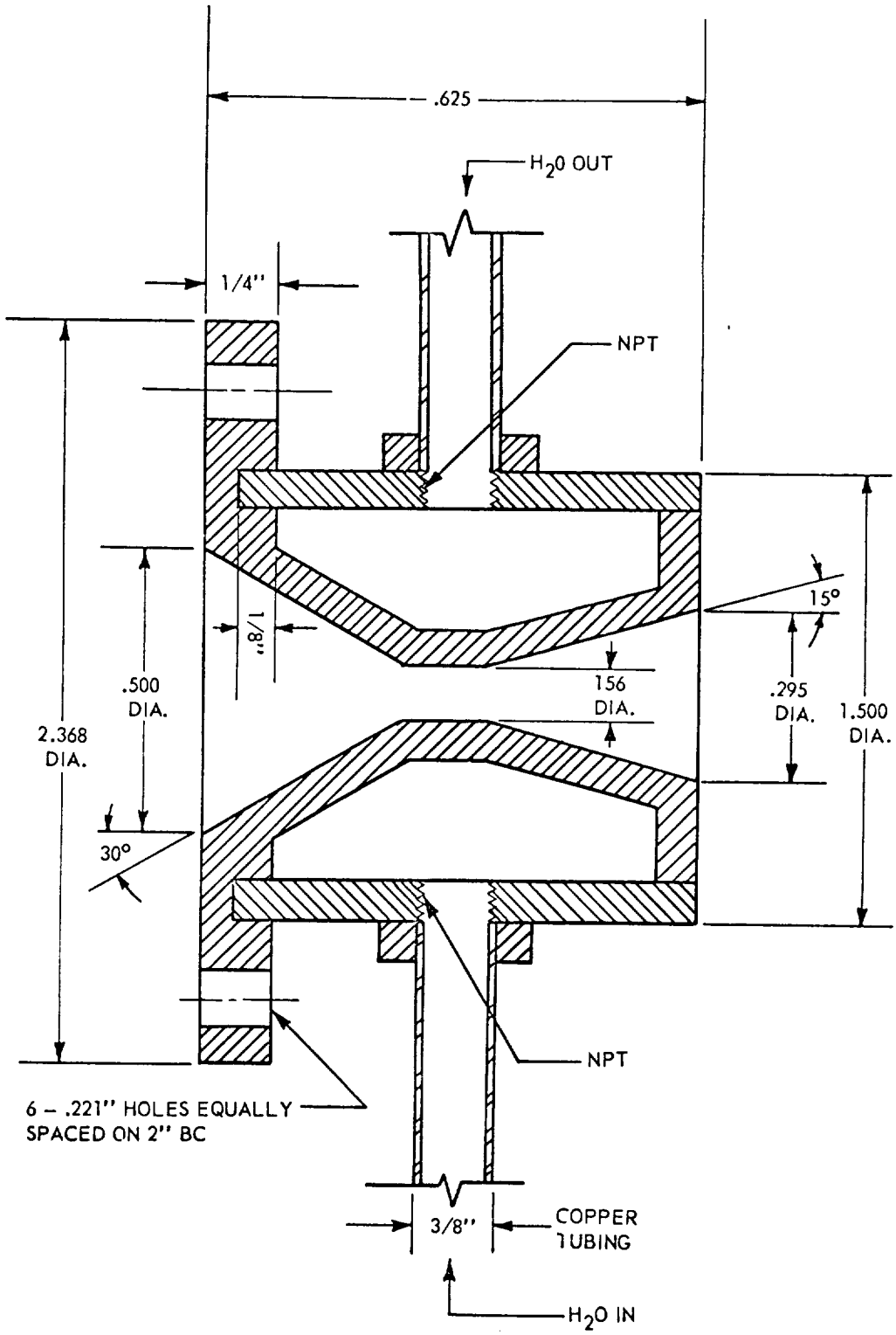

Figure 6. Water-Cooled Copper Nozzle for Use on Small Oxyhydrogen Rocket Motor.

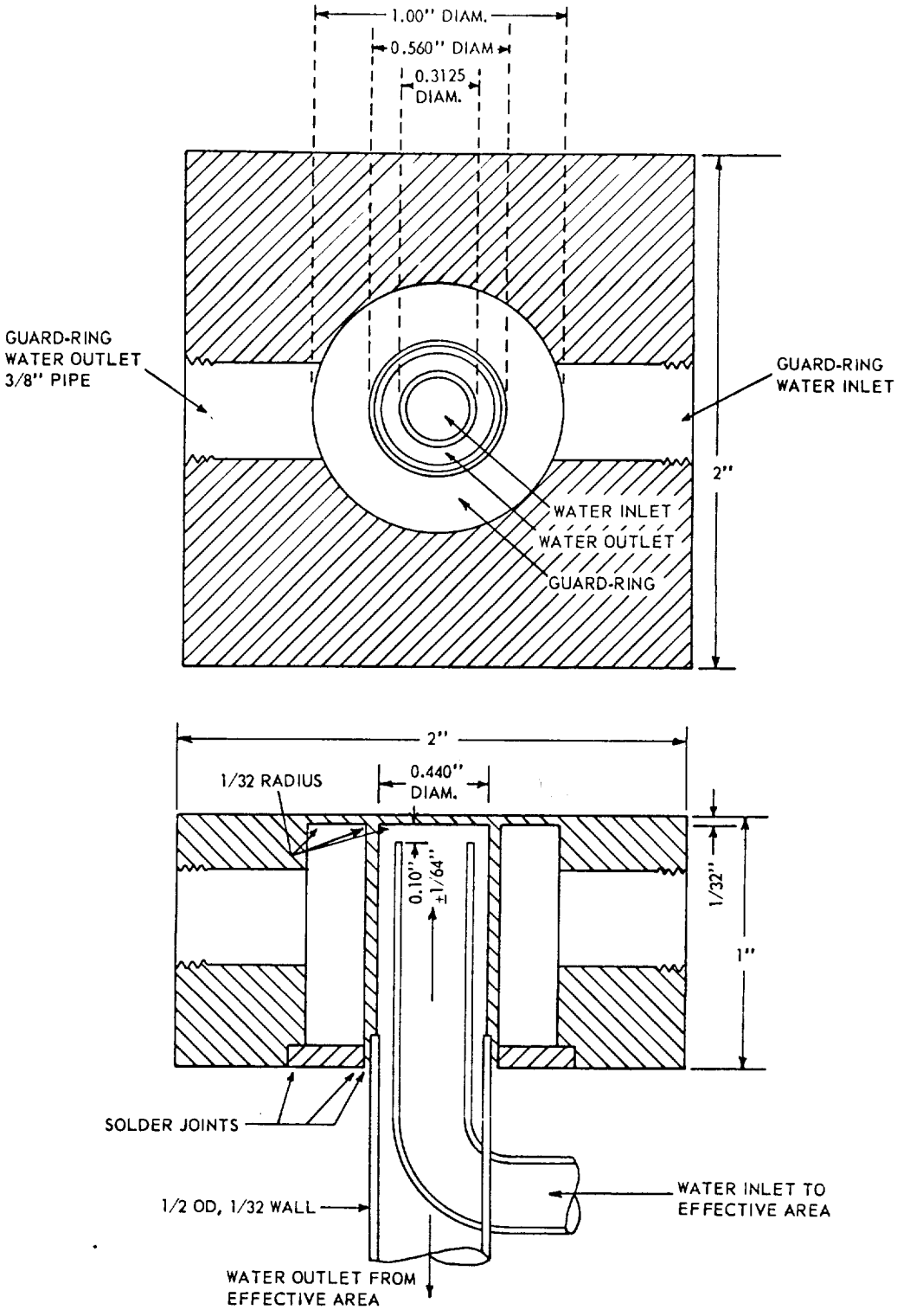

Figure 7. Copper Calorimeter for Heat-Flux Measurements.

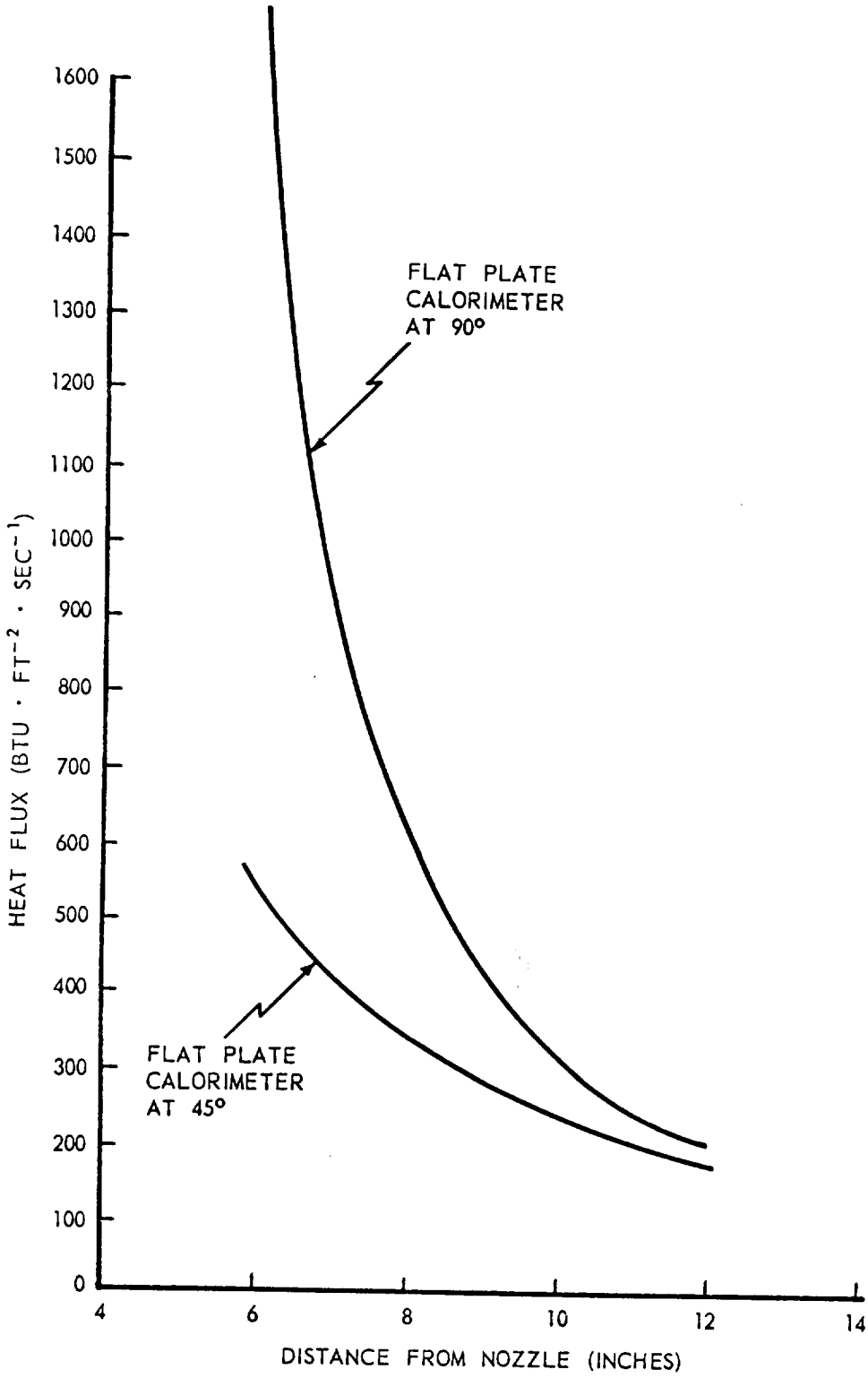

Figure 8. Water Calorimeter Heat-Flux in Rocket Motor Exhaust as Function of Distance from Exit Plane.

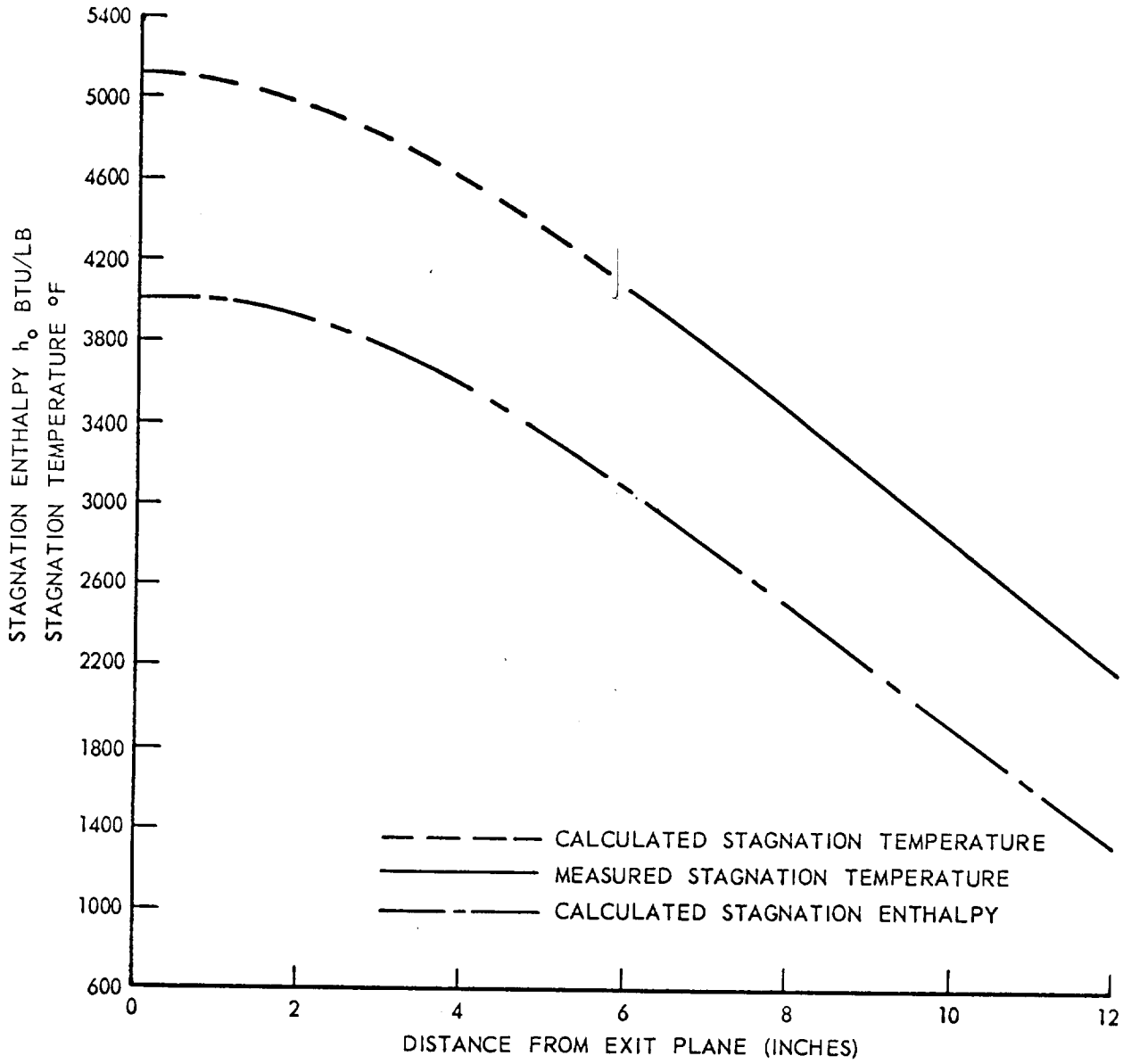

Figure 9. Stagnation Temperature and Stagnation Enthalpy in Rocket Motor Exhaust as a Function of Distance from the Exit Plane.

TABLE I

OPERATING CONDITIONS OF OXYHYDROGEN ROCKET MOTOR

Fuel	Gaseous hydrogen
Oxidizer	Gaseous oxygen
Fuel-Oxidizer Ratio by Volume	4:1
Fuel Flow Rate	36 scf/min
Oxygen Flow Rate	9 scf/min
Upstream Fuel Pressure[+]	860 psi
Upstream Oxygen Pressure[+]	840 psi
Chamber Pressure[++]	275 psi
Starting Chamber Pressure Peak[+++]	400 psi
Estimated Flame Temperature	3800° F
Heat Flux in Nozzle Area[++++] (approx)	1250 $Btu \cdot ft^{-2} \cdot sec^{-1}$
Exhaust Velocity (approx)	7500 fps

[+] Pressure upstream of critical flow orifice.

[++] Continuous chamber pressure using water-cooled nozzle.

[+++] Pressure peaks at 400 psi due to external ignition procedure.

[++++] Measured through a water-cooled copper nozzle.

as open-faced honeycomb. Its adaptability to composite structures enhanced its attractiveness for use under hyperthermal-hypervelocity conditions, i.e., the honeycomb structure would offer the mechanical strength and adaptability to other component parts of the missile while the hydrated cement--fused silica aggregate mixes would act as a filler material and would offer the insulation and cooling of the nose cone through the release of the water of crystallization of the cement and ablation of the composite structure. It has previously been demonstrated that the chemical or combined water of the hydrated material could be utilized for transpiration cooling.

A preliminary investigation was made to determine: (1) the effect of an increase in the water-to-cement ratio from 0.67 to 1.67 on the ablation and physical properties of portland, Lumnite and special Lumnite cement compositions;

(2) the effect of an increase in Aerolith (Vinsol resin) additions from 0.5 oz per 94 lb cement to 4 oz per 94 lb cement on the ablation and physical properties of portland and Lumnite cement compositions; and (3) the effect of a change in aggregate size from -100+200-mesh to -50+100-mesh fused silica on the ablation and physical properties of 30, 40, 60, and 80 per cent Lumnite cement compositions.

It was planned to incorporate the best compositions into honeycomb composite structures and evaluate them in the exhaust gases of the oxyhydrogen rocket motor. A complete analysis was anticipated at this time; however, due to time limitations this was not possible and therefore sample 1246-01-C of Table III was chosen, before the preliminary investigation was completed, to be incorporated into the composite structure. This composite structure is discussed in section D of this chapter.

The test sample for the preliminary investigation of hydrated compositions were prepared by following the standard procedure for preparing and curing of cements outlined in Table II. The samples investigated are shown in Table III. A chemical analysis of the hydrated cements is shown in the Appendix.

Physical properties (bulk density, per cent water absorption, and per cent apparent porosity) were determined for each sample. Test samples 3/4 x 3/4 x 4 inches were used for the determinations. The physical properties are shown in Table IV. The probable transverse strength range of these samples is 400 to 600 psi for the Lumnite and special Lumnite samples while the range for the portland

TABLE II

STANDARD PROCEDURE FOR PREPARING AND CURING CEMENTS

Step Number	
	Preparation of Molds
1	Apply thin coat of vaseline jelly to the brass molds for releasing purposes.
	Preparation of Mixture
2	Add 3 per cent water based on dry weight of aggregate to the fused silica aggregate and roll on a ball mill for a minimum of 16 hours.
3	Mix dry cement and wetted fused silica aggregate in a Hobart N-50 mixer for 5 minutes.
4	Add the required amount of water to the mixture and mix in a Hobart N-50 mixer for an additional 5 minutes.
5	Vibrate resultant slurry into prepared molds. Vibrate for approximately 5 minutes.
	Curing of Test Samples
6	Allow mixture to set in air for 6 to 8 hours.
7	Cover the molds with wetted burlap cloth and place in moisture box for 24 hours.
8	Remove samples from the molds and cover with wetted burlap cloth for 2 days, slowly allowing the cloth to dry.
9	Remove burlap cloth.
	Drying and Firing Procedure
10	Air dry samples for 5 days.
11	Dry and fire at desired temperatures and times.
	Testing of Samples
12	Test samples immediately after step 11.

TABLE III

COMPOSITIONS OF HYDRATED CEMENTS--FUSED SILICA AGGREGATE MIXES

Ga. Tech Sample No.	Lumnite Cement (%)	Portland Cement (%)	Special Lumnite Cement (%)	Fused Silica Aggregate -100+200 (%)	Fused Silica Aggregate -50+100 (%)	Water-Cement Ratio
1246-01-A	30	-	-	70	-	0.67
1246-01-B	30	-	-	70	-	1.00
1246-01-C	30	-	-	70	-	1.33
1246-01-D	30	-	-	70	-	1.67
1248-02-AP	-	30	-	70	-	0.67
1248-02-BP	-	30	-	70	-	1.00
1248-02-CP	-	30	-	70	-	1.33
1248-02-DP	-	30	-	70	-	1.67
1246-04-ASL	-	-	30	70	-	0.67
1246-04-BSL	-	-	30	70	-	1.00
1246-04-CSL	-	-	30	70	-	1.33
1246-04DSL	-	-	30	70	-	1.67
1246-03-1L+	30	-	-	70	-	1.11
1246-03-2L++	30	-	-	70	-	1.11
1246-03-3L+++	30	-	-	70	-	1.11
1246-03-4L++++	30	-	-	70	-	1.11
1248-01-5P+	-	30	-	70	-	0.84
1248-01-6P++	-	30	-	70	-	0.84
1248-01-7P+++	-	30	-	70	-	0.84
1248-01-8P++++	-	30	-	70	-	0.84

(Continued)

TABLE III (Continued)

COMPOSITIONS OF HYDRATED CEMENTS--FUSED SILICA AGGREGATE MIXES

Ga. Tech Sample No.	Lumnite Cement (%)	Portland Cement (%)	Special Lumnite Cement (%)	Fused Silica Aggregate -100+200 (%)	Fused Silica Aggregate -50+100 (%)	Water-Cement Ratio
1248-01-5XP+	-	30	-	70	-	1.11
1248-01-6XP++	-	30	-	70	-	1.11
1248-01-7XP+++	-	30	-	70	-	1.11
1248-01-8XP++++	-	30	-	70	-	1.11
1246-02-01	30	-	-	70	-	1.11
1246-02-02	40	-	-	60	-	0.75
1246-02-03	60	-	-	40	-	0.42
1246-02-04	80	-	-	20	-	0.34
1246-02-05	30	-	-	-	70	1.11
1246-02-06	40	-	-	-	60	0.75
1246-02-07	60	-	-	-	40	0.42
1246-02-08	80	-	-	-	20	0.34

+0.5 oz Aerolith per 94 lb cement.

++1.0 oz Aerolith per 94 lb cement.

+++2.0 oz Aerolith per 94 lb cement.

++++4.0 oz Aerolith per 94 lb cement.

samples is 600 to 800 psi. The probable linear shrinkage at room temperature for the Lumnite and special Lumnite samples is 0.2 to 0.6 per cent and 0.3 to 1.0 per cent for the portland samples while the probable linear shrinkage at 2150° F is 2 to 6 per cent for the Lumnite samples and 2 to 6 per cent for the portland samples. These values are based on previous work.

TABLE IV

PHYSICAL PROPERTIES
OF HYDRATED CEMENTS--FUSED SILICA AGGREGATE MIXES

Ga. Tech Sample No.	Avg. Apparent Porosity (%)	Avg. Water Absorption (%)	Avg. Bulk Density (Gm/CC)
1246-01-A	25.9	16.0	1.64
1246-01-B	21.1	12.4	1.71
1246-01-C	24.1	14.8	1.63
1246-01-D	27.8	16.9	1.59
1248-02-AP	33.5	23.1	1.45
1248-02-BP	19.7	12.0	1.65
1248-02-CP	28.1	18.4	1.53
1248-02-DP	28.2	19.2	1.55
1246-04-ASL	30.6	20.3	1.51
1246-04-BSL	24.7	15.3	1.61
1246-04-CSL	28.5	18.7	1.52
1246-04-DSL	34.6	24.7	1.40
1246-03-1L	32.3	21.8	1.48
1246-03-2L	32.4	32.1	1.47
1246-03-3L	35.0	24.7	1.42
1246-03-4L	37.8	28.2	1.34
1248-01-5P	27.5	17.6	1.56
1248-01-6P	21.3	13.9	1.54
1248-01-7P	19.5	11.7	1.67
1248-01-8P	23.8	16.5	1.44
1248-01-5XP	22.4	13.6	1.65

(Continued)

TABLE IV (Continued)

PHYSICAL PROPERTIES
OF HYDRATED CEMENTS--FUSED SILICA AGGREGATE MIXES

Ga. Tech Sample No.	Avg. Apparent Porosity (%)	Avg. Water Absorption (%)	Avg. Bulk Density (Gm/CC)
1248-01-6XP	28.8	19.3	1.49
1248-01-7XP	34.1	25.9	1.32
1248-01-8XP	40.2	34.5	1.17
1246-02-01	20.8	12.2	1.71
1246-02-02	18.2	10.2	1.77
1246-02-03	11.6	5.9	1.97
1246-02-04	9.3	4.4	2.10
1246-02-05	26.1	19.7	1.52
1246-02-06	23.8	14.1	1.68
1246-02-07	16.5	8.5	1.93
1246-02-08	15.9	7.8	2.06

A DTA was made for each point of study using a calcined Lumnite cement test pellet as the reference for the Lumnite samples and a calcined portland cement test pellet as the reference for the portland samples. The composition of the reference pellets was the same as the samples tested. The variations in the water-cement ratio, Aerolith additions, and change in aggregate particle size were studied to determine their effect on the magnitude of the endothermic peak caused by the release of the water of crystallization. The results of this analysis are shown in Figures 10 through 25, section E of this chapter.

Backside temperature and ablation properties were determined for each point of this study. The ablation properties of the test plates are shown in Table XI while the transpiration cooling data are shown in Table XII, section XII, section F of this chapter. The backside temperature determinations are shown

in Figures 30 through 37, section F of this chapter. Also, the test plates after ablation tests are shown in Figures 41 through 48.

From the results of the water of plasticity study of Lumnite, special Lumnite, and portland cements--fused silica aggregate it was indicated that a correlation could be made between the DTA data (Table IX and Figures 10 through 25) and the ablation data (Tables XI and XII and Figures 30 through 37); that is, the greater the endothermic area of the DTA curves the greater the transpiration cooling period. This correlation was also noted in the change in aggregate particle size and in the Aerolith addition study.

A DTA was made on 100 per cent Lumnite, portland, and Gypsum plaster cements. The results are shown in Table IX and Figures 26 and 27. The Gypsum plaster had the greatest endothermic area of approximately 10 in^2 with portland cement next with 5.5 in^2 and then Lumnite cement with 5.1 in^2. Two endothermic peaks were noted for the Lumnite and portland cement test pellets.

A study was made to determine the effect of replacing part or all of the water used in the cement with Ludox LS (colloidal silica). Rocket motor test plates, transverse strength bars, and DTA test pellets were cast using the composition listed in Table V.

The average transverse strength of the samples was approximately 220 psi, average bulk density was 1.4 gm/cc and average apparent porosity was 34 per cent. The DTA data are shown in Table IX and Figures 28 and 29. The highest endothermic area of 2.66 in^2 was obtained with sample 1246-02-X2A. However, the transpiration cooling effect was less than the Lumnite samples containing only water.

Three rocket motor test plates of sample 1246-01-B were prepared, cured, and fired at 2150° F for 4 hours to remove the majority of the combined or

TABLE V

TEST SAMPLES INVESTIGATED (LUDOX ADDITION)

Ga. Tech Sample No.	Lumnite Cement (%)	Fused Silica Aggregate (-100+200 Mesh) (%)	Water-Cement Ratio	Ludox-Cement Ratio
1246-06-X1	30	70	0.67	0.87
1246-06-X2[+]	30	70	-	1.72
1246-06-X2A[++]	30	70	-	1.72

[+]Composition troweled in mold after gelling.

[++]Composition poured in mold before gelling.

chemical water. The test plates were then placed in a desiccator until exposed to the exhaust gases of the oxyhydrogen rocket motor at a heat flux value of 260 $Btu \cdot ft^{-2} \cdot sec^{-1}$. Figure 30 shows the amount of cooling that was due to the release of the combined water (samples A, B, C, D) and the amount of cooling that is almost entirely due to ablation (sample BF). The weight loss rate was increased from 0.113 to 0.163 $gm \cdot sec^{-1}$ while the ablation rate was increased from 0.0009 to 0.0038 $in \cdot sec^{-1}$ due to the removal of the combined water. The results of this investigation offer evidence to validate the theory that the majority of the cooling is accomplished through the release of the combined water.

C. Reinforced Ceramic Fiber Ceramics

A study was initiated to determine the feasibility of reinforcing (1) 30 per cent Lumnite cement--fused silica aggregate compositions and (2) 8 per cent Pyropreg AC bonding resin--fused silica slip compositions with H. I. Thompson Fiber Glass Company's F100-1/4, F100-1/2, F100-1 fibers and

FL100 flakes, and General Electric Company's pure fused silica fibers. These reinforcing materials were added to the 30 per cent Lumnite cement and the 8 per cent Pyropreg AC resin composition (see Table VI) in increments of 0.25 per cent up to 1.0 per cent.

The compositions are listed in Table VI. This table is for sample number reference purposes.

The fibers and flakes were washed in 5 per cent solution of TSPP and then rinsed in water but not dried. The fibers and flakes were then introduced into the 30 per cent Lumnite cement and the 8 per cent Pyropreg AC bonding resin--slip compositions. The mixtures were then thoroughly mixed using a Hobart Model N-50 mixer. The Lumnite cement mixtures were then poured into brass molds until set and the resin--slip mixtures were poured into plaster molds until cast solid. The Lumnite cement test samples were cured following the standard curing procedure for cements shown in Table II. The Pyropreg AC bonding resin test samples were cured by air drying for 16 hours, drying at 230° F for 8 hours, and curing at 400° F for 16 hours. The physical properties were then determined for each test sample and are shown in Tables VII and VIII.

The strength of the fiber-reinforced 30 per cent Lumnite cement--70 per cent -100+200-mesh fused silica aggregate was increased for each fiber addition with sample 1246-05-F7 exhibiting the highest strength of 660 psi. This value represents a 135.7-per-cent increase in strength from the standard (no fiber addition) composition, strength which is 280 psi. This highest strength was obtained using 0.25 per cent addition of H. I. Thompson Fiber Glass Company's Refraisil F100-1 fiber. The G. E. pure fused silica random length fibers also increased the strength of the Lumnite cement compositions, the highest strength, 430 psi, being exhibited by sample 1246-05-14. This sample

TABLE VI

COMPOSITIONS OF REINFORCED CERAMIC FIBERS CERAMICS

Ga. Tech Sample No.	H. I. Thompson Refrasil Fibers F100-1/4 (%)+++	H. I. Thompson Refrasil Fibers F100-1/2 (%)+++	H. I. Thompson Refrasil Fibers F100-1 (%)+++	H. I. Thompson Refrasil Flakes FL100 (%)+++	G. E. Pure Fused Silica Random Length Fibers (%)+++	30% Lumnite Cement Comp+	8% Pyropreg AC Resin Comp++
1246-05-F1	0.25	-	-	-	-	X	-
1246-05-F2	0.50	-	-	-	-	X	-
1246-05-F3	1.00	-	-	-	-	X	-
1246-05-F4	-	0.25	-	-	-	X	-
1246-05-F5	-	0.50	-	-	-	X	-
1246-05-F6	-	1.00	-	-	-	X	-
1246-05-F7	-	-	0.25	-	-	X	-
1246-05-F8	-	-	0.50	-	-	X	-
1246-05-F9	-	-	1.00	-	-	X	-
1246-05-F10	-	-	-	0.25	-	X	-
1246-05-F11	-	-	-	0.50	-	X	-
1246-05-F12	-	-	-	1.00	-	X	-
1246-05-F13	-	-	-	-	-	X	-
1246-05-F14	-	-	-	-	0.25	X	-
1246-05-F15	-	-	-	-	0.50	X	-
1246-05-F16	-	-	-	-	1.00	X	-
1249-01-R1	0.25	-	-	-	-	-	X
1249-01-R2	0.50	-	-	-	-	-	X

(Continued)

TABLE VI (Continued)

COMPOSITIONS OF REINFORCED CERAMIC FIBERS CERAMICS

Ga. Tech Sample No.	H. I. Thompson Refrasil Fibers F100-1/4 (%)+++	H. I. Thompson Refrasil Fibers F100-1/2 (%)+++	H. I. Thompson Refrasil Fibers F100-1 (%)+++	H. I. Thompson Refrasil Flakes FL100 (%)+++	G. E. Pure Fused Silica Random Length Fibers (%)+++	30% Lumnite Cement Comp+	8% Pyropreg AC Resin Comp++
1249-01-R3	1.00	-	-	-	-	-	X
1249-01-R4	-	0.25	-	-	-	-	X
1249-01-R5	-	0.50	-	-	-	-	X
1249-01-R6	-	1.00	-	-	-	-	X
1249-01-R7	-	-	0.25	-	-	-	X
1249-01-R8	-	-	0.50	-	-	-	X
1249-01-R9	-	-	1.00	-	-	-	X
1249-01-R10	-	-	-	0.25	-	-	X
1249-01-R11	-	-	-	0.50	-	-	X
1249-01-R12	-	-	-	1.00	-	-	X
1249-01-R13	-	-	-	-	-	-	X
1249-01-R14	-	-	-	-	0.25	-	X
1249-01-R15	-	-	-	-	0.50	-	X
1249-01-R16	-	-	-	-	1.00	-	X

+Composed of 30 per cent Lumnite cement--70 per cent -100+200 mesh fused silica aggregate, water-cement ratio 1.33.

++Composed of 8 per cent Pyropreg AC bonding resin added to fused silica slip with 1.5 ml concentrated hydrochloric acid per 300 gm fused silica slip.

+++Per cent addition based on dry weight of Lumnite cement and fused silica aggregate or on weight of fused silica slip used to prepare 8 per cent Pyropreg AC bonding resin composition.

TABLE VII

PHYSICAL PROPERTIES
OF REINFORCED 30 PER CENT LUMNITE CEMENT COMPOSITIONS
WITH FIBERGLAS FIBERS AND FLAKES

Ga. Tech Sample No.	Avg. Apparent Porosity (%)	Avg. Water Absorption (%)	Avg. Bulk Density (Gm/CC)	Avg. Transverse Strength (PSI)	Per Cent Increase or Decrease from Standard (%)
1246-05-F1	34.8	23.7	1.47	380	+35.7
1246-05-F2	36.4	25.5	1.43	320	+14.3
1246-05-F3	36.4	25.6	1.42	290	+3.6
1246-05-F4	29.6	19.1	1.55	450	+60.7
1246-05-F5	34.4	23.5	1.47	390	+39.3
1246-05-F6	32.2	21.6	1.49	580	+107.1
1246-05-F7	30.8	20.2	1.52	660	135.7
1246-05-F8	29.0	18.6	1.56	630	+125.0
1246-05-F9	37.4	26.7	1.40	420	+50.0
1246-05-F10	33.9	22.8	1.49	500	+78.6
1246-05-F11	31.7	20.8	1.52	630	+125.0
1246-05-F12	29.9	19.3	1.55	530	+89.3
1246-05-F13*	39.8	29.7	1.34	280	--
1246-05-F14	31.7	20.1	1.51	430	+53.6
1246-05-F15	35.1	24.3	1.44	340	+21.4
1246-05-F16	35.7	24.1	1.45	400	+42.9

*Sample 1246-05-F13 contained no fiber or flake additions and is used as a standard.

TABLE VIII

PHYSICAL PROPERTIES
OF REINFORCED 8 PER CENT PYROPREG AC BONDING RESIN--
FUSED SILICA SLIP COMPOSITIONS WITH FIBERGLAS FIBERS AND FLAKES

Ga. Tech Sample No.	Avg. Apparent Porosity (%)	Avg. Water Absorption (%)	Avg. Bulk Density (Gm/CC)	Avg. Transverse Strength (PSI)	Per Cent Increase or Decrease from Standard (%)
1249-01-R1	18.6	11.4	1.63	4840	-18.0
1249-01-R2	16.0	9.7	1.64	4080	-30.8
1249-01-R3	21.8	13.7	1.59	2910	-50.7
1249-01-R4	14.0	8.8	1.70	4480	-24.1
1249-01-R5	13.0	7.6	1.72	2570	-56.4
1249-01-R6	24.5	15.3	1.60	5930	+ 0.5
1249-01-R7	19.6	11.7	1.68	5270	-10.7
1249-01-R8	18.9	11.2	1.70	4840	-18.0
1249-01-R9	21.6	13.7	1.58	4260	-27.8
1249-01-R10	14.1	8.4	1.66	6000	+ 1.7
1249-01-R11	18.6	11.3	1.65	6100	+ 3.4
1249-01-R12	14.4	8.5	1.70	6030	- 2.2
1249-01-R13*	10.6	6.3	1.65	5900	-
1249-01-R14	14.7	9.0	1.66	5430	- 8.0
1249-01-R15	18.8	11.0	1.71	6350	+ 7.6
1249-01-R16	17.3	10.4	1.66	5920	+ 0.3

*Sample 1249-01-R13 contained no fiber or flake additions and is used as a standard.

contained 0.25 per cent addition and its strength represents an increase of 53.6 per cent from standard.

The strength of the fiber-reinforced 8 per cent Pyropreg AC bonding resin--fused silica slip was not improved as significantly as the fiber-reinforced Lumnite cement compositions. The highest strength was exhibited by sample 1249-01-R15. (See Table VIII.) This sample contained 0.50 per cent G. E. pure fused silica fibers. Its strength was 6350 psi, which is a 7.6 per cent increase of strength from standard (5900 psi). The Refrasil fibers and flakes did not fare as well as the G. E. pure fused silica fibers. The highest strength obtained using Refrasil was for the 0.50-per-cent-Refrasil F100-1-fiber addition. This strength was 6100 psi, which is a 3.4 per cent increase from standard (5900 psi) and is sample 1249-01-R11. The fiber or flake reinforcement of the Pyropreg AC bonding resin compositions was generally poor. The strengths of these compositions were in general decreased rather than increased as was the case for the Lumnite compositions.

D. Composite Structures

Studies performed under U. S. Army Ordnance Contract No. DA-01-009-ORD-777, of which this reported work is a continuation, indicated the feasibility of directing the transpiration cooling effect of the combined water or water of crystallization of hydrated materials such as Lumnite cements, portland cements, clays, plasters, etc., in such a manner as to improve the backside temperatures and ablative properties of such materials. The directing of the transpiration cooling effect was accomplished through the use of honeycomb structures which acted as the mechanical strength reinforcement agent of the system. The honeycomb structure should lend itself to

ease in adapting the launch vehicle to other component parts of the missile. The hydrated filler material furnished the transpiration cooling agent of the composite structure system.

It is thought that the channels of the honeycomb structure directed the combined water, after its release by the application of extreme temperatures to the surface of the composite structure, through the system to the back plate and then redirected it back through the sample, thus establishing a cooling cycle.

The 30 per cent Lumnite cement--70 per cent -100+200 mesh-fused silica aggregate, 1.33 water-cement ratio-composition used for the composite structure studies was selected from the preliminary water-cement ratio studies. This composition was selected before all of the work on the water-cement ratio studies was completed because of the limited time of the present contract. It was the best composition studied to date.

The composite substructure was formed from type Ph-15-7M0 stainless steel 1- x 2- x 7-inch honeycomb panels obtained from Lockheed Aircraft Corporation, Marietta, Georgia. The 1- x 2- x 7-inch panels were cut in half, forming 1/2- x 2- x 7-inch open-faced honeycomb panels. The core area of these panels was 0.0625 square inch and the web thickness was 0.002 inch.

The selected Lumnite compositions were vibrated into the cells of the open-faced honeycomb test panels until the cells were filled. The surface was troweled smooth and the resulting composite was then cured, following the standard procedure outlined in Table II. The cured composites were exposed to the exhaust gases of the oxyhydrogen rocket motor at a heat flux value of 260 $Btu \cdot ft^{-2} \cdot sec^{-1}$. The results of this exposure are listed in Tables XI and XII, and shown in Figures 39 and 50.

For the purpose of determining any heat sink effect of the backplate of the test panel, a 1/2-inch-diameter x 1/8-inch-width groove was cut in the backplate of two test panels and centered directly behind the planned point of flame impingement. The spring-loaded backside-temperature-sensing thermocouple was centered on the resulting disk of the grooved backplate during the exposure of the test panel to the exhaust gases of the oxyhydrogen rocket motor.

Figure 39 is a comparison of the change in backside temperature of the composites having a 1/2-inch-diameter groove cut in the backplates, sample 1249-02-0, with similar composites without the grooved ring, sample 1249-02-R. The heat sink effect of the backplate is graphically shown by the lower change in backside temperature for the same time and by the masking or hiding of the flat portion of curve '0', Figure 39, of the transpiration cooling effect of the Lumnite cement filler material.

A composite that is formed by applying a thick ceramic coating to a metal substrate was studied. Sandblasted 2- x 7- x 1/8-inch mild steel plates were coated with a film of Nalcoag (colloidal silica). The aggregate compositions A and B listed below were troweled onto the surface of the substrates until a 1/2-inch-thick test plate was formed. The test plates were then dried in a 160° F dryer for approximately 16 hours, and then exposed to the exhaust gases of the oxyhydrogen rocket motor at a heat flux value of 260 $Btu \cdot ft^{-2} \cdot sec^{-1}$.

Composition B

100 parts by weight fused silica slip
100 parts by weight -20+50-mesh fused silica aggregate
0.50 part by weight water
0.50 part by weight Nalcoag

Composition D

100 parts by weight fused silica slip
75 parts by weight -50+100-mesh fused silica aggregate
0.67 part by weight water
0.67 part by weight Nalcoag

The backside-temperature-vs-time curve is shown in Figure 40 and the test plates are shown in Figure 51 after the ablation test. There was negligible ablation at this heat flux value. The substrate for composition D separated after the rocket motor was cut off.

These results indicate that there is a possibility of easily coating a metal nose cone with a ceramic material for thermal protection (in this case fused silica), and still retaining the desired properties of both the metal and ceramic.

E. Differential Thermal Analysis (DTA)

A DTA study was made to determine the temperature range in which the combined water of Lumnite and portland cements and Gypsum plaster is released.

Test pellets described in Section A were made from various combinations of Lumnite and portland cements--fused silica aggregate and Gypsum plaster. The water of plasticity (water-cement ratio) was varied so as to determine its effect on the magnitude of the endothermic peak (negative millivolts) caused by the release of the water of crystallization. The effect of the fused silica aggregate size from -100+200 mesh to -50+100 mesh and Aerolith additions from 0.5 oz Aerolith per 94 lb of cement to 4 oz Aerolith per 94 lb of cement on the magnitude of the endothermic peak was investigated. Table IX lists the DTA data obtained and Figures 10 through 29 the plots of the DTA data.

TABLE IX

DIFFERENTIAL THERMAL ANALYSIS DATA

Ga. Tech Sample No.	Endothermic Peak (°C)	Endothermic Area (In^2)	Water Release Temperature Range (°C)	Exothermic Peak (°C)	Exothermic Area (In^2)
1246-01-A	175	1.80	25-290	315	0.40
1246-01-B	140	1.28	25-250	265	1.29
1246-01-C	150	1.62	30-270	310	1.28
1246-01-D	105	1.60	25-225	290	1.29
1248-02-AP	155	0.81	45-220	325	1.96
1248-02-BP	155	1.29	40-255	325	1.87
1248-02-CP	170	0.40	45-205	320	3.01
1248-02-DP	145	1.12	25-245	320	0.70
1246-04-ASL	200,300	2.29	25-310	350	3.09
1246-04-BSL	135,285	1.37	40-303	350	3.16
1246-04-CSL	155,275	2.58	30-298	330	2.96
1246-04-DSL	175,290	3.26	40-305	350	2.22
1246-03-1L	150	1.79	25-250	315	3.00
1246-03-2L	125	0.66	60-235	320	2.41
1246-03-3L	165	0.83	45-230	340	2.84
1246-03-4L	175	1.57	55-258	320	3.82
1248-01-5P	150	1.18	30-230	330	3.03
1248-01-6P	165	0.84	35-225	320	2.96
1248-01-7P	150	0.87	25-230	335	1.64
1248-01-8P	140	0.72	25-220	330	1.63
1248-01-5XP	125	1.25	40-240	300	0.55
1248-01-6XP	85	0.94	25-205	300	1.65
1248-01-7XP	125	0.97	25-200	300	1.78
1248-01-8XP	150	0.87	30-230	310	1.30
1246-02-01	175	1.10	40-225	320	2.10
1246-02-02	165	3.15	15-257	310	2.25
1246-02-03	150,275	3.60	10-305	355	1.45

(Continued)

TABLE IX (Continued)

DIFFERENTIAL THERMAL ANALYSIS DATA

Ga. Tech Sample No.	Endothermic Peak (°C)	Endothermic Area (In^2)	Water Release Temperature Range (°C)	Exothermic Peak (°C)	Exothermic Area (In^2)
1246-02-04	150,285	4.04	30-320	360	1.55
1246-02-05	140	1.86	35-280	310	0.67
1246-02-06	165	2.70	15-285	310	1.00
1246-02-07	160,305	4.32	10-355	380	0.47
1246-02-08	155,285	4.50	15-305	375	1.39
1246-00-01+	190,330	5.14	30-375	415	0.98
1248-00-01++	220,560	6.69	40-345,395-650	360	0.23
1249-00-01+++	230	10.37	40-960	-	-
1246-06-X1	170	2.24	25-270	310	0.75
1246-06-X2	180	2.34	35-260	310	1.11
1246-02X2A	170	2.66	25-280	320	0.73

+100 per cent Lumnite cement (water-cement ratio 0.28).

++100 per cent portland cement (water-cement ratio 0.34).

+++100 per cent Gypsum plaster (water-cement ratio 1.50).

For a detailed description of the method used to obtain the DTA data see section A. A discussion of the results for each test sample can be found in their respective sections.

F. Ablation Studies

This section contains the backside temperature determinations and ablation properties of all the material systems evaluated. A detailed discussion is given for each material system in its respective subsection.

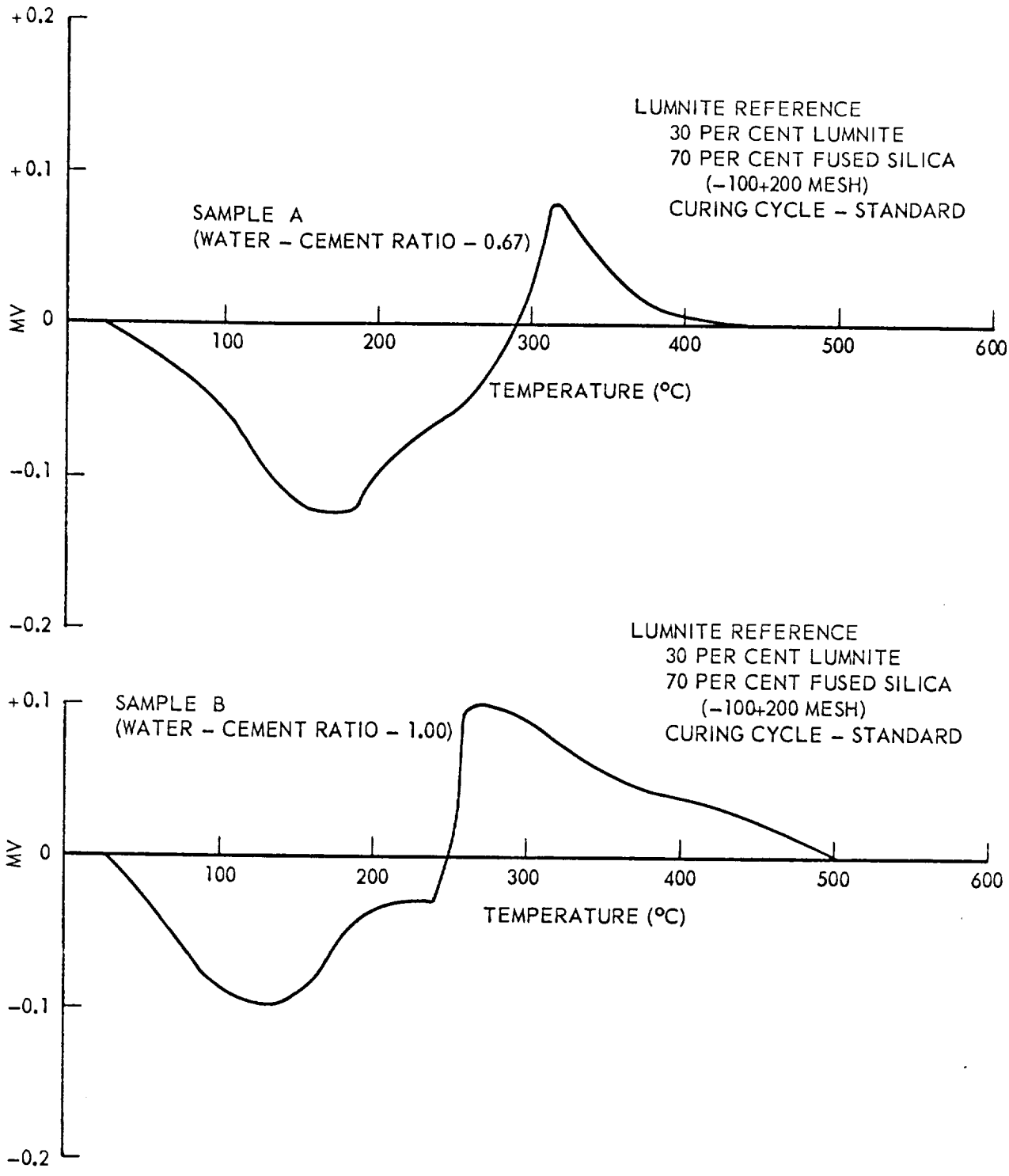

Figure 10. Differential Thermal Analysis Samples 1246-01-A, B.

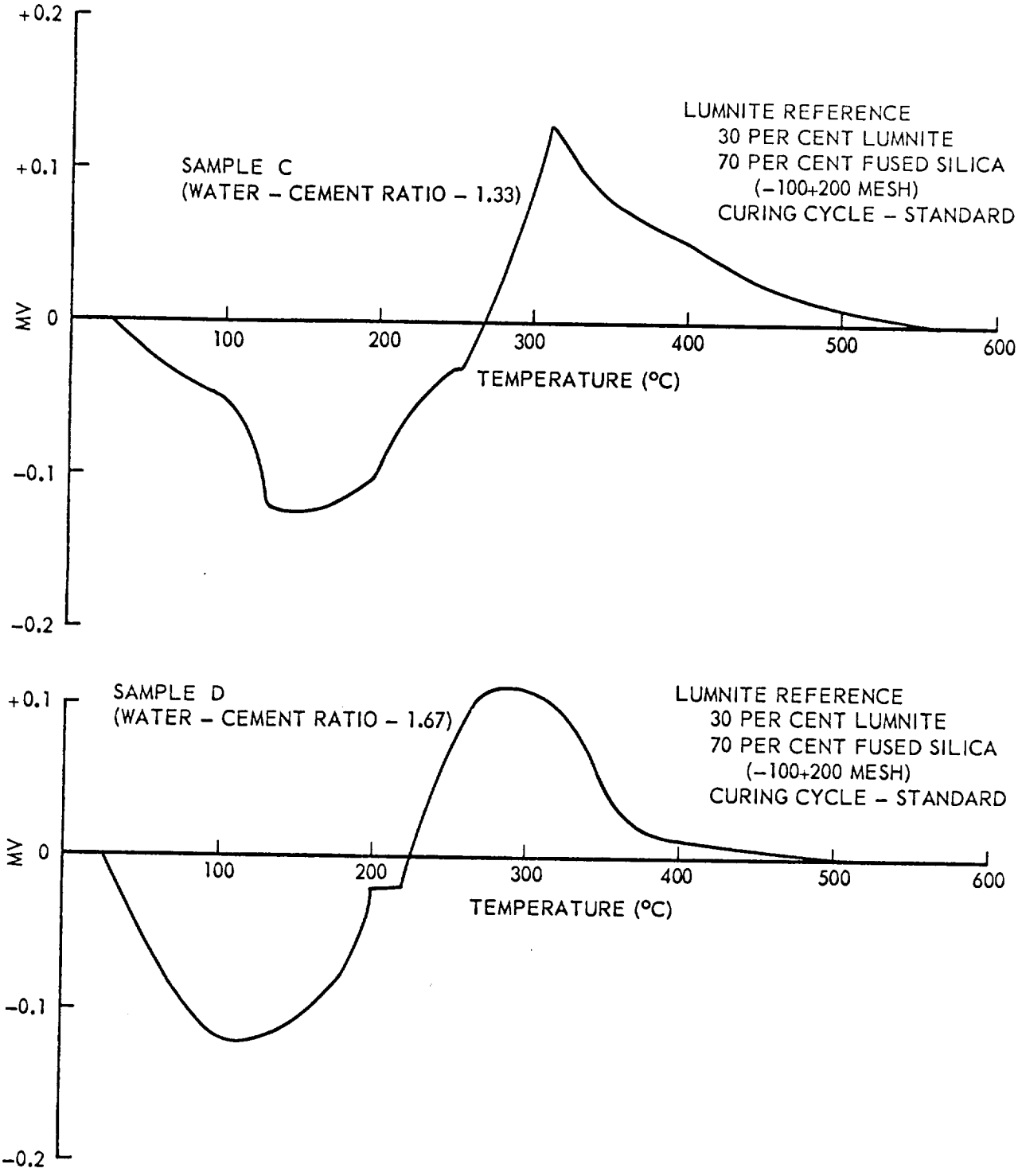

Figure 11. Differential Thermal Analysis Samples 1246-01-C, D.

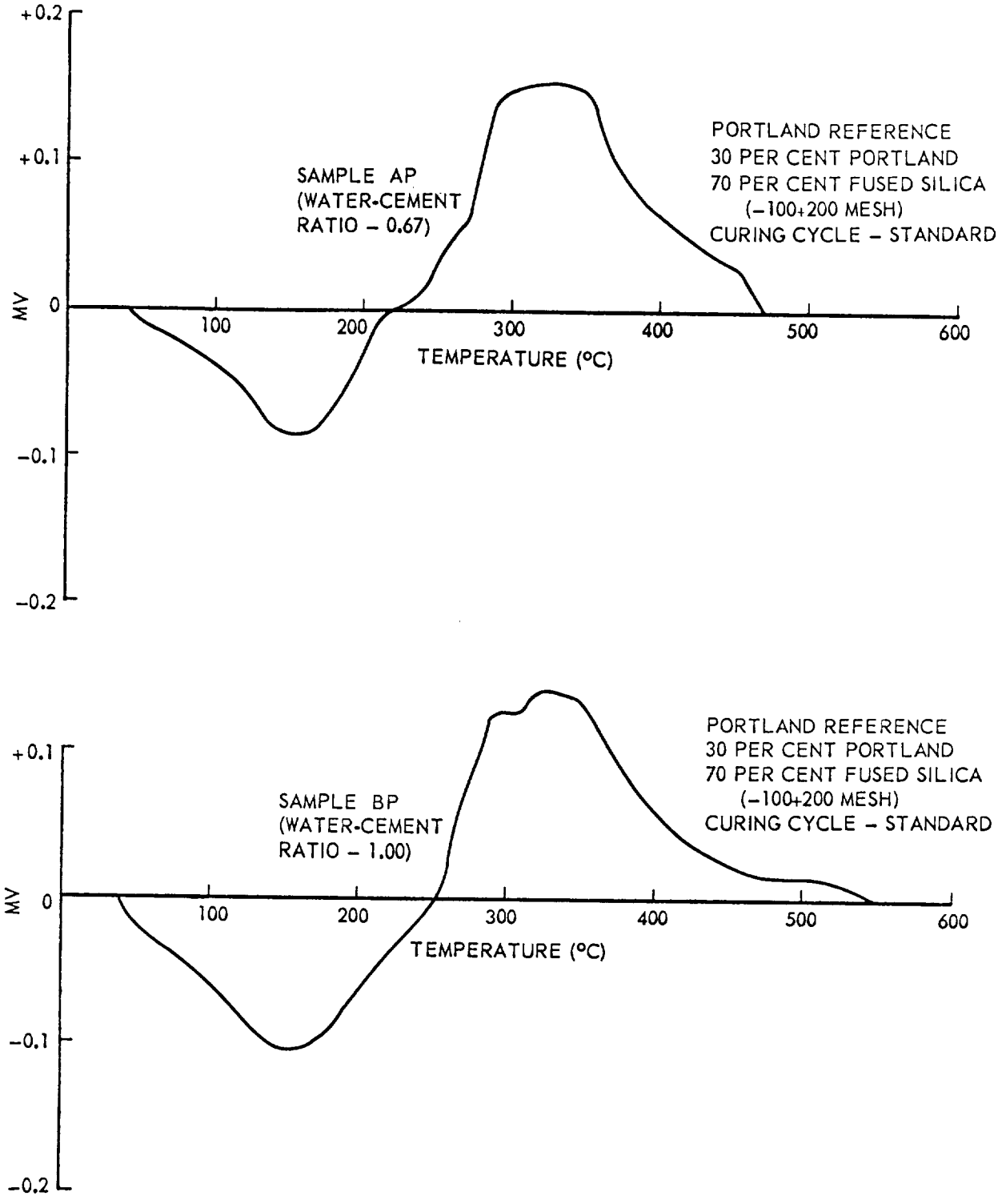

Figure 12. Differential Thermal Analysis Samples 1248-02-AP,BP.

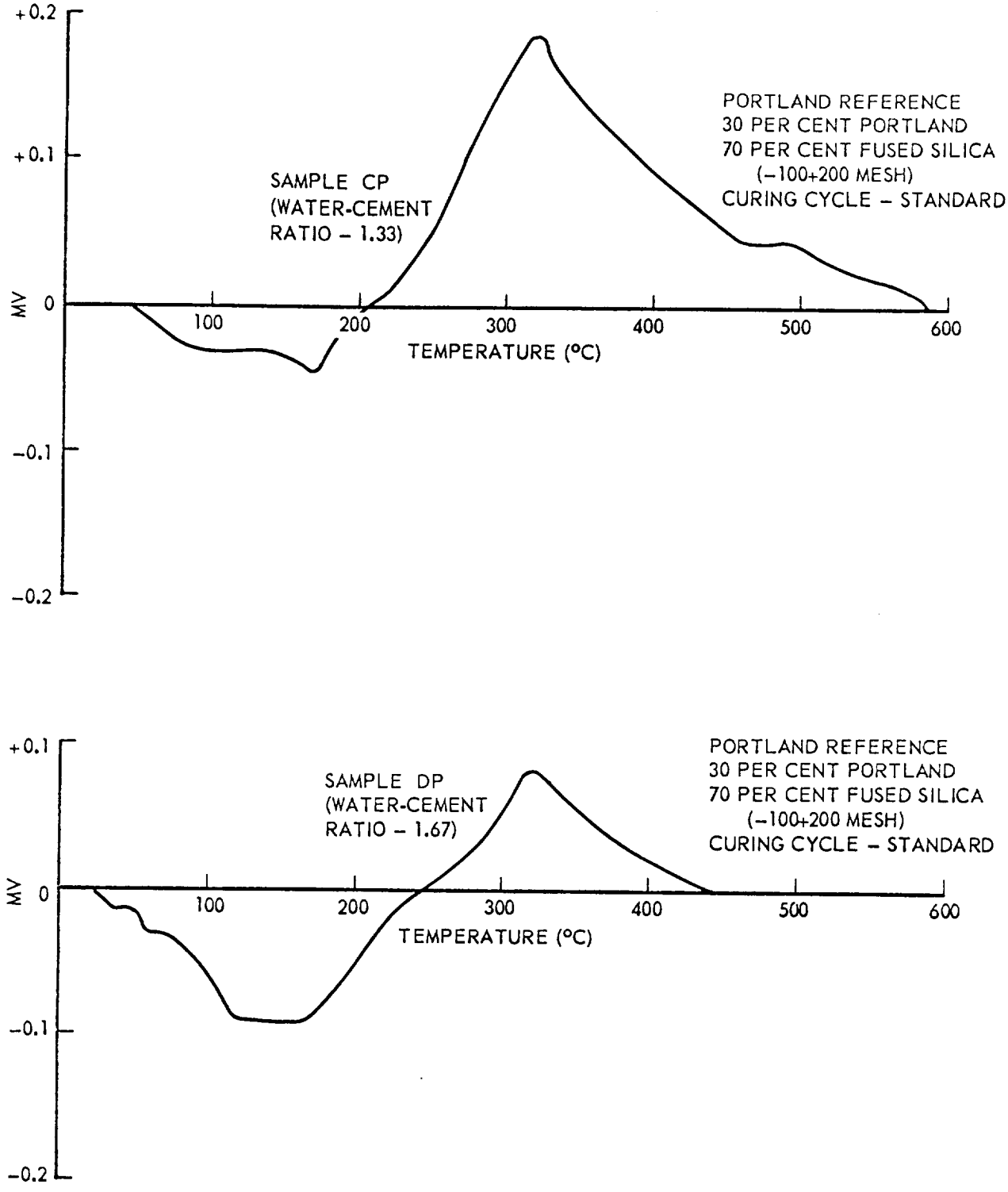

Figure 13. Differential Thermal Analysis Samples 1248-02-CP, DP.

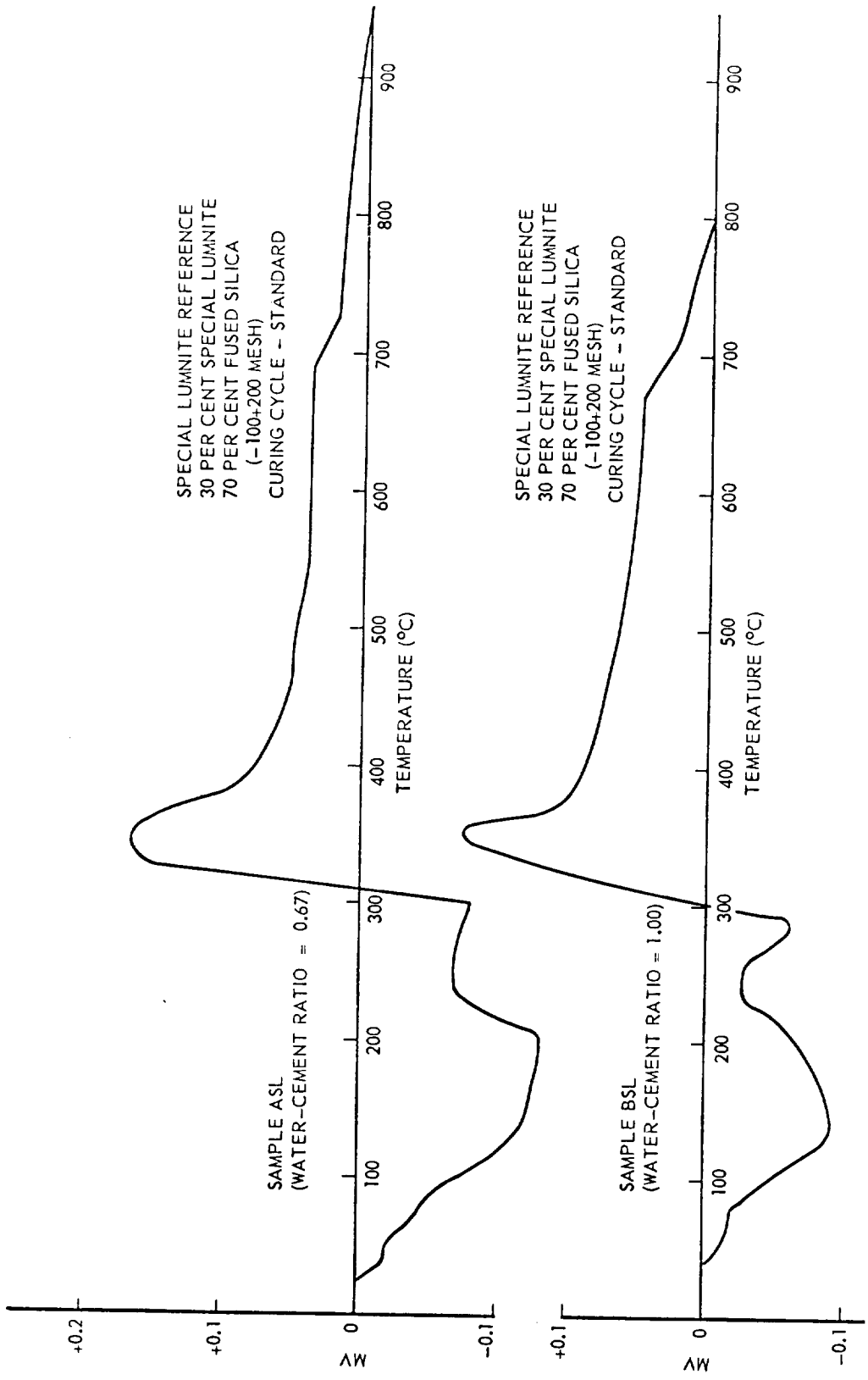

Figure 14. Differential Thermal Analysis Samples 1246-04-ASL, ESL.

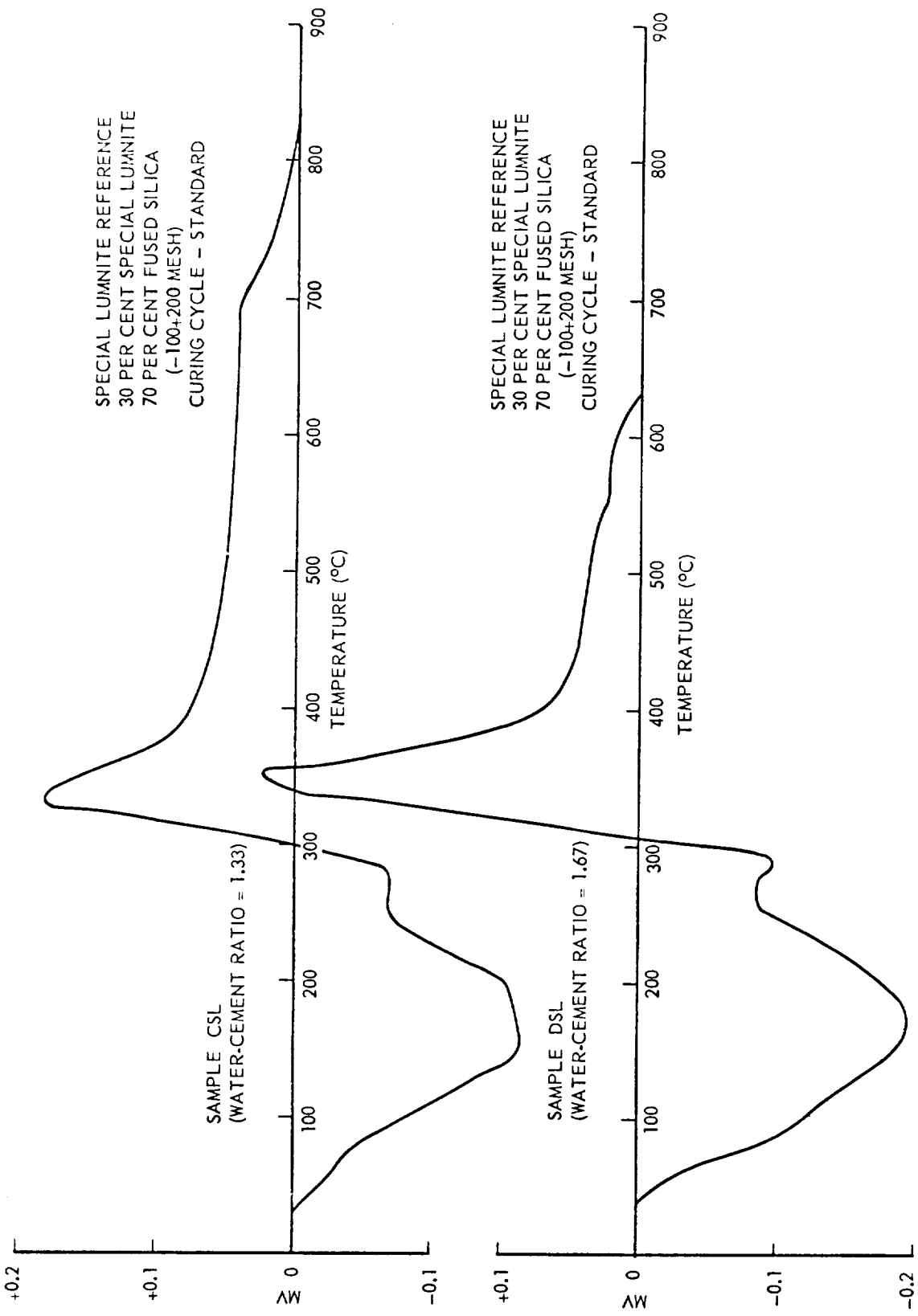

Figure 15. Differential Thermal Analysis Samples 1246-04-CSL, DSL.

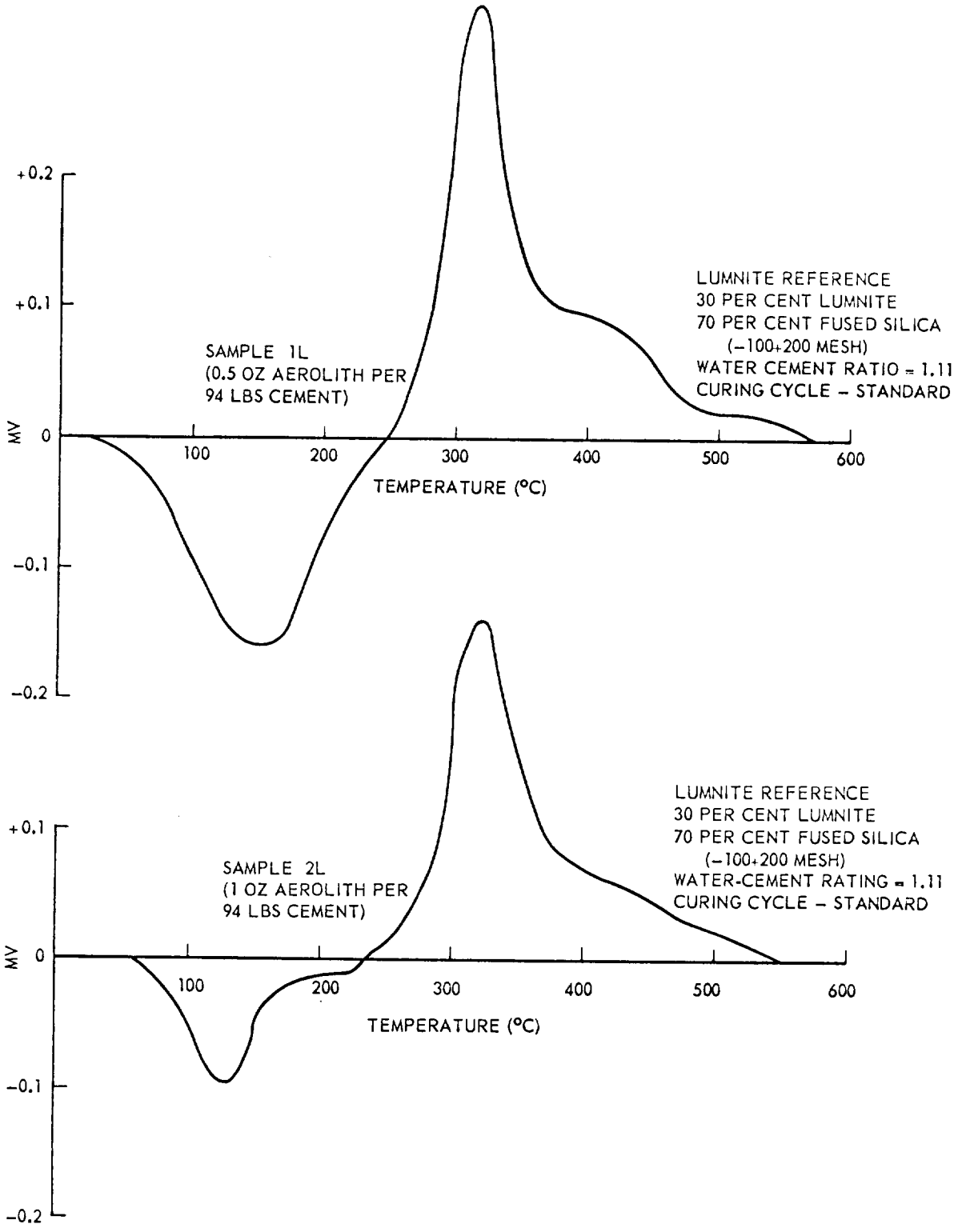

Figure 16. Differential Thermal Analysis Samples 1246-03-1L, 2L.

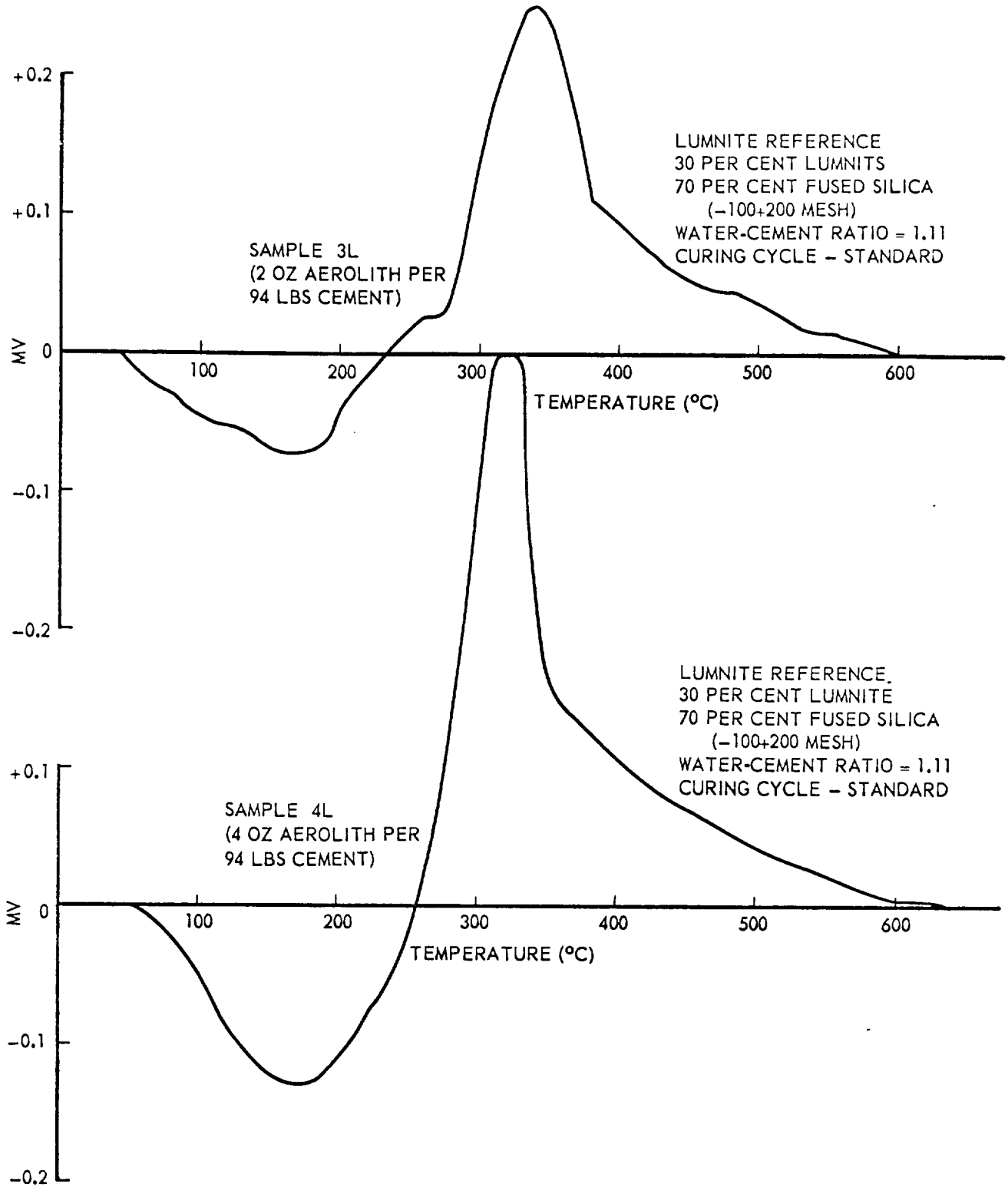

Figure 17. Differential Thermal Analysis Samples 1246-03-3L, 4L.

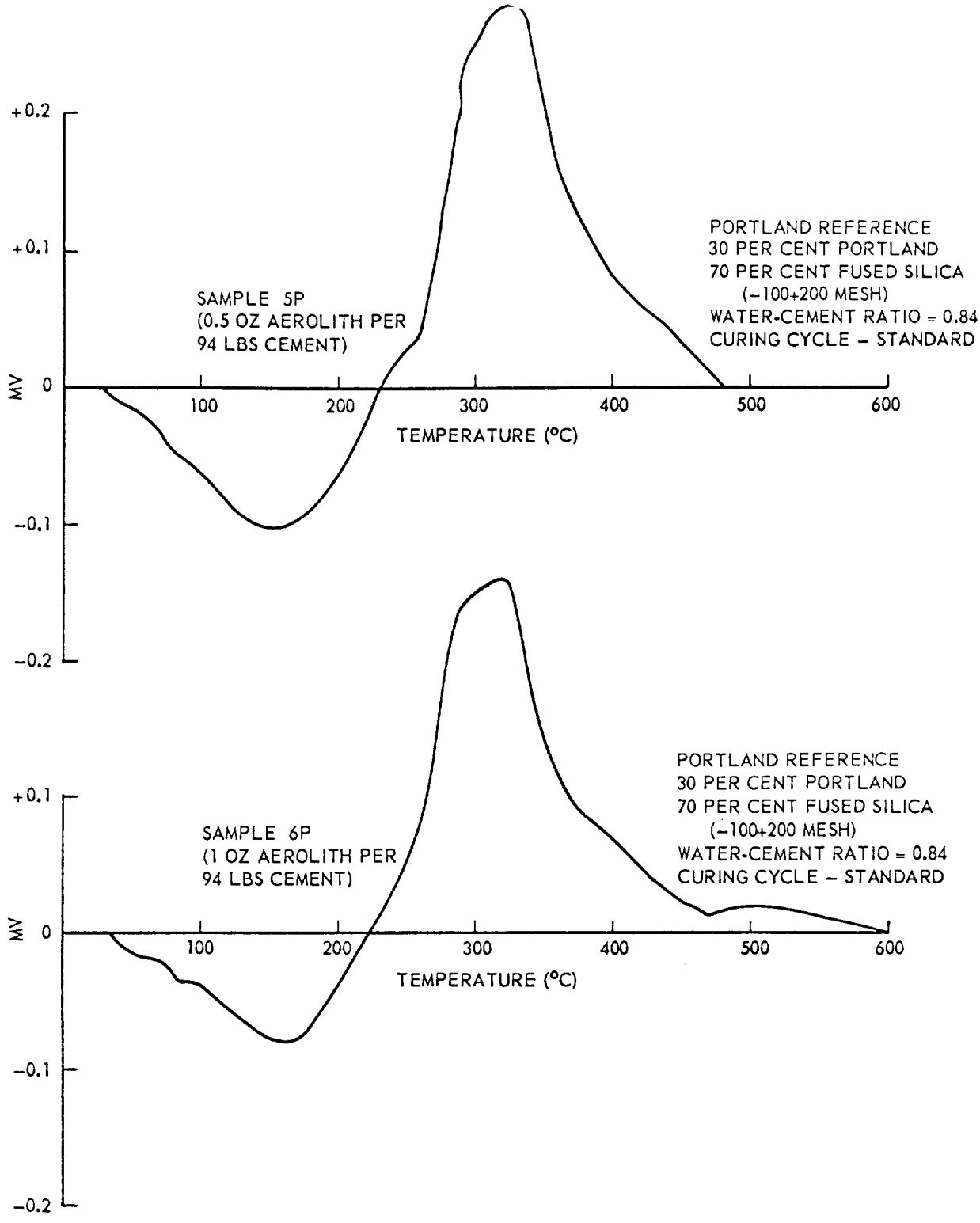

Figure 18. Differential Thermal Analysis Samples 1248-01-5P, 6P.

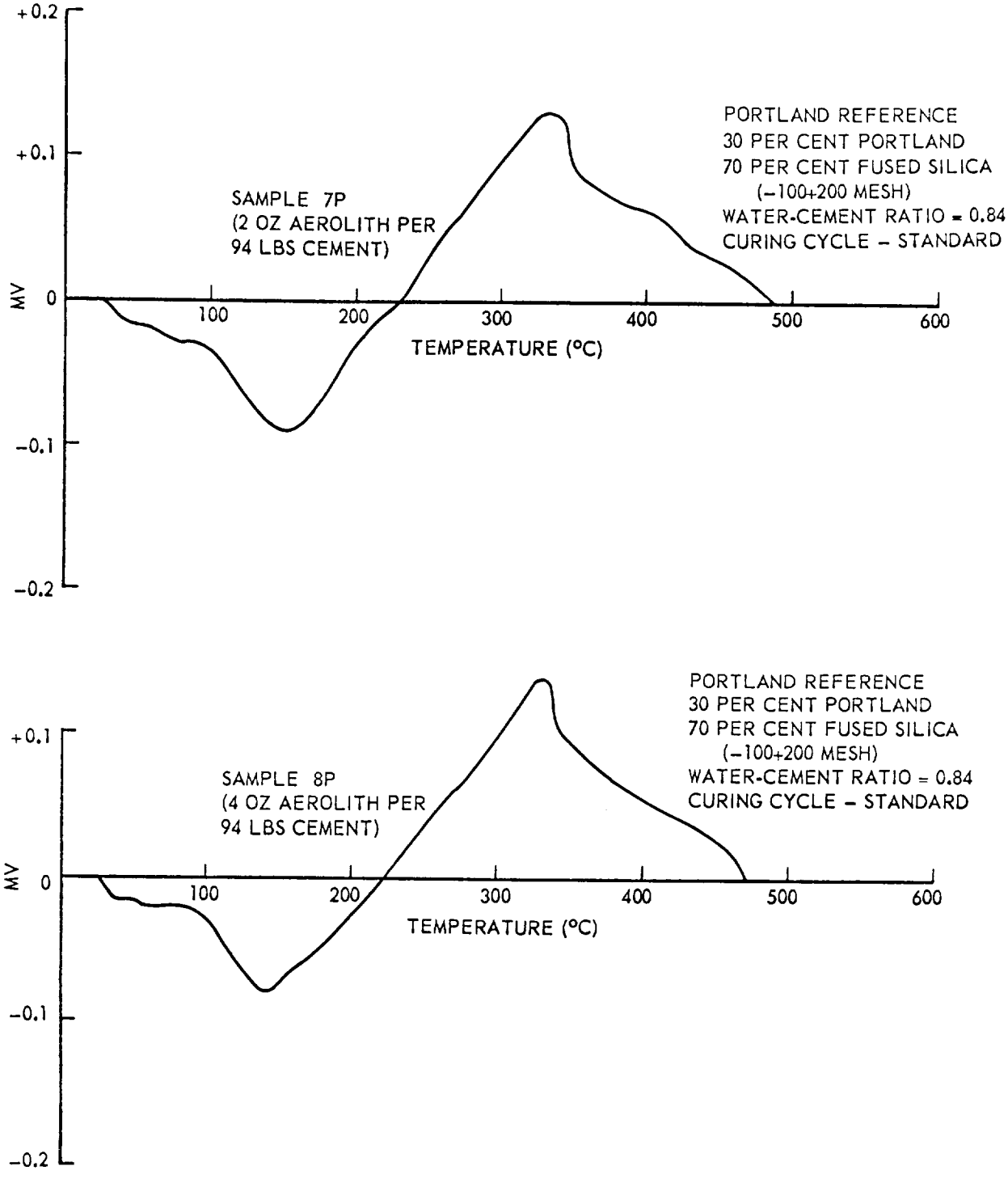

Figure 19. Differential Thermal Analysis Samples 1248-01-7P, 8P.

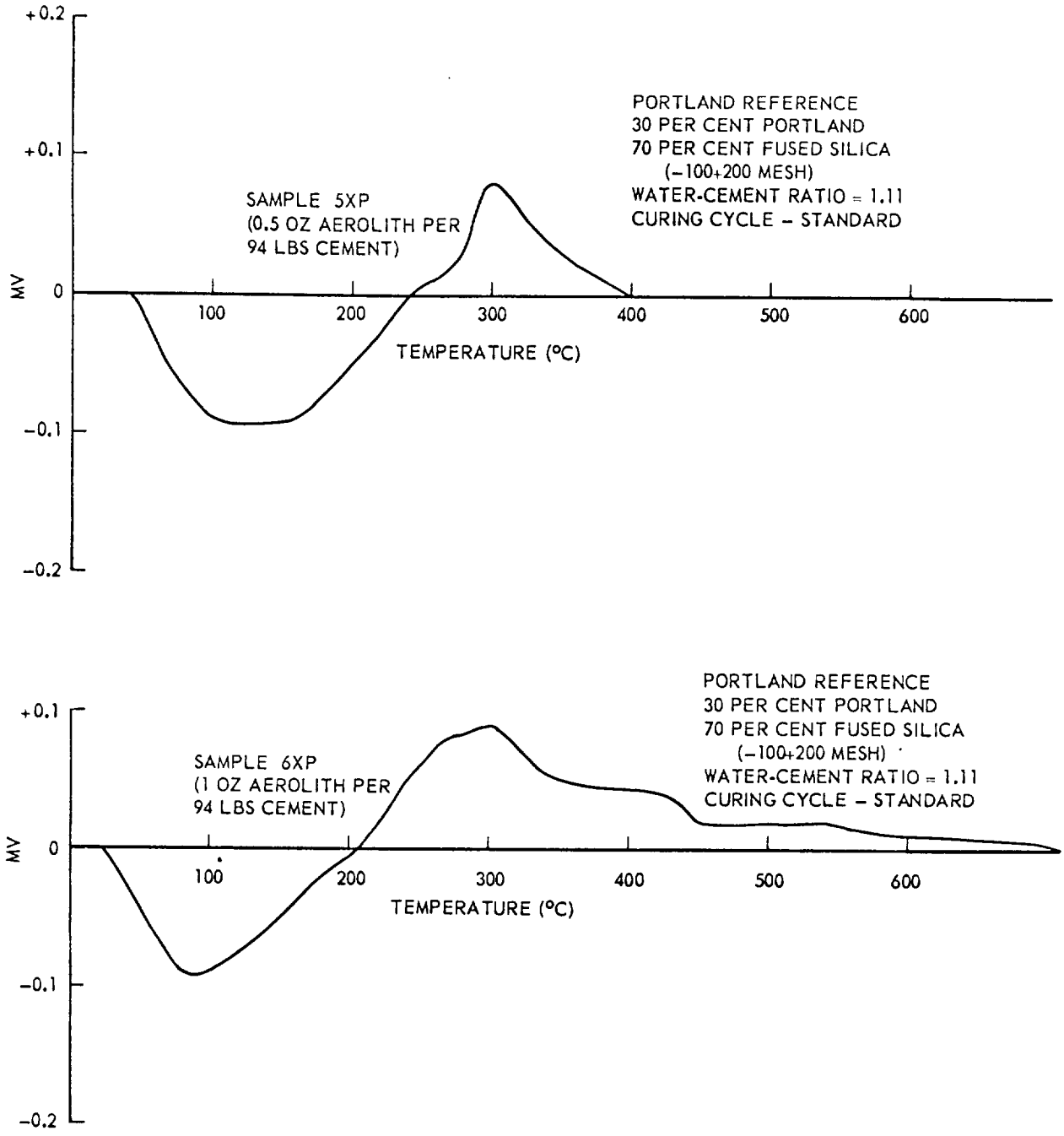

Figure 20. Differential Thermal Analysis Samples 1248-01-5XP, 6XP.

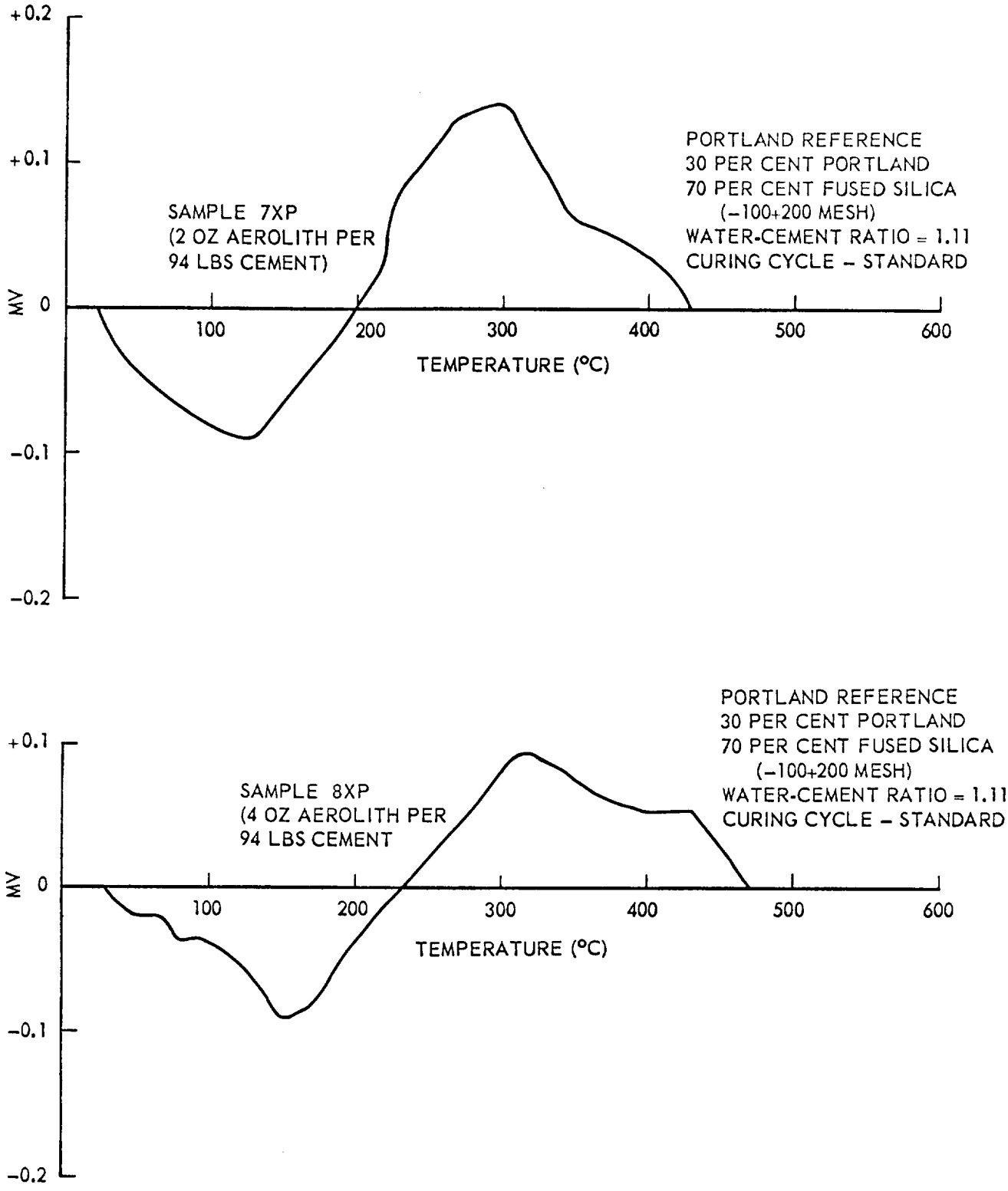

Figure 21. Differential Thermal Analysis Samples 1248-01-7XP, 8XP.

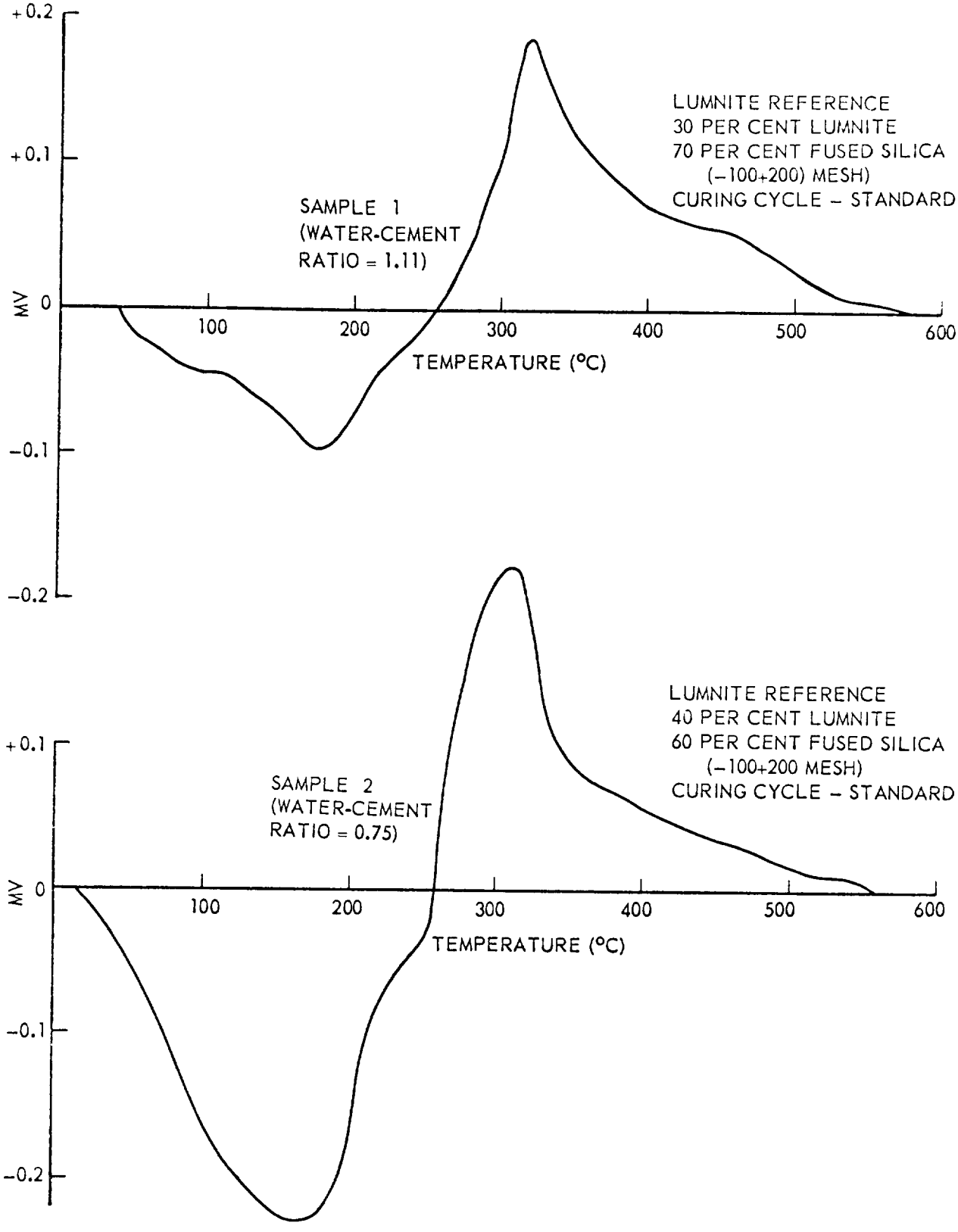

Figure 22. Differential Thermal Analysis Samples 1246-02-01, 02.

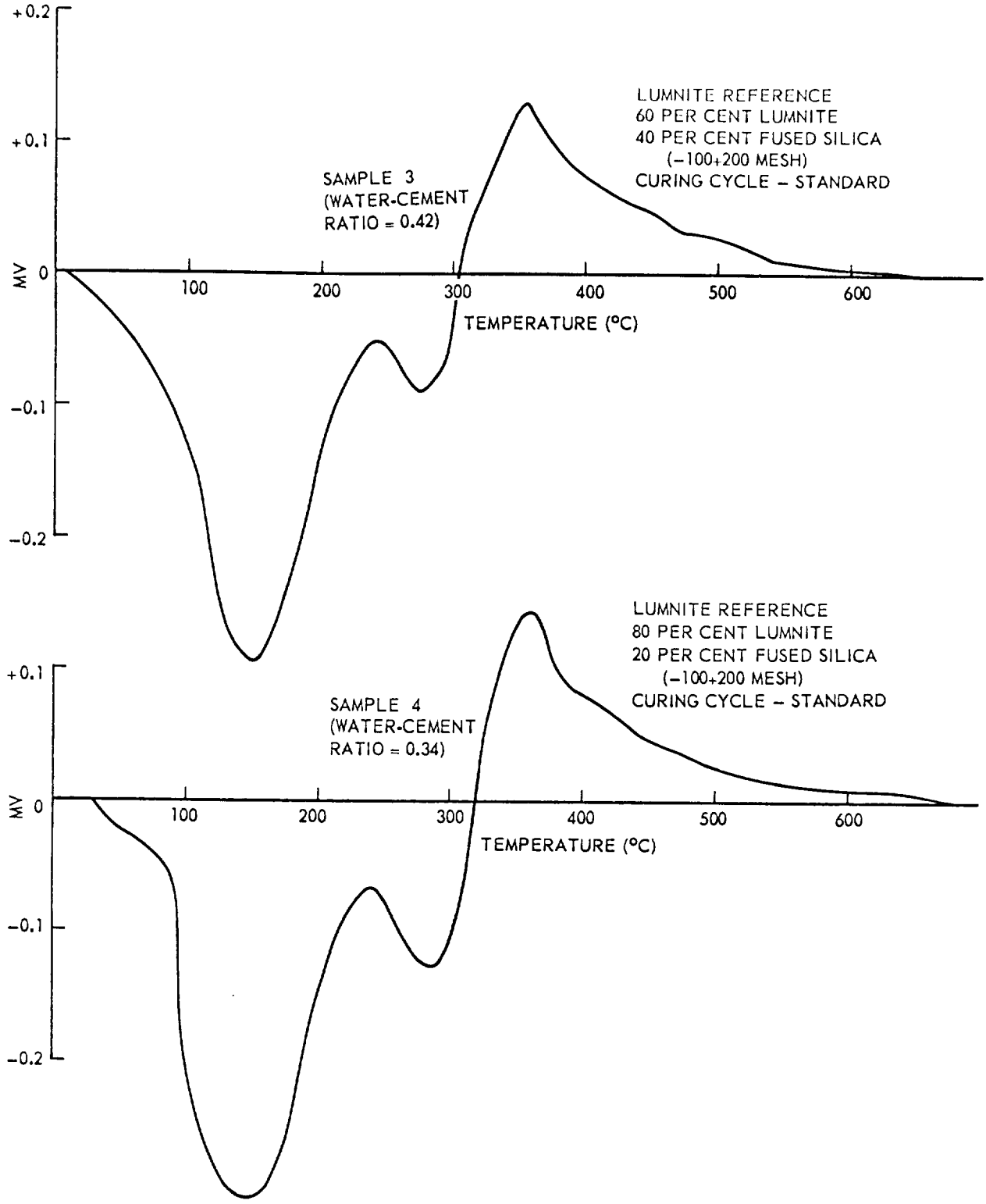

Figure 23. Differential Thermal Analysis Samples 1246-02-03, 04.

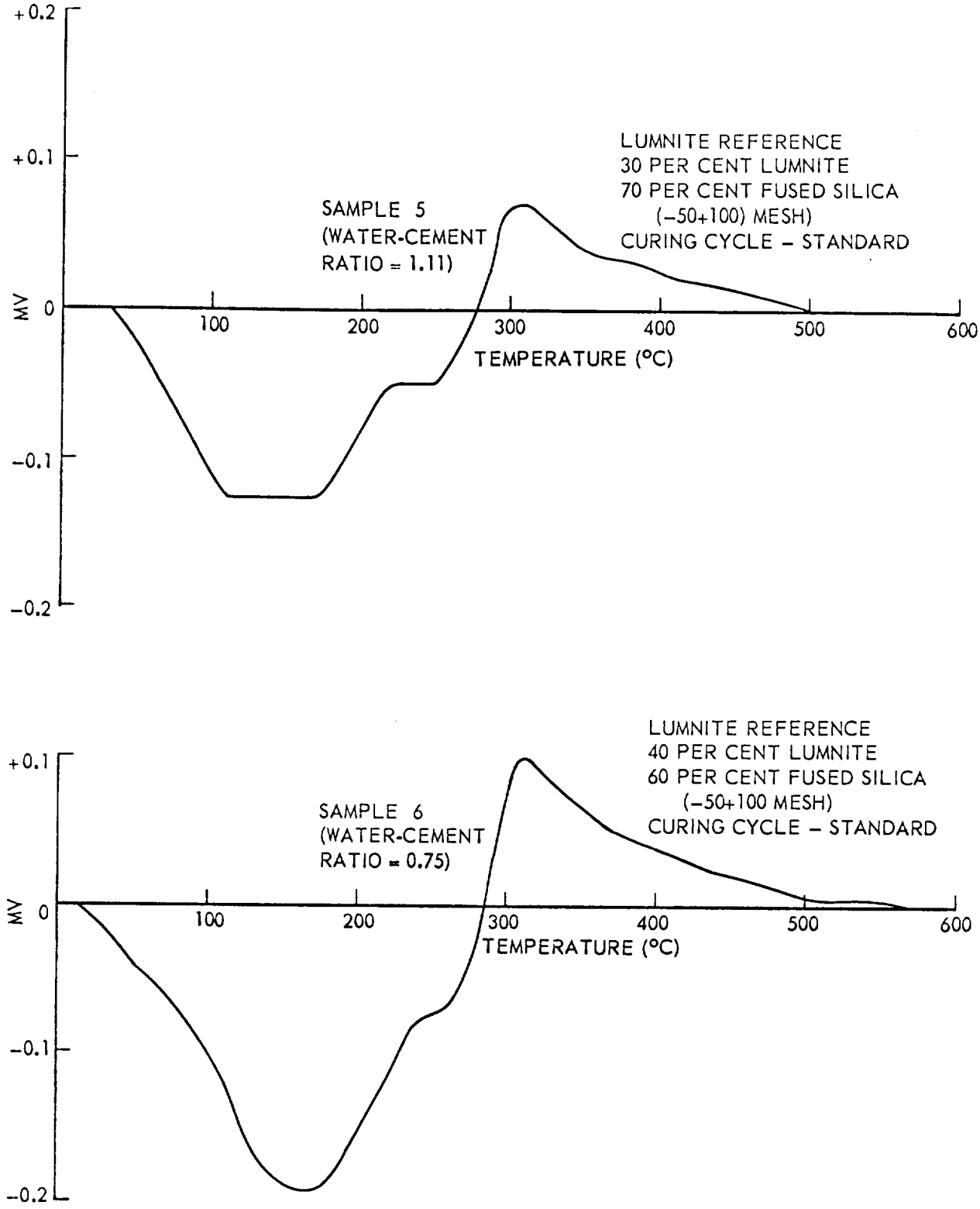

Figure 24. Differential Thermal Analysis Samples 1246-02-05, 06.

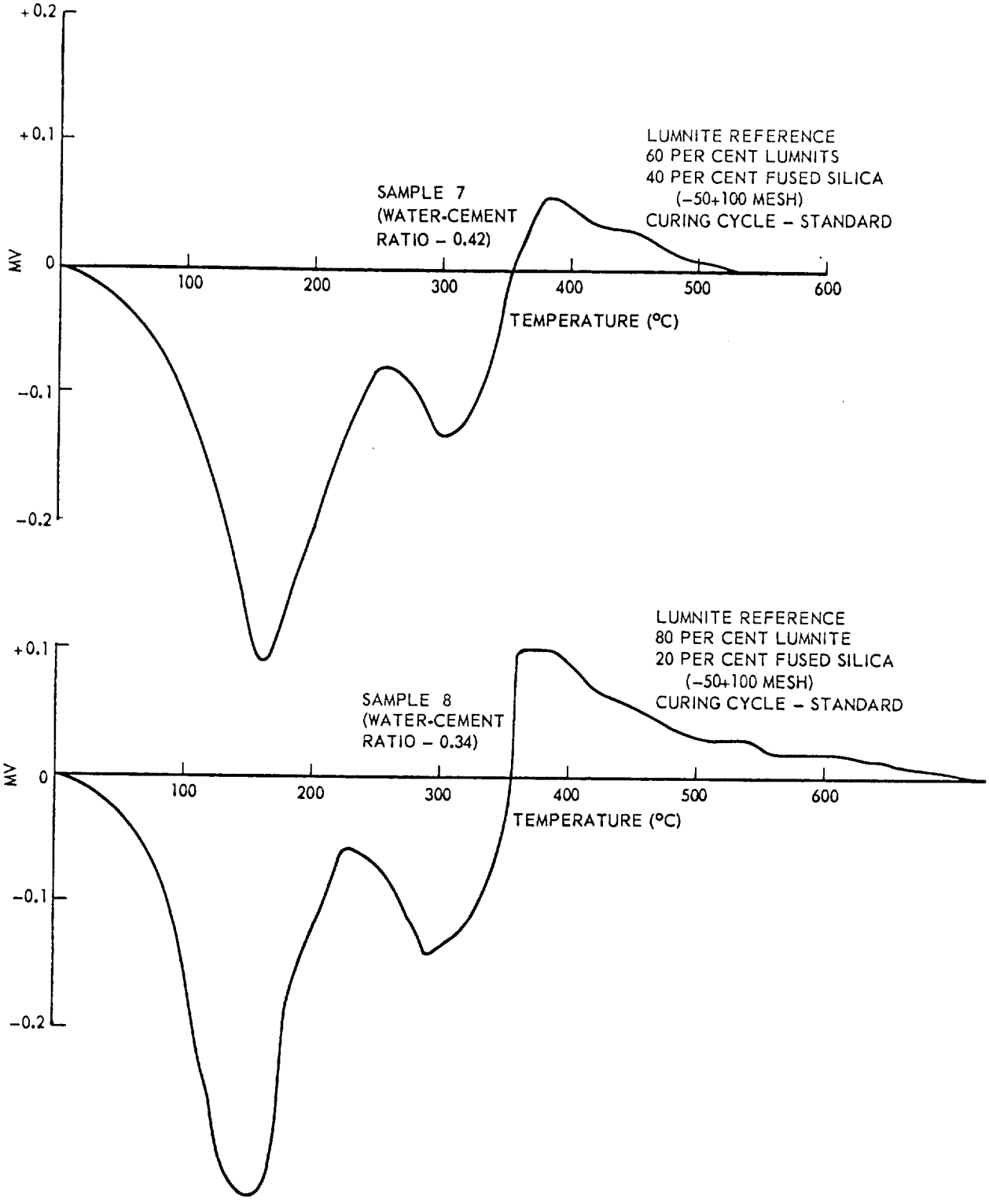

Figure 25. Differential Thermal Analysis Samples 1246-02-07,08.

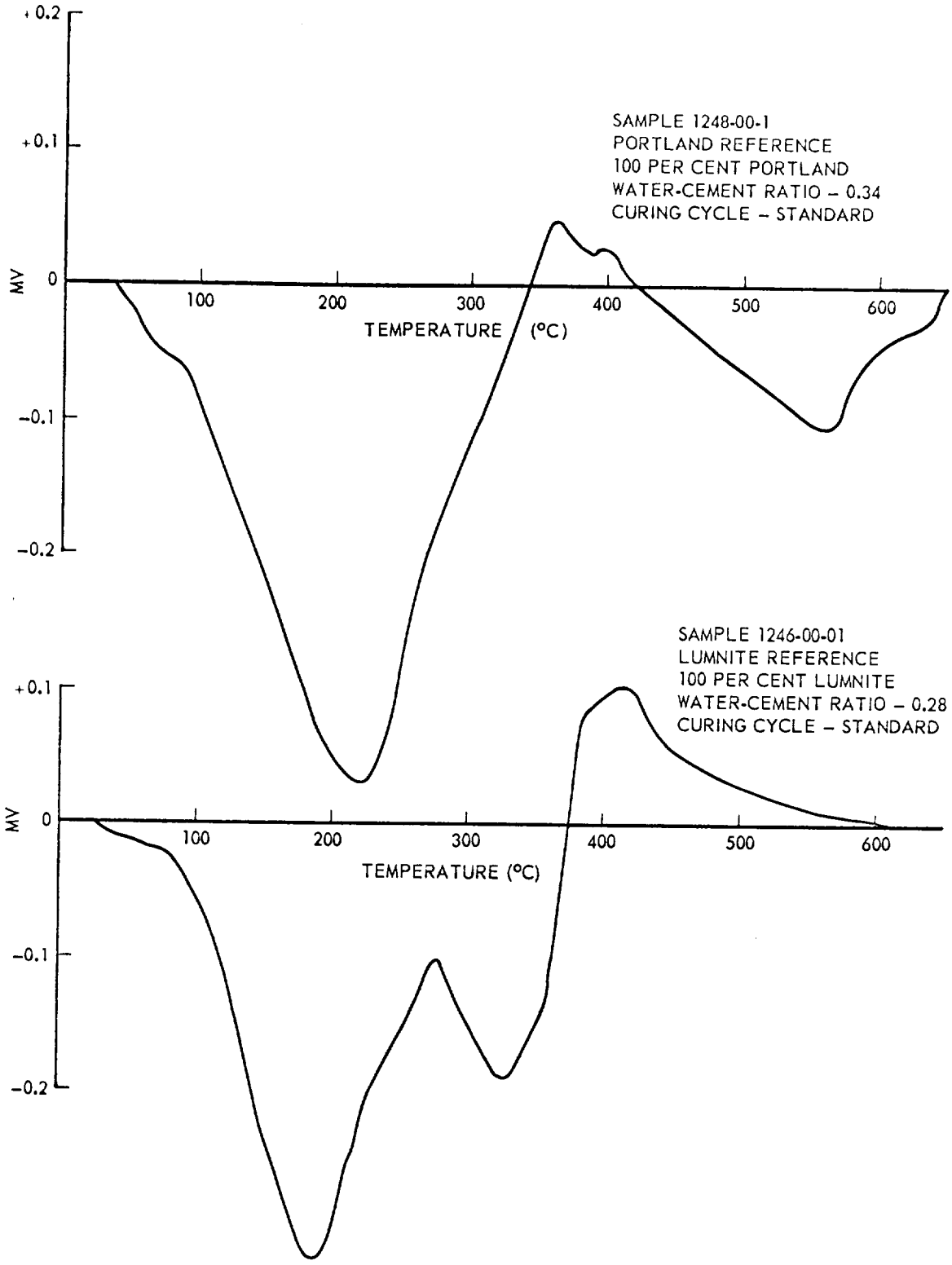

Figure 26. Differential Thermal Analysis Samples 1248-00-01 and 1246-00-01.

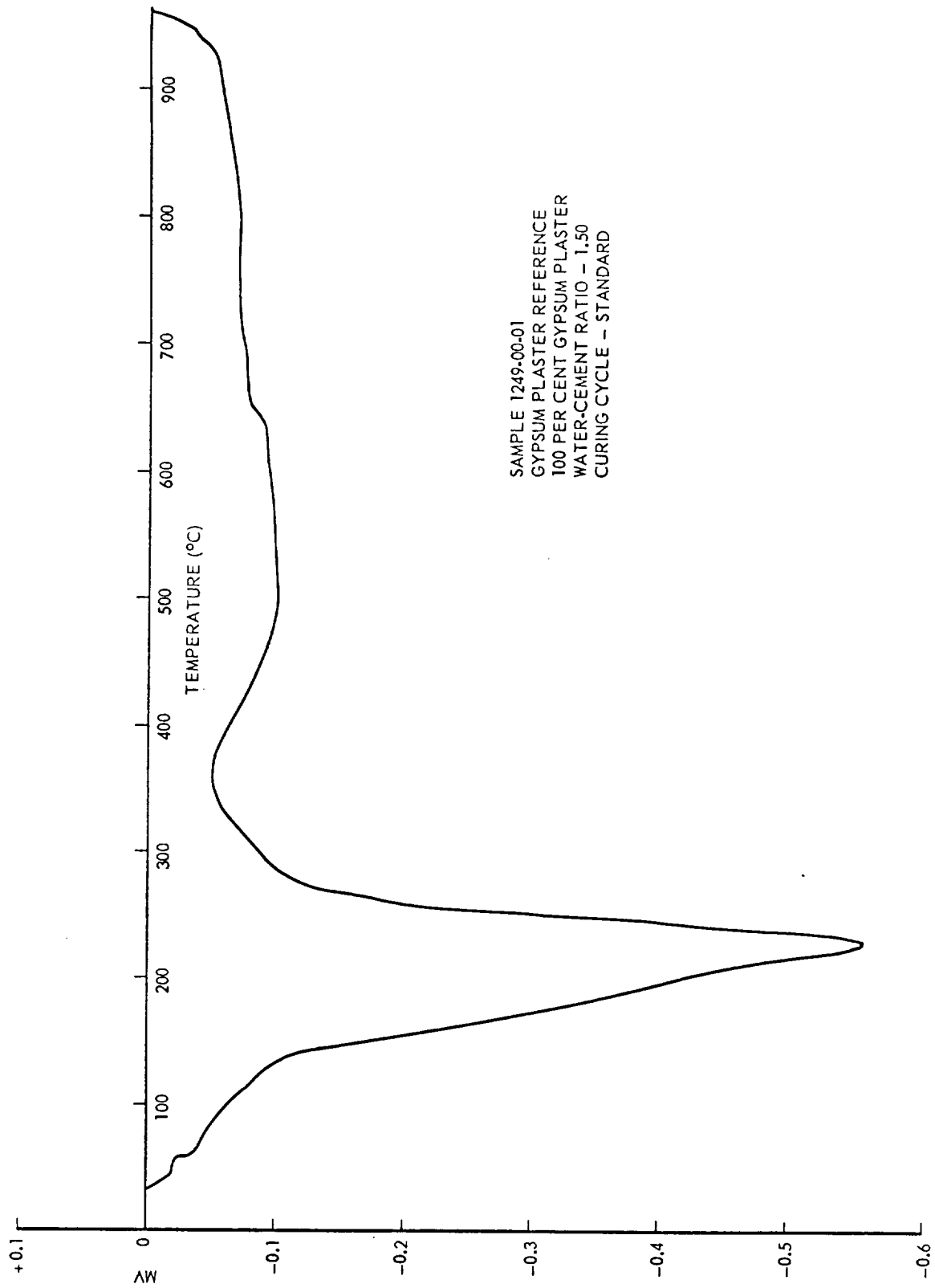

Figure 27. Differential Thermal Analysis Samples 1249-00-01.

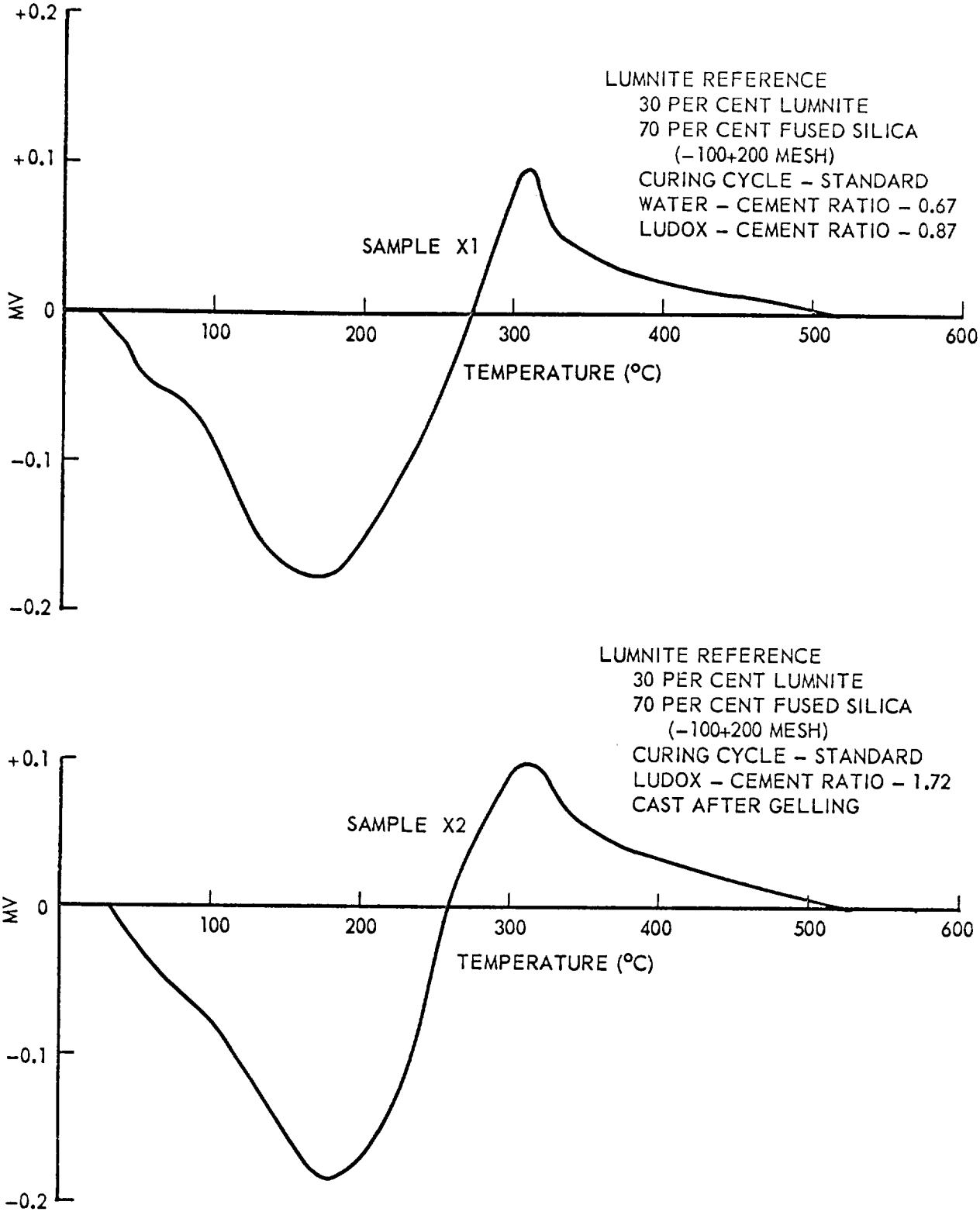

Figure 28. Differential Thermal Analysis Samples 1246-06-X1, X2.

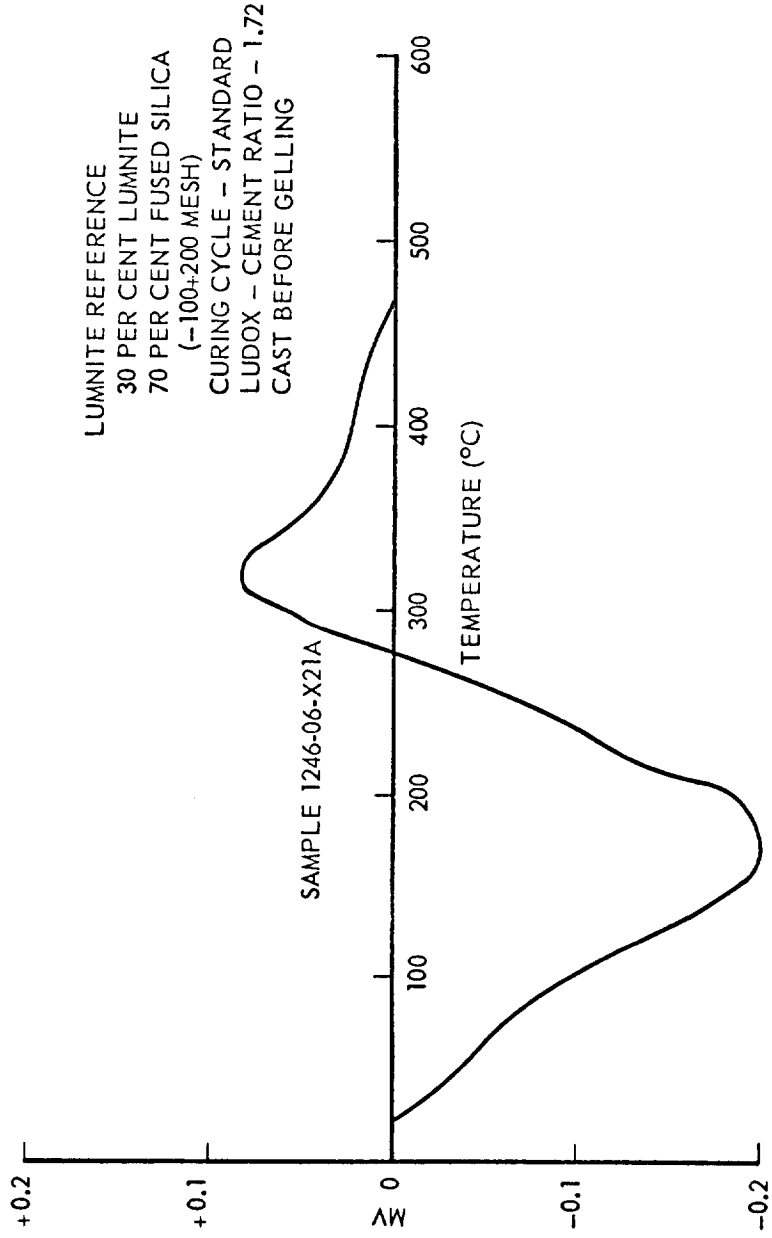

Figure 29. Differential Thermal Analysis Sample 1246-06-X2A.

Shown in Tables X, XI, and XII are the history of each rocket motor test plate and the data obtained from each test plate or test group. Unless otherwise stated all test plates were exposed to the exhaust gases of the oxyhydrogen rocket motor at 9-1/2 inches from the exit plane of the rocket nozzle at a flame impingement angle of 45°; the water calorimeter heat flux value at this distance and angle is 260 $Btu \cdot ft^{-2} \cdot sec^{-1}$. Backside temperature measurements were made with an iron-constantan thermocouple automatically recorded on a Wheelco Model 8000 recorder at a chart speed of 180 inches per hour. For a more detailed explanation of the method used to obtain ablation data, see section A. Figures 30 through 40 show the backside-temperature-vs-time curves (ambient temperature between 25° and 30° C) for all test plates exposed to the exhaust gases of the oxyhydrogen rocket motor. Unless otherwise stated these curves are an average of two test plates. Figures 41 through 51 show the rocket motor test plates after ablation tests.

TABLE X

HISTORY OF ROCKET MOTOR TEST PLATE SAMPLES

Ga. Tech Sample No.	History, Section B
1246-01-A, 1246-01-B, 1246-01-C, 1246-01-D, 1248-02-AP, 1248-02-BP, 1248-02-CP, 1248-02-DP, 1248-04-ASL, 1246-04-BSL, 1246-04-CSL, 1246-04-DSL, 1246-03-1L, 1246-03-2L, 1246-03-3L, 1246-03-4L, 1248-01-5P, 1248-01-6P, 1248-01-7P, 1248-01-8P, 1248-01-5XP, 1248-01-6XP, 1248-01-7XP, 1248-01-8XP, 1246-02-01, 1246-02-02, 1246-02-03, 1246-02-04, 1246-02-05, 1246-02-06, 1246-02-07, 1246-02-08	Composition shown in Table III, section B and cured according to procedure outline in Table II, section B.
1246-01-BF	Same as 1246-01-B except fired at 2150° F for 4 hours.

(Continued)

TABLE X (Continued)

HISTORY OF ROCKET MOTOR TEST PLATE SAMPLES

Ga. Tech Sample No.	History, Section B
1246-06-X1	30 per cent Lumnite cement--70 per cent fused silica aggregate (-100+200 mesh), water-cement ratio 0.67 and Ludox-cement ratio 0.87. Cured following standard curing procedure.
1246-06-X2	Same as 1246-06-X1 except it has no water but has a Ludox-cement ratio of 1.72. The sample was cast after gelling occurred.
1246-06-X2A	Same as 1246-06-X2 except it was cast before gelling occurred.
1249-02-0	Honeycomb composite structure with 30 per cent Lumnite cement composition. 1/2-inch groove cut in back plate directly behind point of flame impingement.
1249-02-R	Same as 1249-02-0 except it has no groove cut in the back plate.
1249-03-B	1/8-inch-thick metal substrate coated with approximately 3/8-inch fused silica aggregate coating, composition B fired at 160° F for 16 hours.
1249-03-D	Same as 1249-03-B except composition D was used to coat the substrate.

TABLE XI

ABLATION TEST DATA

Ga. Tech Sample No.	Exposure Time (Sec)	Max. Change in Backside Temp. (°C)	Weight Loss Rate (Gm/Sec)	Maximum Ablation and/or Erosion Rate (In/Sec)
1246-01-A_1	114	192	0.145	0.0026
1246-01-A_3	126	210	0.185	0.0025
1246-01-B_1	136	217	0.117	0.0011
1246-01-B_2	155	215	0.101	0.0006
1246-01-C_2	156	229	0.113	0.0014
1246-01-C_3	164	222	0.098	0.0011
1246-01-D_2	128	204	0.127	0.0012
1248-02-AP_1	118	220	0.140	0.0020
1248-02-AP_2	111	219	0.141	0.0024
1248-02-BP_1	122	217	0.170	0.0022
1248-02-BP_2	123	217	0.172	0.0019
1248-02-CP_1	147	220	0.069	0.0022
1248-02-CP_2	135	218	0.139	0.0018
1248-02-DP_1	134	220	0.113	0.0019
1248-02-DP_2	135	222	0.135	0.0017
1246-04-ASL_1	127	210	0.179	0.0021
1246-04-ASL_2	133	222	0.173	0.0021
1246-04-BSL_1	121	218	0.198	0.0024
1246-04-BSL_2	123	220	0.185	0.0019
1246-04-CSL_1	115	192	0.200	0.0022
1246-04-CSL_2	131	219	0.158	0.0020

(Continued)

TABLE XI (Continued)

ABLATION TEST DATA

Ga. Tech Sample No.	Exposure Time (Sec)	Max. Change in Backside Temp. (°C)	Weight Loss Rate (Gm/Sec)	Maximum Ablation and/or Erosion Rate (In/Sec)
1246-04-DSL$_1$	104	219	0.217	0.0025
1246-04-DSL$_2$	113	220	0.178	0.0024
1246-03-1L$_1$	147	219	0.108	0.0009
1246-03-1L$_3$	140	222	0.111	0.0009
1246-03-2L$_1$	148	223	0.105	0.0013
1246-03-2L$_3$	143	217	0.099	0.0011
1246-03-3L$_1$	138	218	0.108	0.0011
1246-03-3L$_2$	158	221	0.101	0.0010
1246-03-4L$_1$	160	197	0.101	0.0014
1246-03-4L$_2$	151	222	0.082	0.0009
1248-01-5P$_1$	96	223	0.151	0.0026
1248-01-5P$_2$	106	221	0.150	0.0028
1248-01-6P$_1$	101	208	0.165	0.0029
1248-01-7P$_1$	140	221	0.072	0.0002
1248-01-7P$_2$	149	221	0.073	0.0002
1248-01-8P$_1$	144	225	0.062	0.0001
1248-01-8P$_3$	155	209	0.057	0.0002
1248-01-5XP$_2$	200	216	0.054	0.0000
1248-01-5XP$_3$	181	182	0.115	0.0000
1248-01-6XP$_2$	160	220	0.062	0.0001
1248-01-6XP$_3$	195	222	0.053	0.0001

(Continued)

TABLE XI (Continued)

ABLATION TEST DATA

Ga. Tech Sample No.	Exposure Time (Sec)	Max. Change in Backside Temp. (°C)	Weight Loss Rate (Gm/Sec)	Maximum Ablation and/or Erosion Rate (In/Sec)
1248-01-7XP$_1$	100	223	0.121	0.0022
1248-01-8XP$_1$	89	207	0.183	0.0044
1246-02-01	87	188	0.214	0.0026
1246-02-02	101.4	203	0.214	0.0030
1246-02-03	104.0	201	0.370	0.0022
1246-02-04	132.0	200	0.211	0.0018
1246-02-05$_1$	140	225	0.111	0.0009
1246-02-05$_2$	156	226	0.097	0.0010
1246-02-06$_1$	99	225	0.286	0.0050
1246-02-06$_2$	112	118	0.258	0.0039
1246-02-07$_1$	123	193	0.202	0.0042
1246-02-07$_2$	116	225	0.238	0.0038
1246-02-08$_1$	152	222	0.209	0.0028
1246-06-X1$_1$	92	188	0.258	0.0034
1246-06-X1$_2$	96	157	0.267	0.0036
1246-06-X2$_1$	89	218	0.277	0.0033
1246-06-X2$_2$	99	204	0.258	0.0029
1246-06-X2A$_1$	113	218	0.216	0.0024
1246-06-X2A$_2$	100	221	0.192	0.0022
1246-01-BF$_1$	49	222	0.128	0.0033
1246-01-BF$_3$	50	244	0.135	0.0042

(Continued)

TABLE XI (Continued)

ABLATION TEST DATA

Ga. Tech Sample No.	Exposure Time (Sec)	Max. Change in Backside Temp. (°C)	Weight Loss Rate (Gm/Sec)	Maximum Ablation and/or Erosion Rate (In/Sec)
1249-02-O_1	74	219	0.191	0.0022
1249-02-O_2	65	223	0.179	0.0036
1249-02-R_2	86	229	0.162	0.0033
1249-03-B	86	223	0.008	0.0000
1249-03-D*	107	223	0.014	-

*Separated from back plate after test.

TABLE XII

TRANSPIRATION COOLING DATA

Ga. Tech Sample No.	Cooling Temperature (ΔT) (°C)	Cooling Period (Sec)
1246-01-A	60	76
1246-01-B	68	76
1246-01-C	69	114
1246-01-D	68	58
1248-02-AP	64	34
1248-02-BP	66	56
1248-02-CP	60	58
1248-02-DP	69	54
1246-04-ASL	64	38

(Continued)

TABLE XII (Continued)

TRANSPIRATION COOLING DATA

Ga. Tech Sample No.	Cooling Temperature (ΔT) (°C)	Cooling Period (Sec)
1246-04-BSL	63	39
1246-04-CSL	61	55
1246-04-DSL	61	48
1246-03-1L	71	62
1246-03-2L	71	62
1246-03-3L	70	114
1246-03-4L	70	82
1248-01-5P	-	-
1248-01-6P	59	26
1248-01-7P	67	41
1248-01-8P	64	46
1248-01-5XP	72	56
1248-01-6XP	68	52
1248-01-7XP	66	20
1248-01-8XP	60	20
1246-02-01	64	44
1246-02-02	-	-
1246-02-03	66	20
1246-02-04	-	-
1246-02-05	68	52
1246-02-06	71	40

(Continued)

TABLE XII (Continued)

TRANSPIRATION COOLING DATA

Ga. Tech Sample No.	Cooling Temperature (ΔT) (°C)	Cooling Period (Sec)
1246-02-07	56	26
1246-02-08	64	68
1246-06-X1	60	30
1246-06-X2	-	-
1246-06-X2a	66	42
1249-02-0	63	22
1249-02-R	-	-
1246-01-BF	58	14
1249-03-B	-	-
1249-03-D	-	-

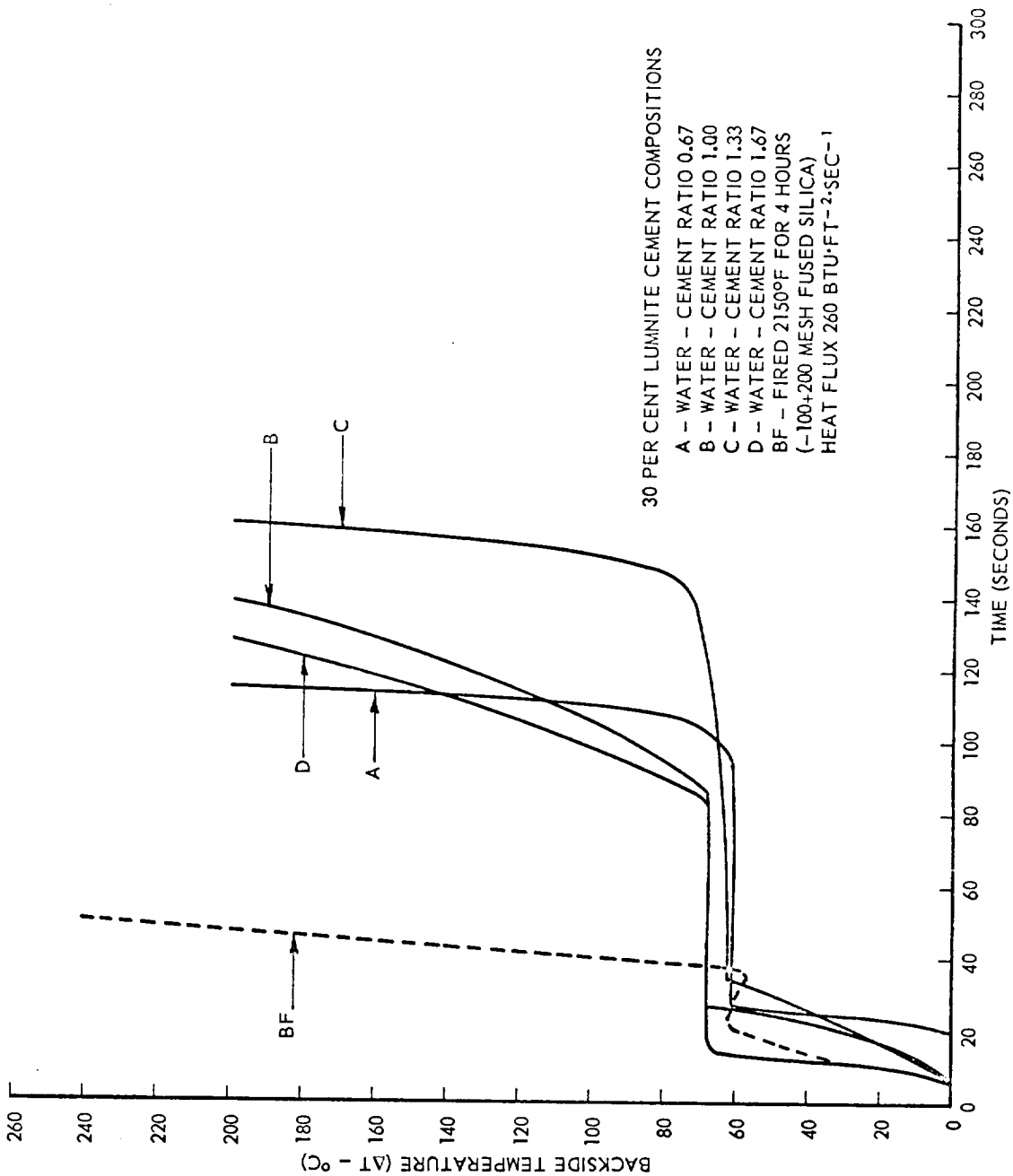

Figure 30. Change in Backside Temperature Vs. Time (Samples 1246-01-A, B, C, D, BF.)

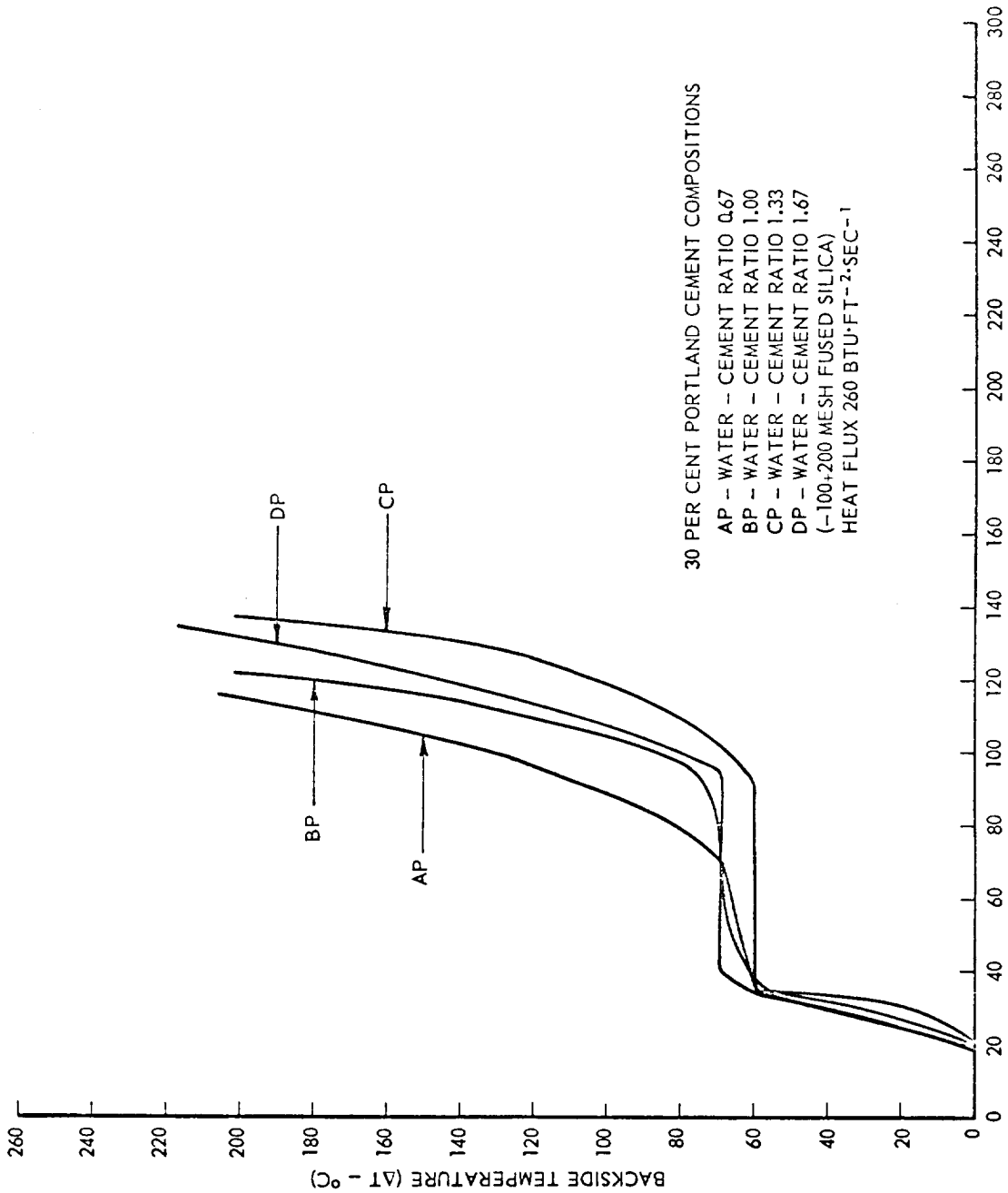

Figure 31. Change in Backside Temperature Vs. Time (Samples 1248-02-AP, BP, CP, DP).

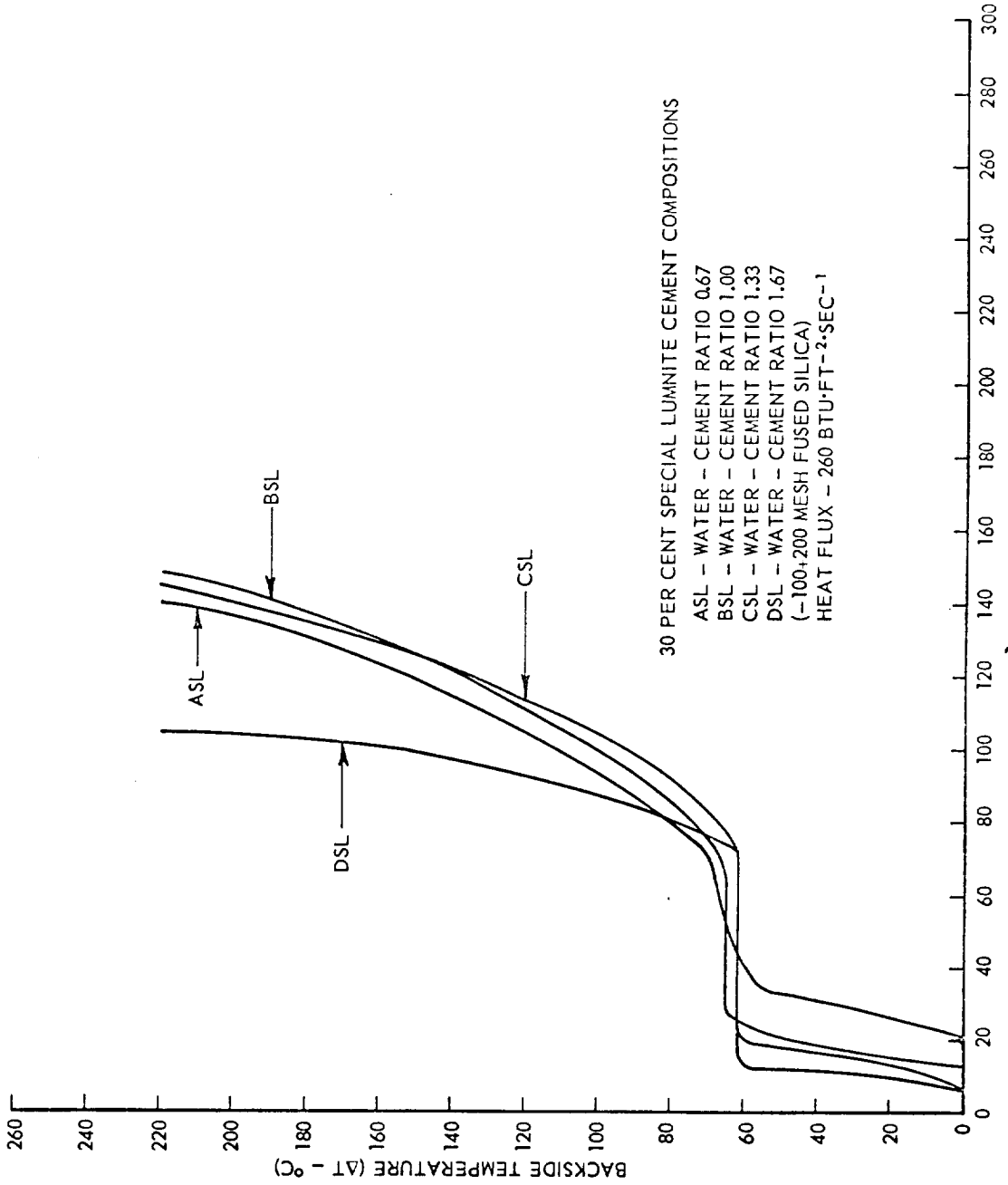

Figure 32. Change in Backside Temperature Vs. Time (Samples 1246-04-ASL, BSL, CSL, DSL).

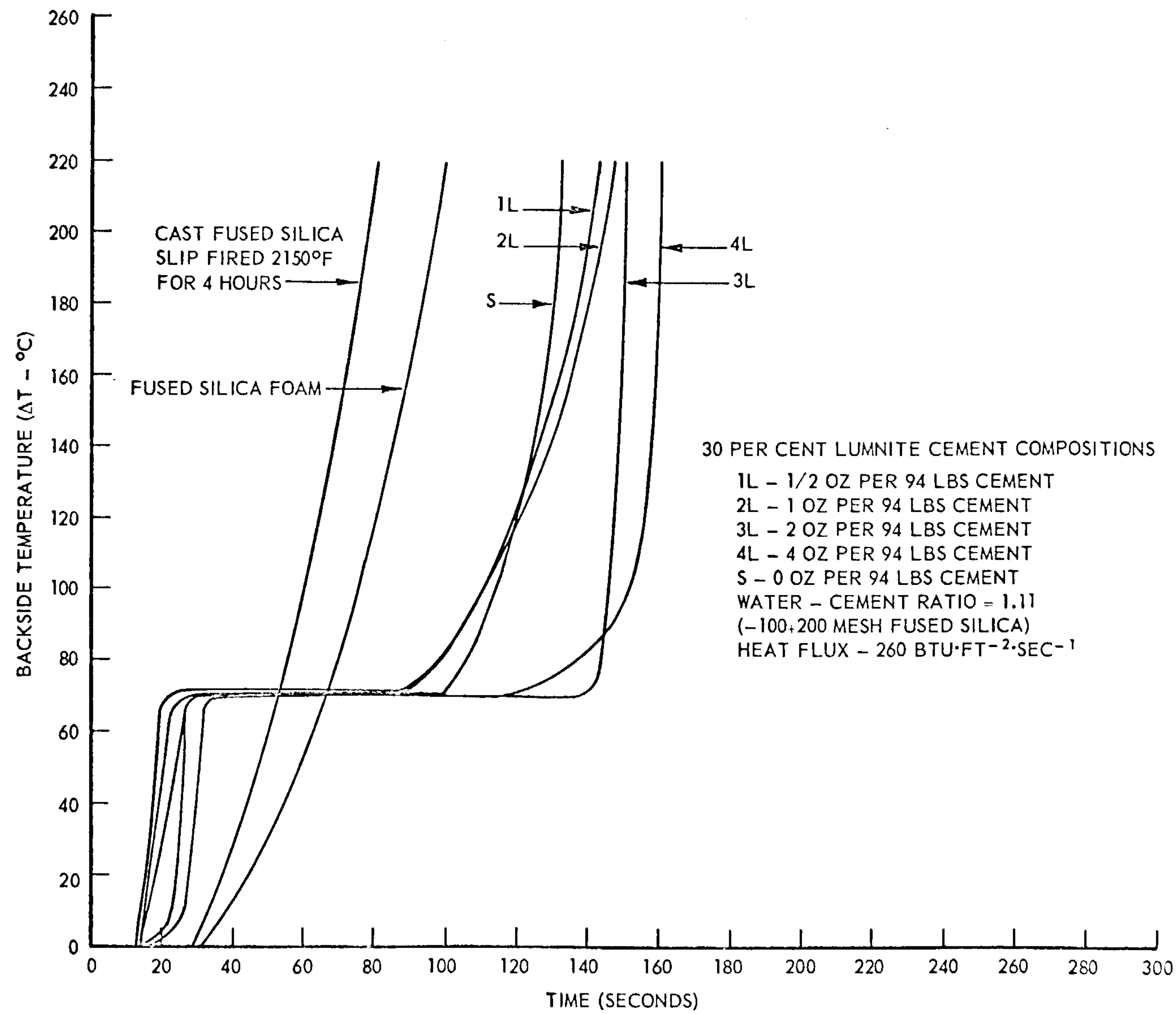

Figure 33. Change in Backside Temperature Vs. Time (Samples 1246-03-1L, 2L, 3L, 4L).

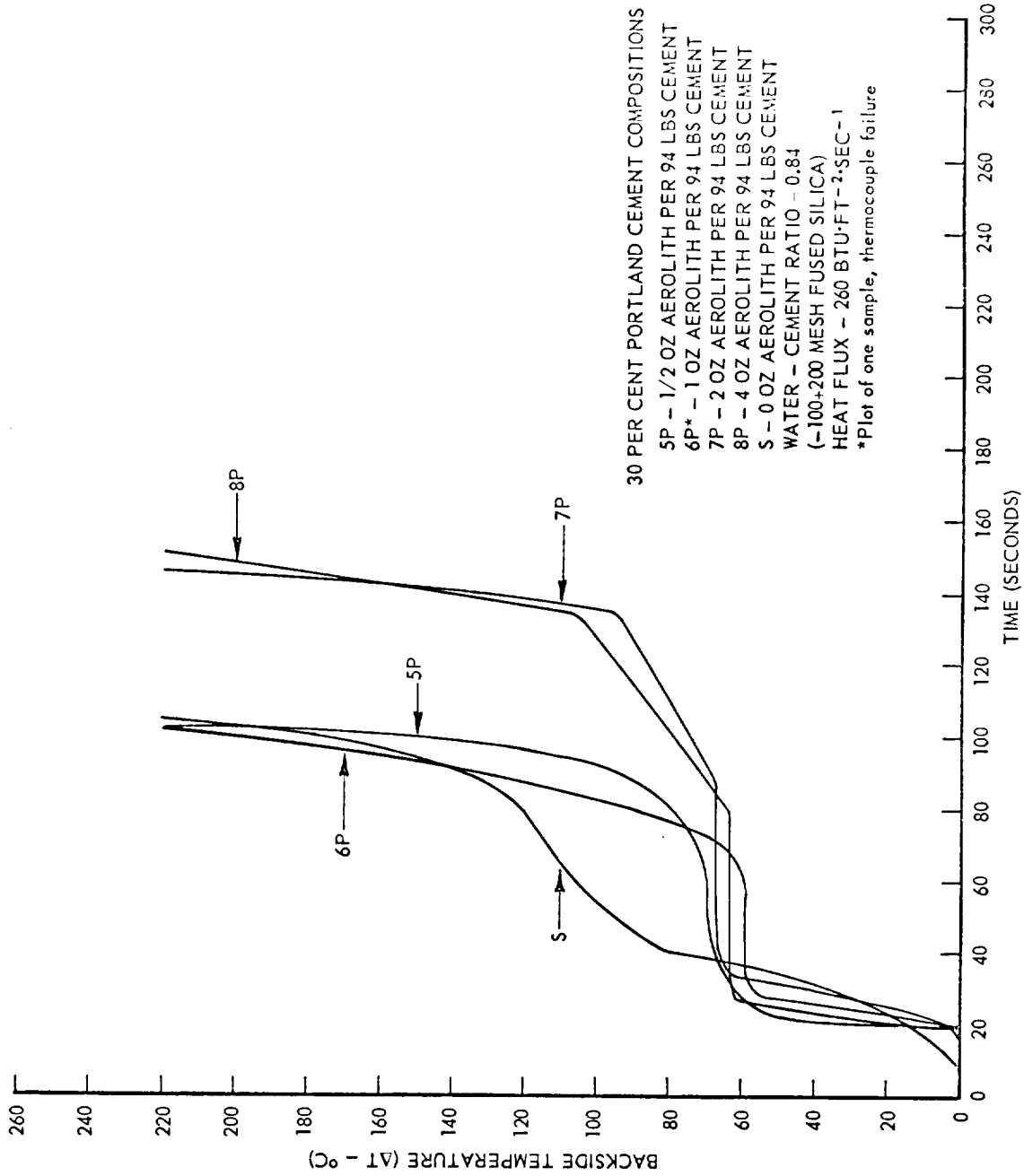

Figure 34. Change in Backside Temperature Vs. Time (Samples 1248-01-5P, 6P, 7P, 8P).

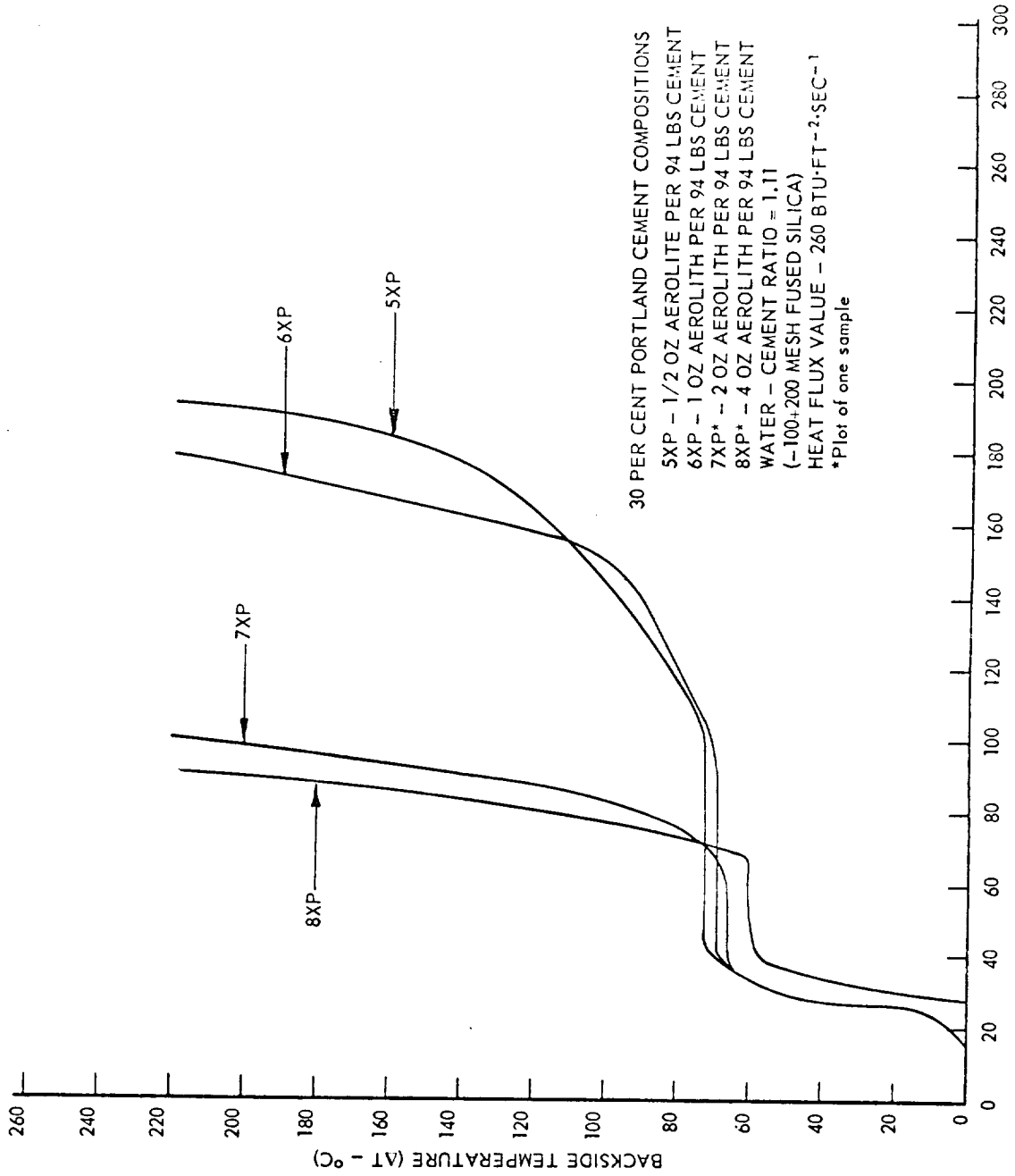

Figure 35. Change in Backside Temperature Vs. Time (Samples 1248-01-5XP, 6XP, 7XP, 8XP).

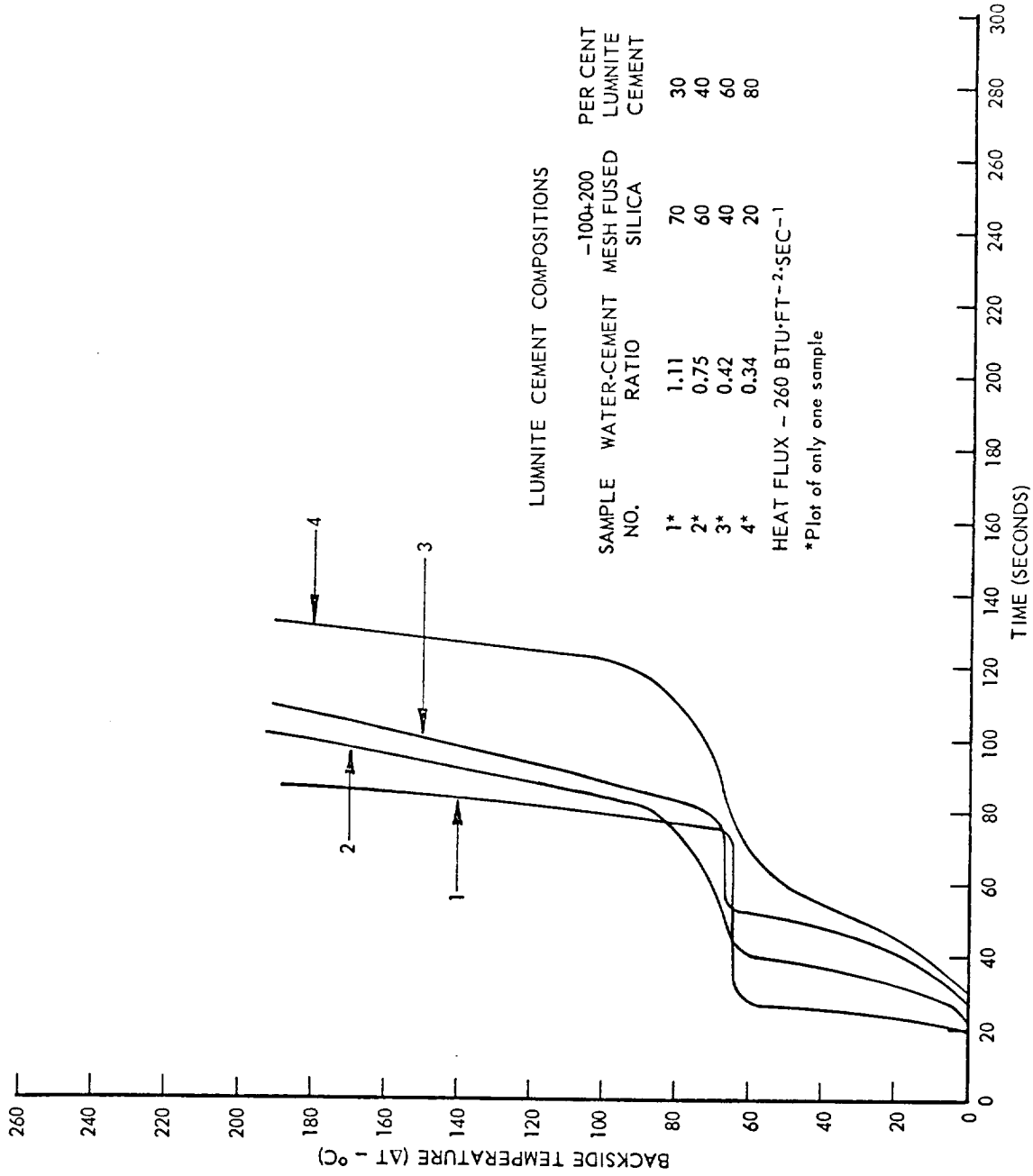

Figure 36. Change in Backside Temperature Vs. Time (Samples 1246-02-01, 02, 03, 04.)

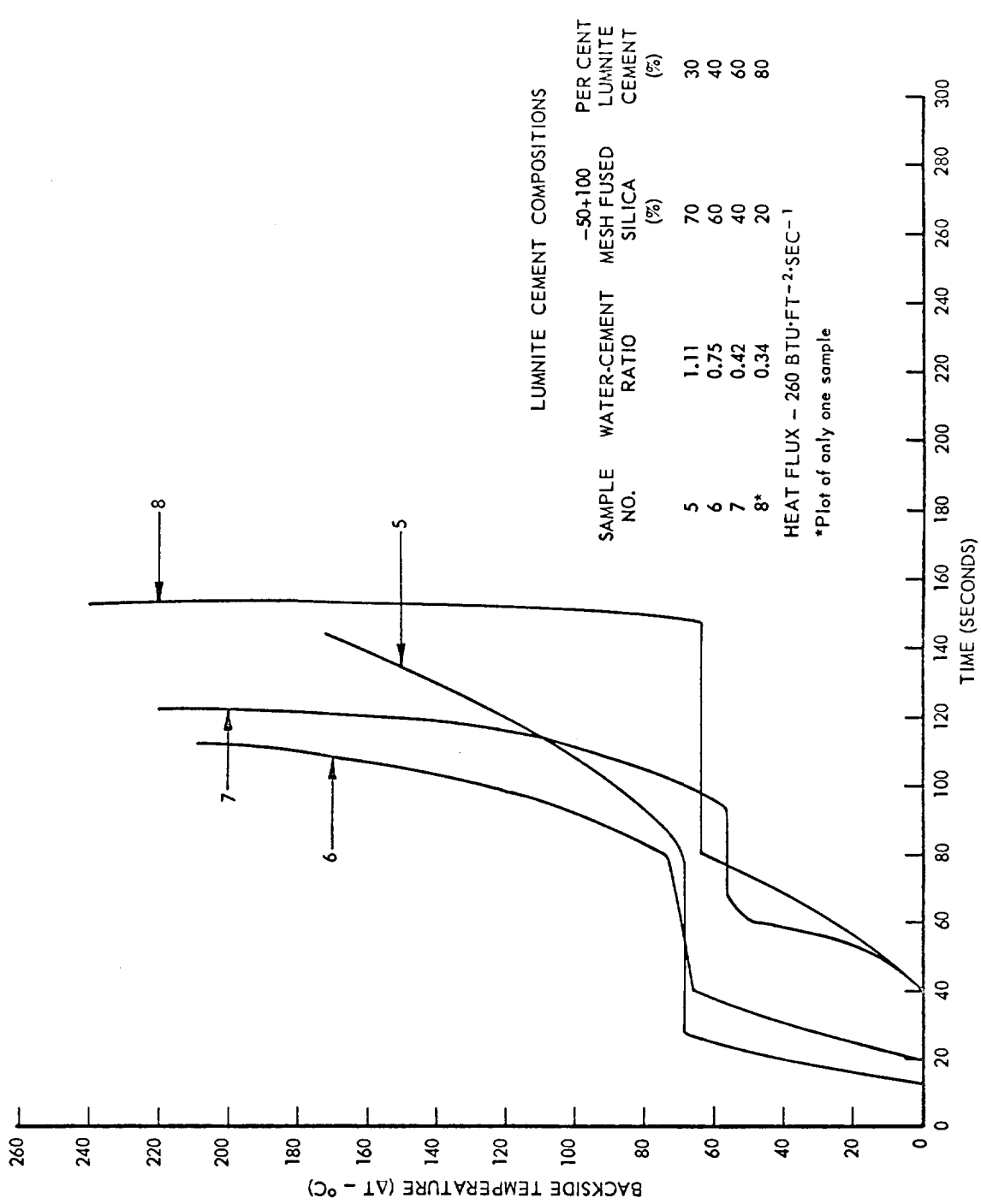

Figure 37. Change in Backside Temperature Vs. Time (Samples 1246-02-05, 06, 07, 08).

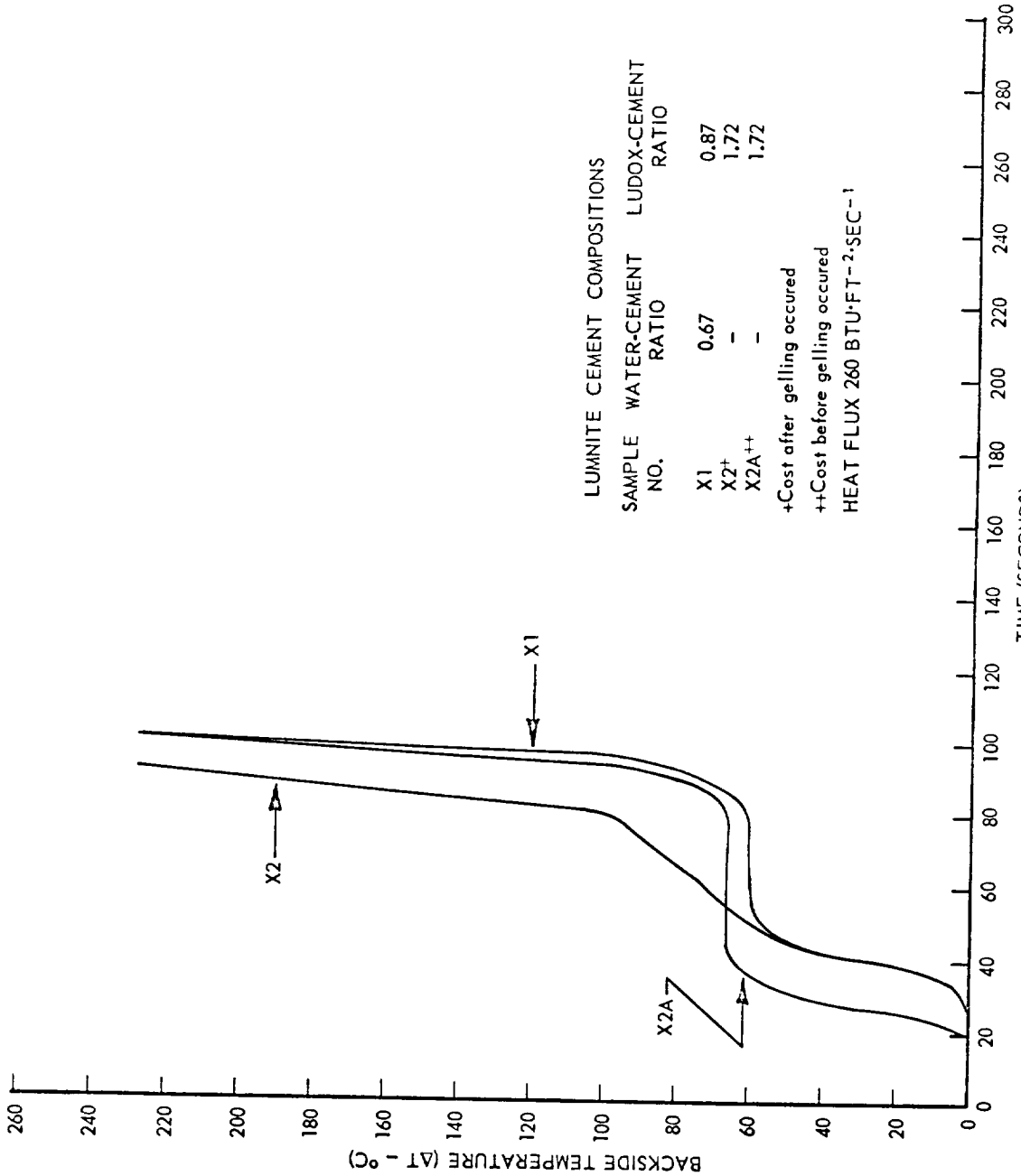

Figure 38. Change in Backside Temperature Vs. Time (Samples 1246-06-X1, X2, X2A).

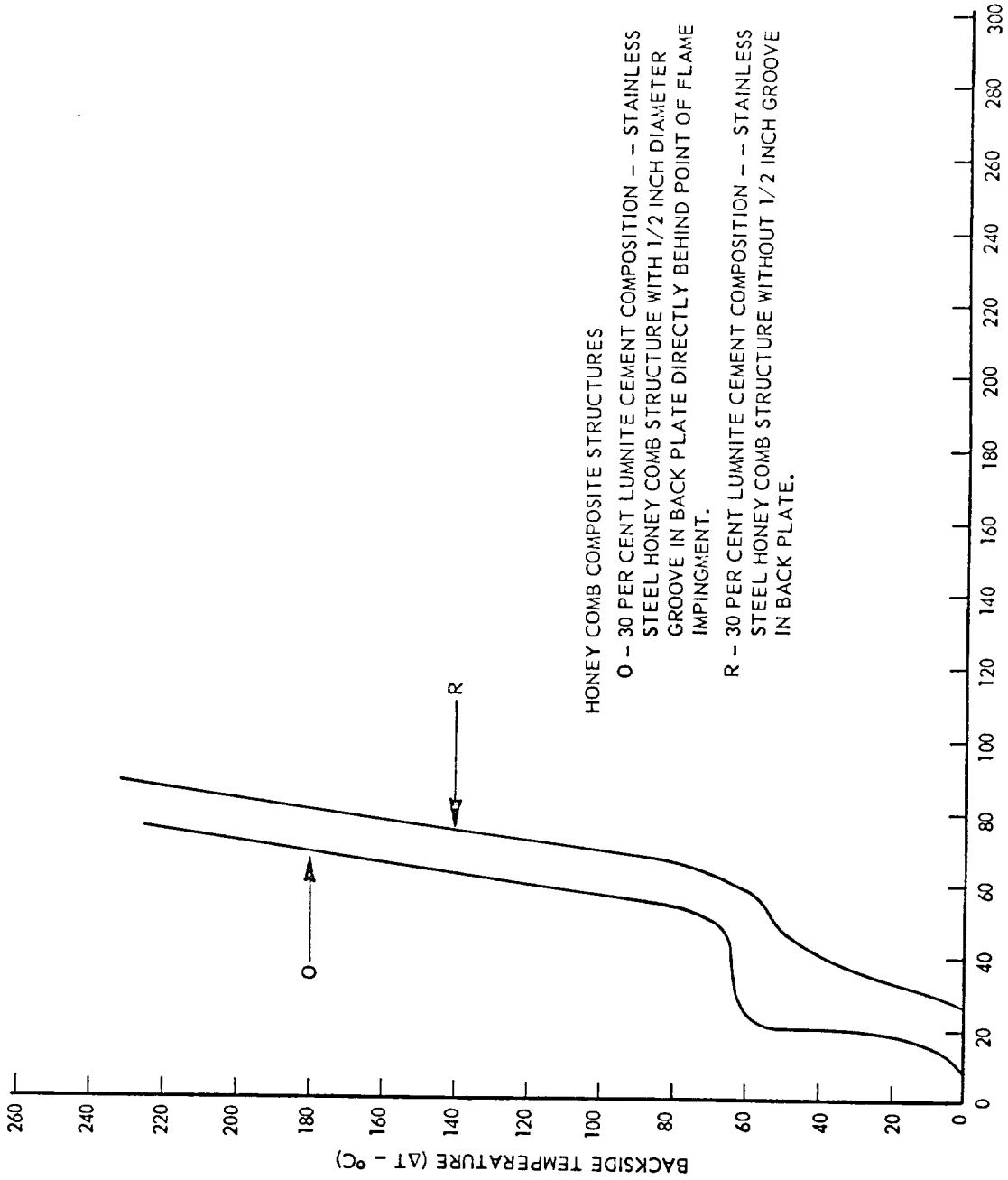

Figure 39. Change in Backside Temperature Vs. Time (Samples 1249-02-O, R).

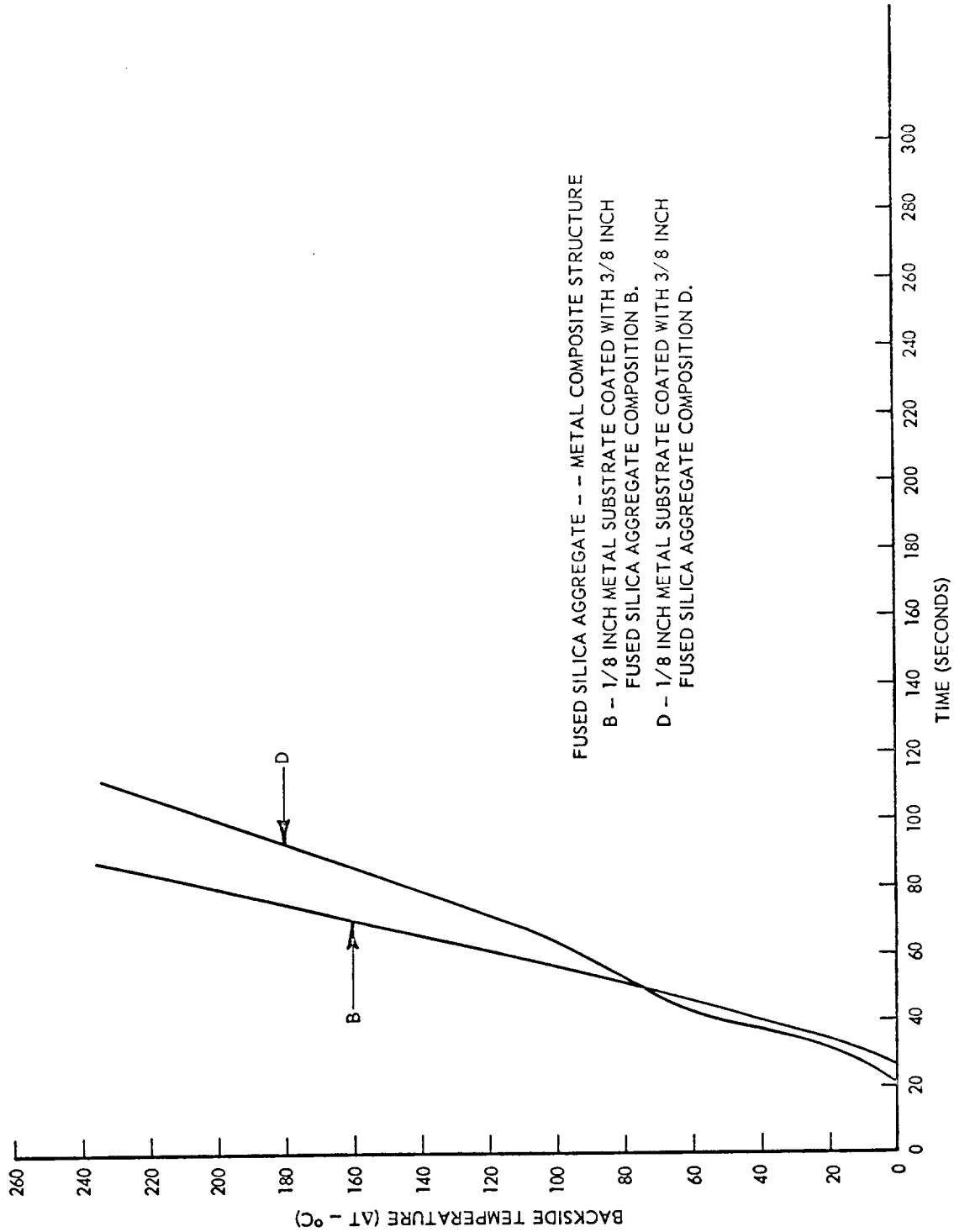

Figure 40. Change in Backside Temperature Vs. Time (Samples 1249-03, B, D).

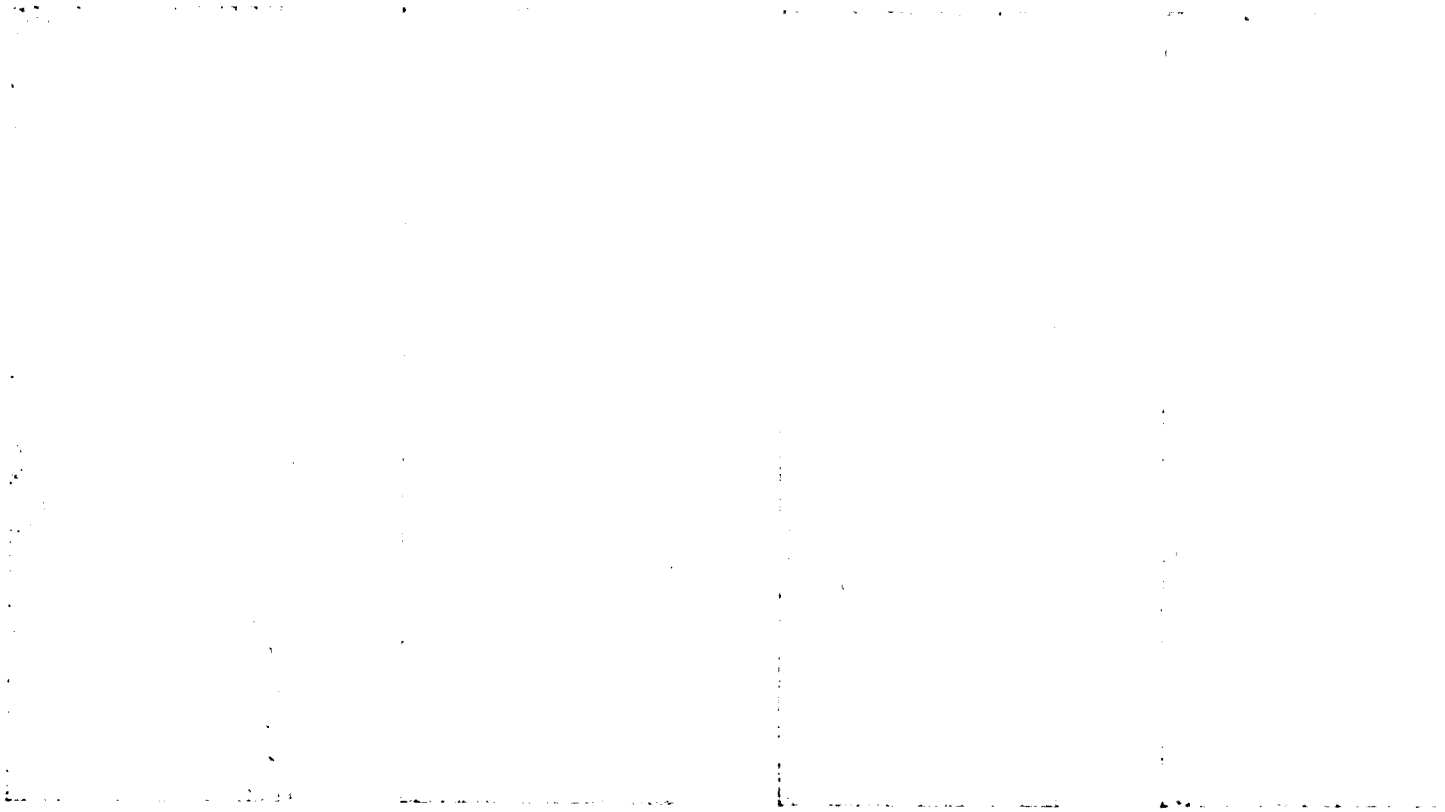

Figure 41. Rocket Motor Test Plates After Ablation Tests (Samples 1246-01, A, B, C, D).

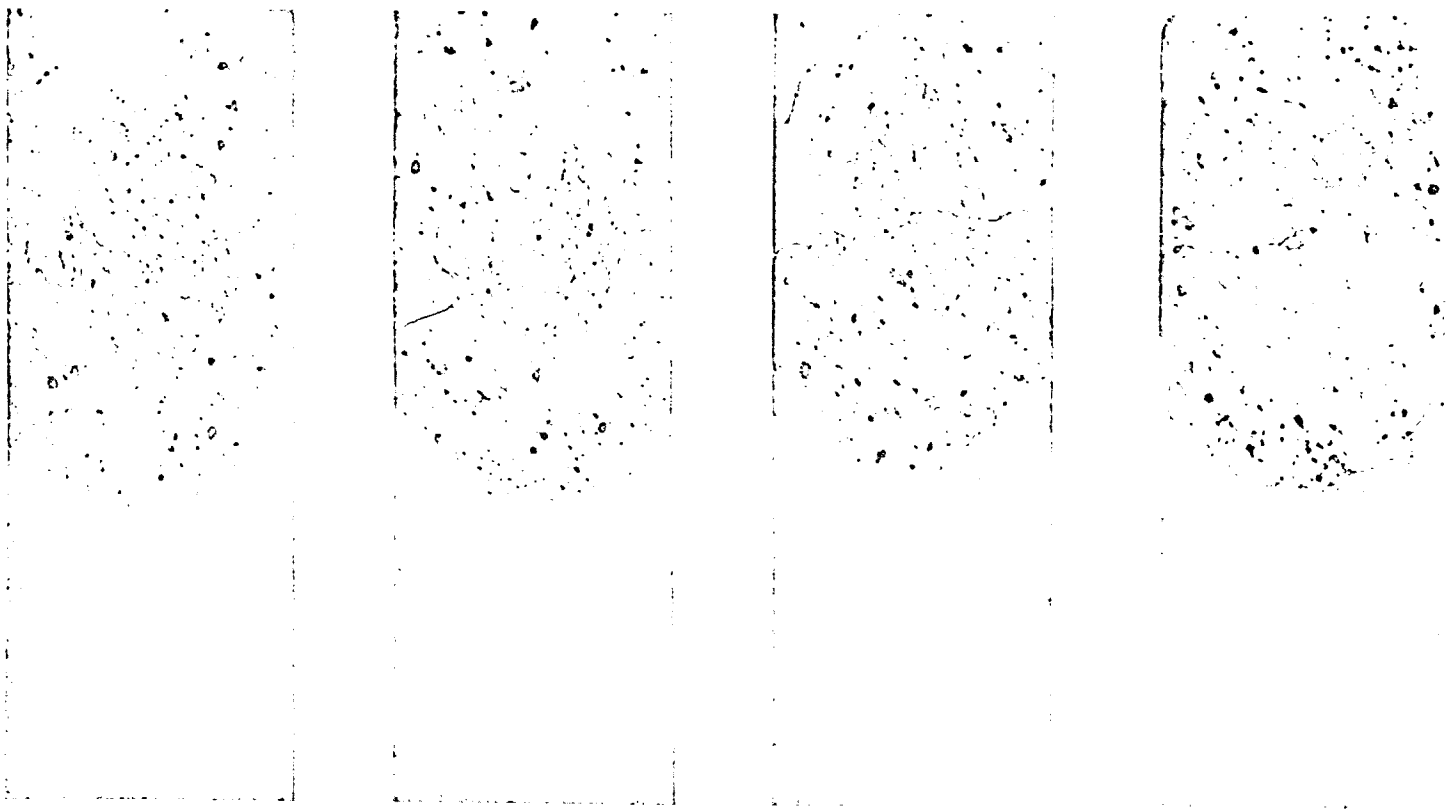

1248-02-AP 1248-02-BP 1248-02-CP 1248-02-DP

Figure 42. Rocket Motor Test Plates After Ablation Tests (Samples 1248-02-AP, BP, CP, DP).

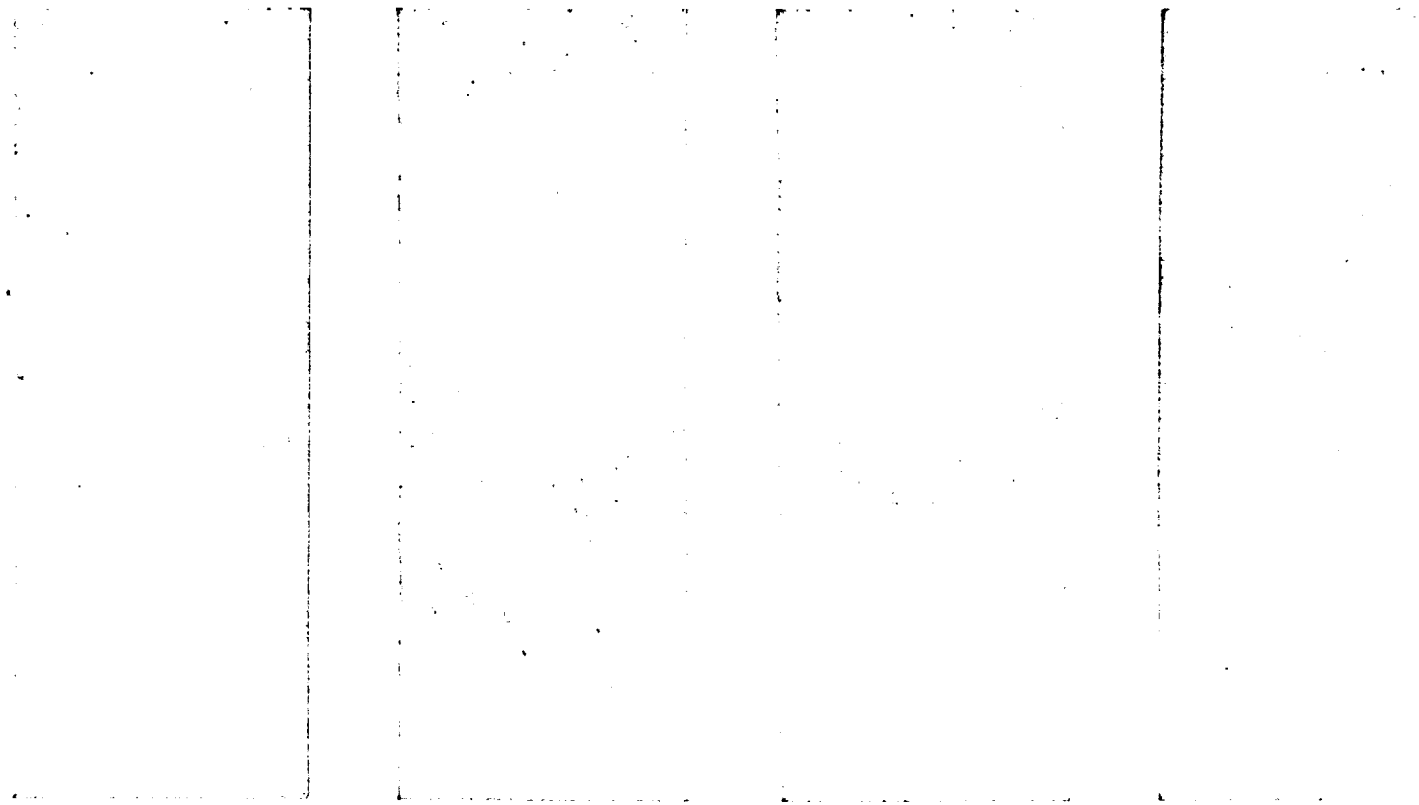

Figure 43. Rocket Motor Test Plates After Ablation Tests (Samples 1246-01-ASL, BSL, CSL, DSL).

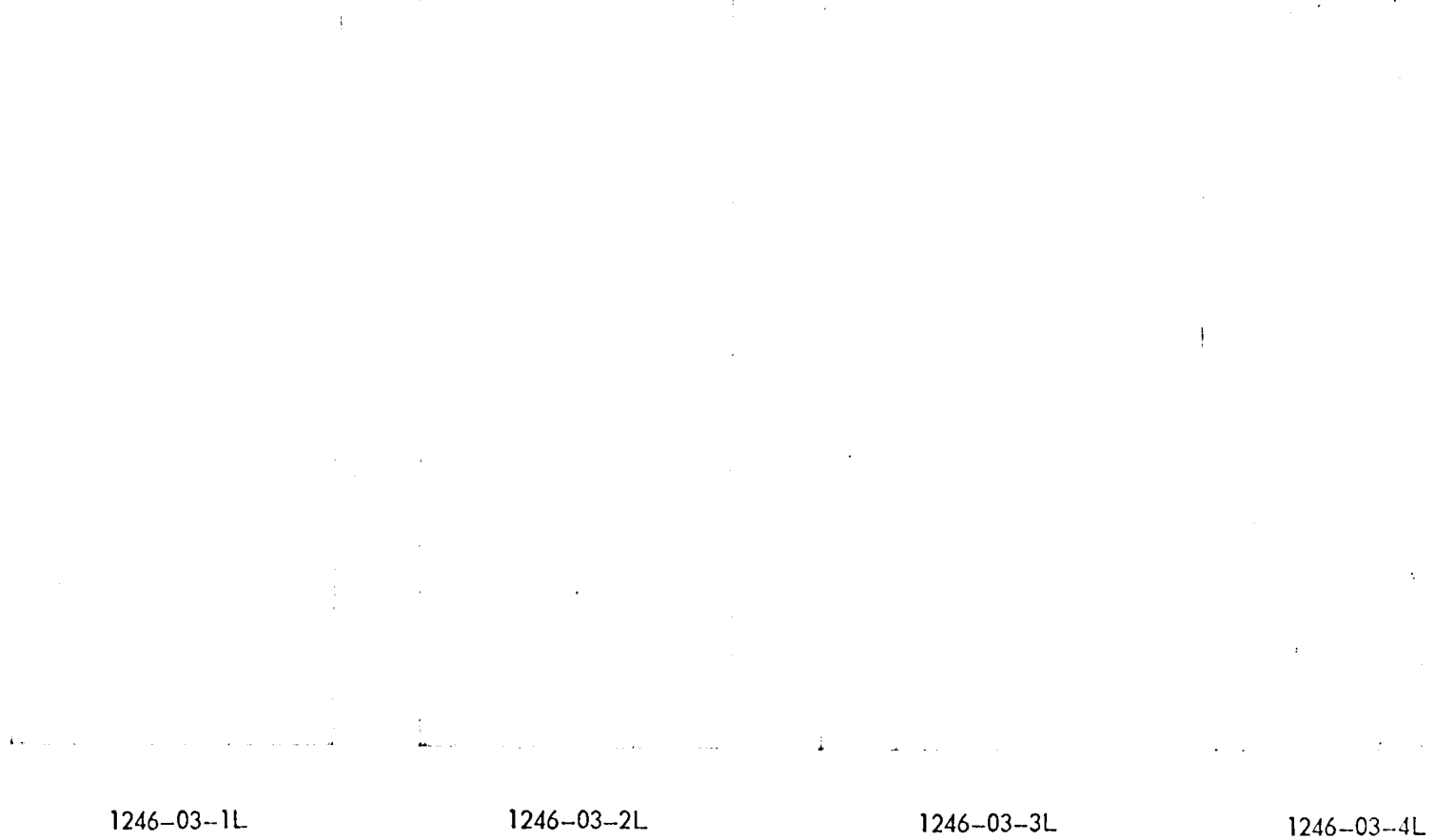

Figure 44. Rocket Motor Test Plates After Ablation Tests (Samples 1246-03-1L, 2L, 3L, 4L).

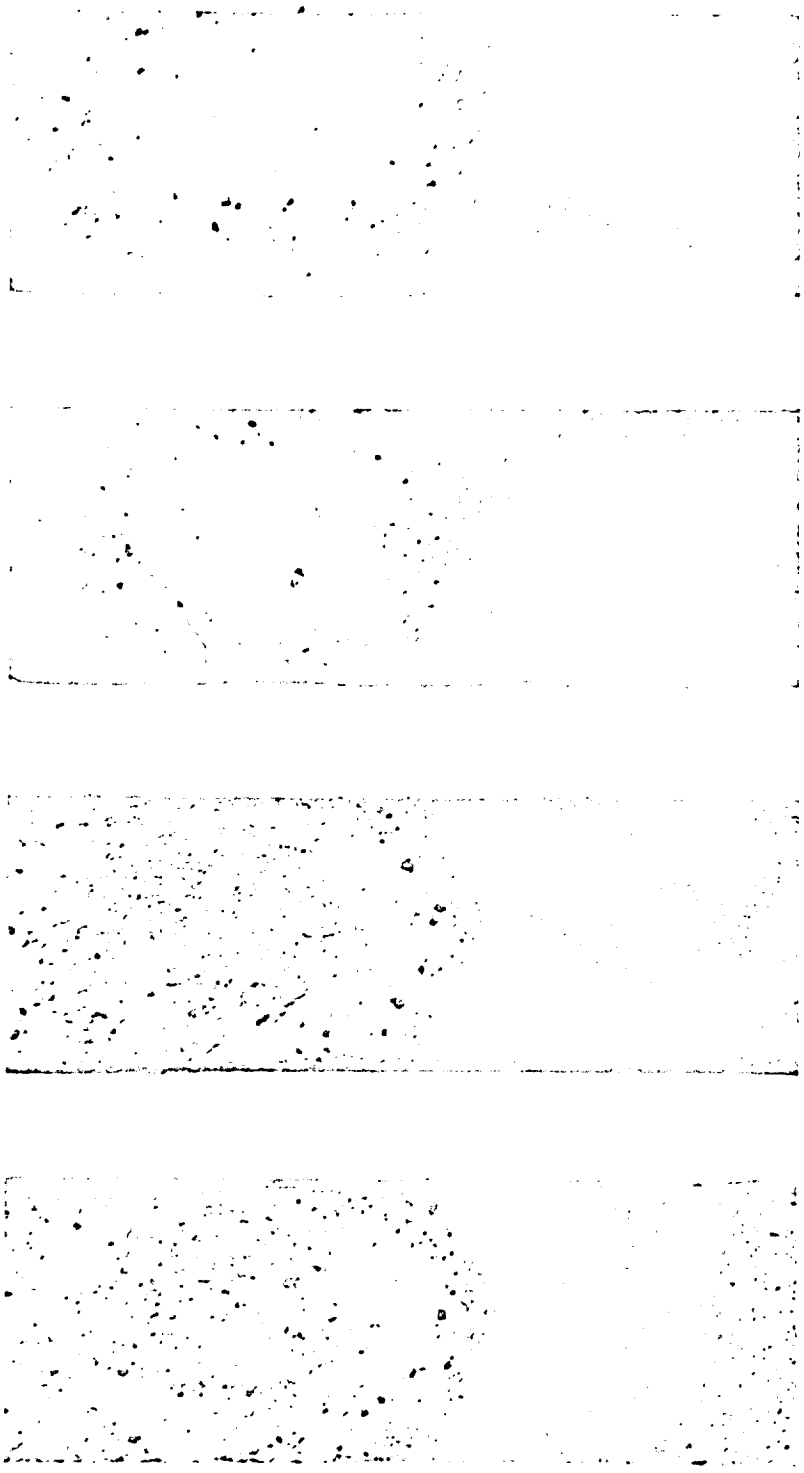

Figure 45. Rocket Motor Test Plates After Ablation Tests (Samples 1248-01-5P, 6P, 7P, 8P).

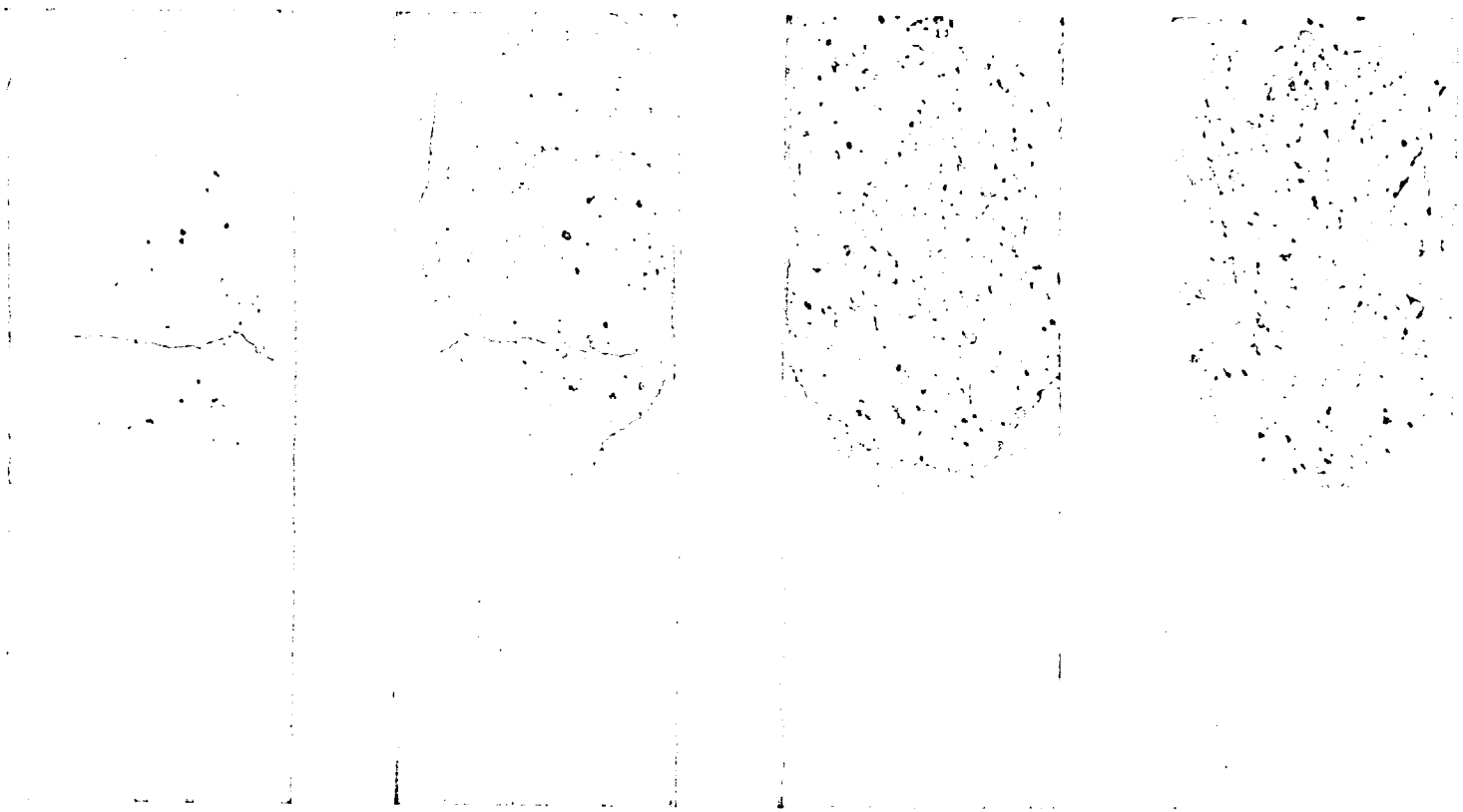

1248-01-5XP 1248-01-6XP 1248-01-7XP 1248-01-8XP

Figure 46. Rocket Motor Test Plates After Ablation Tests (Samples 1248-01-5XP, 6XP, 7XP, 8XP).

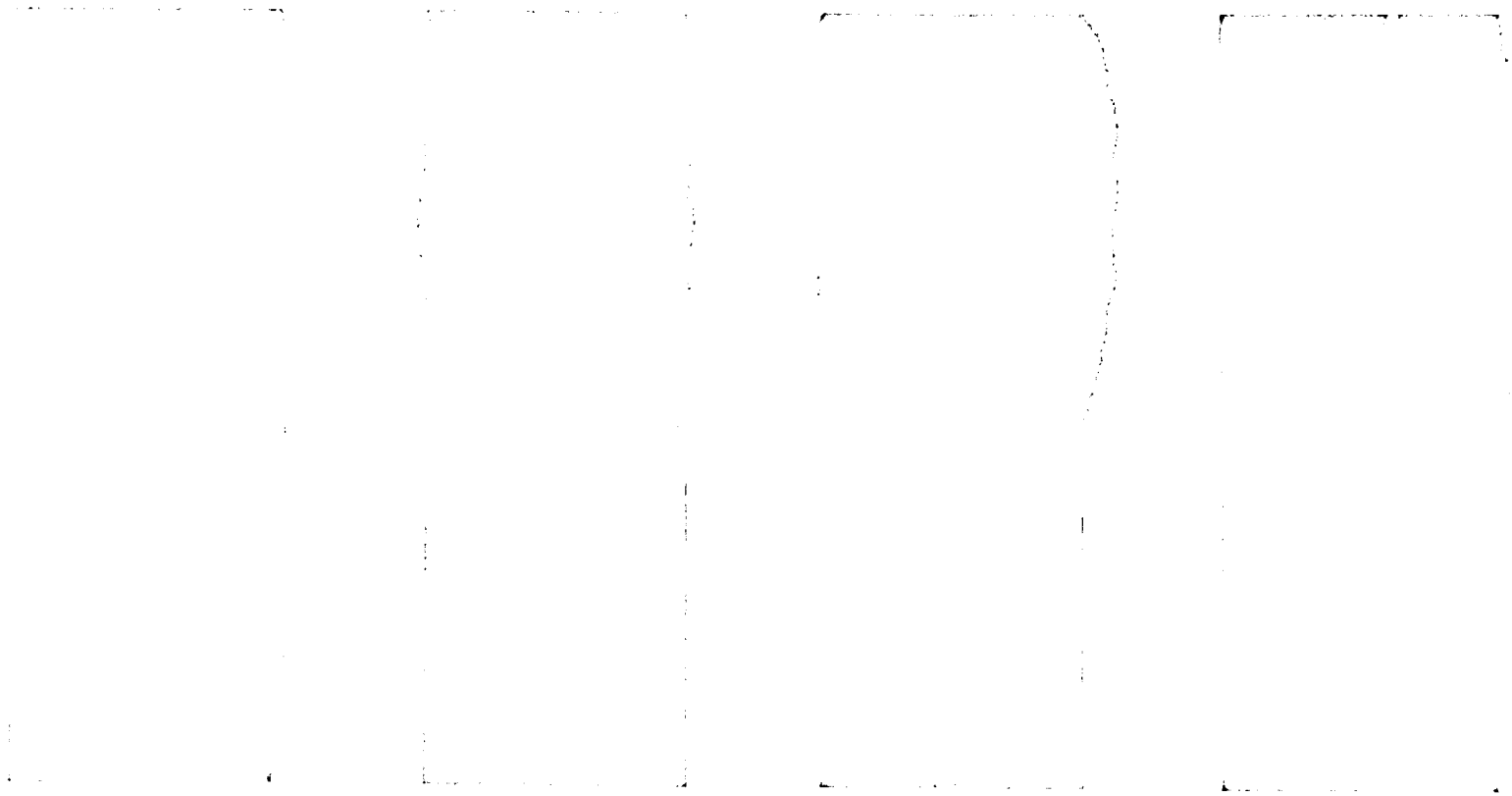

1246-02-01 1246-02-02 1246-02-03 1246-02-04

Figure 47. Rocket Motor Test Plates After Ablation Tests (Samples 1246-02-01, 02, 03, 04).

Figure 48. Rocket Motor Test Plates After Ablation Tests (Samples 1246-02-05, 06, 07, 08).

Figure 49. Rocket Motor Test Plates After Ablation Tests (Samples 1246-06-X1, X2, X2A).

Figure 50. Rocket Motor Test Plates After Ablation Tests (Samples 1249-02-O, R).

Figure 51. Rocket Motor Test Plates After Ablation Tests (Samples 1249-03-B, D).

Figure 52. Rocket Motor Test Plates After Ablation Tests (Sample 1246-01-BF).

IV. CONCLUSIONS

Concluding statements are not necessary for some of the below-listed headings. These headings are listed only for the purpose of continuity.

A. Equipment and Procedures Used for Standard Tests

B. Hydrated Cements--Fused Silica Aggregate Mixes

Evaluations of hydrated materials such as Lumnite, special Lumnite and portland cements and Gypsum plaster indicated that their water of crystallization could be utilized for transpiration cooling. Figures 30 through 37 graphically illustrate the transpiration cooling effect of the combined water of the cement when the rocket motor test plates were exposed to the exhaust gases of the oxyhydrogen rocket motor at a heat flux value of 260 $Btu \cdot ft^{-2} \cdot sec^{-1}$. Cooling time periods as long as 114 seconds were noted. Figure 30 graphically illustrates the amount of cooling that is due to ablation (sample 1246-01-BF) and the amount of cooling that is due to transpiration cooling (samples 1246-01-A, B, C, D). Also the average ablation or erosion rate and weight loss rate were significantly increased due to the removal of the chemical or combined water.

From the results of the water of plasticity (water-cement ratio) study of Lumnite, special Lumnite, and portland cements--fused silica aggregate it was found that a correlation could be made between the DTA data (Table IX and Figures 10 through 25) and the ablation data (Tables XI and XII and Figures 30 through 37); that is the greater the endothermic area of the DTA curves the greater the transpiration cooling period. Sample 1246-01-C exhibited the longest transpiration cooling period of 114 seconds. In general

the water-cement ratio of 1.33 offered the longest cooling period in all three cases. The correlation between the DTA data and the ablation data was also noted in the change in aggregate particle size and the Aerolith addition study.

The results of the DTA data showed that 100 per cent Gypsum plaster had the greatest endothermic area of approximately 10 in^2 with portland cement next with 5.5 in^2 and then Lumnite cement with 5.1 in^2. Two endothermic peaks were noted for the Lumnite and portland cement test pellets.

The average transverse strength of the test samples with water replaced by Ludox LS colloidal silica was approximately 220 psi, average bulk density 1.4 gm/cc and average apparent porosity 34 per cent. The largest DTA endothermic area of these samples was 2.66 in^2 (sample 1246-02-X2A). This area was larger than the samples studied in the water-cement ratio study. However, the transpiration cooling effect was less than the Lumnite samples containing only water.

C. Reinforced Ceramic Fiber Ceramics

The average transverse strength of the 30 per cent Lumnite cement--70 per cent -100+200-mesh fused silica aggregate was increased for each fiber addition with sample 1246-05-F7 exhibiting the highest strength of 660 psi. This value represents a 135.7-per-cent increase in strength from the standard (no fiber addition) composition strength which was 280 psi. This highest strength was obtained using a 0.25-per-cent addition of H. I. Thompson Fiber Glass Company's Refrasil F100-1 fiber. The G. E. pure fused silica random length fibers also increased the strength of the Lumnite cement compositions. The highest strength, 430 psi, being exhibited by sample 1246-05-14. This

sample, contained a 0.25-per-cent addition and its strength represents an increase of 53.6 per cent from standard.

The strength of the fiber-reinforced 8 per cent Pyropreg AC bonding resin--fused silica slip was not improved as significantly as the fiber-reinforced Lumnite cement compositions. The highest strength was exhibited by sample 1249-01-R15 (6350 psi, a 7.6-per-cent increase from standard). This sample contained 0.50 per cent G. E. pure fused silica fibers. The Refrasil fibers and flakes did not fare as well as the G. E. pure fused silica fibers. The highest strength obtained using Refrasil was for the 0.50-per-cent-Refrasil F100-1-fiber addition. This strength was 6100 psi, which is a 3.4-per-cent increase from standard (5900 psi) and is sample 1249-01-R11. The fiber and flake reinforcement of the Pyropreg AC bonding resin compositions were generally poor.

Due to time limitations, ablation properties could not be investigated for these compositions.

D. Composite Structures

It was shown that composite structures could be fabricated by filling openfaced honeycomb panels with Lumnite cement compositions and by coating a mild steel substrate with fused silica aggregate. These composite structures withstood the thermal shock of the exhaust gases of the oxyhydrogen rocket motor.

For the purpose of determining any heat sink effect of the backplate of the honeycomb test panel, a 1/2-inch-diameter x 1/8-width groove was cut in the backplate directly behind the planned point of flame impingement. The heat sink effect of the backplate is graphically shown by the lower change

in backside temperature for the same time by masking or hiding the transpiration cooling effect of the Lumnite cement filler material (the flat portion of curve 'O', Figure 39).

The results of the coating of the substrate with fused silica aggregate indicate that there is a possibility of easily coating a metal nose cone with a ceramic material for thermal protection and still retaining the desired properties of both the metal and ceramics.

E. Differential Thermal Analysis (DTA)

F. Ablation Studies

Respectfully submitted:

N. E. Poulos

N. E. Poulos
Project Director

Approved:

J. D. Walton

J. D. Walton, Jr., Head
Ceramics Branch

Frederick Bellinger

Frederick Bellinger, Chief
Material Sciences Division

J. E. Boyd

J. E. Boyd, Director
Engineering Experiment Station

V. APPENDIX

A. Analysis of Hydrated Cements

Following is a chemical analysis of Lumnite, special Lumnite, and portland cements used for conducting the experimental tests.

LUMNITE CEMENT

$Al_2O_3+TiO_2$	41.5 o/o
CaO	36.4 o/o
Fe_2O_3	5.7 o/o
FeO	5.7 o/o
SiO_2	8.9 o/o
MgO	1.1 o/o
SO_3	0.22 o/o
	0.48 o/o

SPECIAL LUMNITE CEMENT

Al_2O_3	48 o/o
CaO	38 o/o
Fe_2O_3	1 o/o
S	0.7 o/o
SiO_2	6 o/o

PORTLAND CEMENT, TYPE III

Ca_3SiO_5 (or $3CaO \cdot SiO_2$)	53 o/o
Ca_2SiO_4 (or $2CaO \cdot SiO_2$)	19 o/o
$Ca_3Al_2O_6$ (or $3CaO \cdot Al_2O_3$)	10 o/o
$Ca_4Al_2Fe_2O_{10}$ (or $4CaO \cdot Al_2O_3 \cdot Fe_2O_3$)	10 o/o

B. Source of Raw Materials

Colloidal Silica, Ludox LS, E. I. Dupont de Nemours and Company, Incorporated, Grasselli Chemicals Department, Wilmington, Delaware.

Fused Silica Aggregate and Slip, The Glasrock Products, Incorporated, Atlanta, Georgia.

Pyropreg AC Bonding Resin, Cardo Molding Products, Incorporated, Dane and Company, Atlanta, Georgia.

Refrasil F100-1/4, F100-1/2, F100-1, FL100 Fibers and Flakes, H. I. Thompson Fiber Glass Company, Los Angeles, California.

G. E. Pure Fused Silica Fibers, The General Electric Company, Schenectady, New York.

Lumnite Cement, Universal Atlas Cement, Division of United States Steel Corporation, New York, New York.

Portland Cement, High Early, Southern Cement Company, Division of American, Marietta Company, Mingham, Alabama.

U. S. Gypsum Pottery Plaster No. 1, United States Gypsum Company, Chicago, Illinois.

Keltex, Kelco Company, New York, New York.

Aerolith, Vinsol Resin Solution, L. Sonneborn Sons, Incorporated, New York, New York.